LARS Technical Report 052081

Computer-Based Forest Cover Classification Using Multispectral Scanner Data of Different Spatial Resolutions

by R. S. Latty

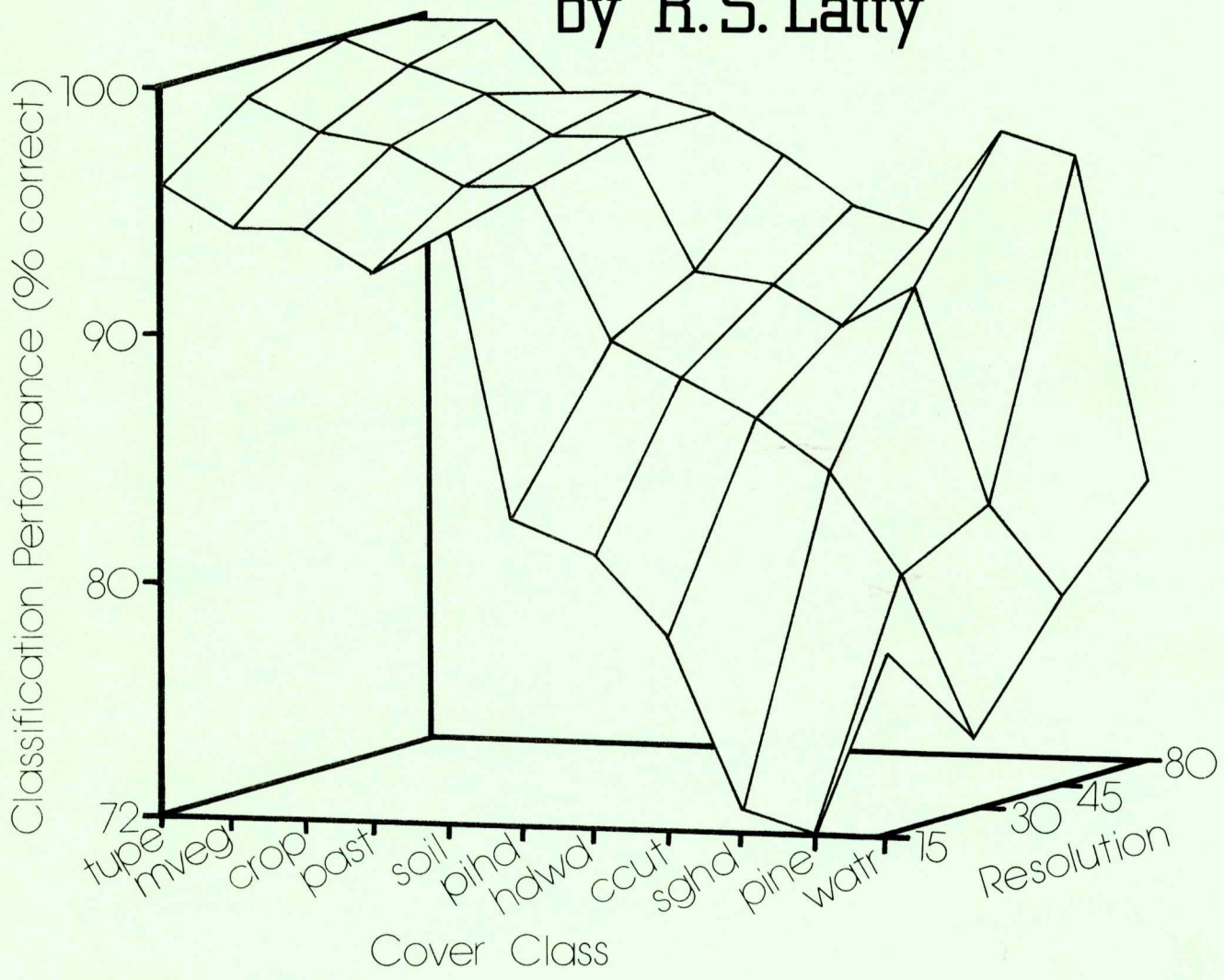

Laboratory for Applications of Remote Sensing
Purdue University West Lafayette, Indiana 47906 USA
1981

LARS Technical Report 052081

COMPUTER-BASED FOREST COVER CLASSIFICATION USING MULTISPECTRAL SCANNER DATA OF DIFFERENT SPATIAL RESOLUTIONS

by

Richard S. Latty

May 1981

The research described in this report was sponsored by NASA under Contract No. NAS9-15889.

Star Information Form

1. Report No.	2. Government Accession No.	3. Recipient's Catalog No.

4. Title and Subtitle	5. Report Date
Computer-Based Forest Cover Classification Using Multispectral Scanner Data of Different Spatial Resolutions	May 1981
	6. Performing Organization Code

7. Author(s)	8. Performing Organization Report No.
Richard S. Latty	052081

9. Performing Organization Name and Address	10. Work Unit No.
Laboratory for Applications of Remote Sensing Purdue University 1220 Potter Drive West Lafayette, IN 47906-1399	11. Contract or Grant No. NAS9-15889

12. Sponsoring Agency Name and Address	13. Type of Report and Period Covered
Mr. Norman Hatcher Exploratory Investigations Branch NASA/Johnson Space Center; Houston, TX 77058	Technical Report
	14. Sponsoring Agency Code

15. Supplementary Notes

16. Abstract The objectives of this study were to: (1) Compare the classification accuracies obtained with data from four different spatial resolutions and (2) to compare the classification accuracies obtained using the per-point classifier with accuracies achieved using a per-field classifier (i.e., the LARSYS *SECHO classifier). Data used were obtained on May 2, 1979 with the NASA NS-001 Thematic Mapper Simulator (TMS) over an area in Northeastern South Carolina from a height of 19,500 feet above ground. Data sets having 15x15, 30x30, 45x45, and 60x75 meter spatial resolutions were generated and compared. Classification accuracies were assessed using both training and test areas.

The results show that the use of successively higher spatial resolution data resulted in lower overall classification performance (i.e., 15x15 meter spatial resolution resulted in significantly lower classification accuracy than Landsat spatial resolution). Differences in classification accuracies for data of different spatial resolutions were not significant among cover classes having relatively low levels of spectral variability across adjacent pixels (i.e., pasture, crops, bare soil or water). However, statistically different classification performances were found for forest cover classes which had relatively large amounts of spectral variability across adjacent pixels. Statistically higher classification accuracies were achieved using *SECHO classifier than were achieved using the per-point GML classifier.

17. Key Words (Suggested by Author(s))	18. Distribution Statement

19. Security Classif. (of this report)	20. Security Classif. (of this page)	21. No. of Pages	22. Price
Unclassified	Unclassified		

*For sale by the National Technical Information Service, Springfield, Virginia 22161

NASA - JSC

TABLE OF CONTENTS

Page

LIST OF TABLES

Appendix Table | Page

LIST OF FIGURES

Figure Page

Figure

Page

ABSTRACT

Latty, Richard S. M. S. in Forestry, Purdue University, May, 1981. Computer-Based Forest Cover Classification Using Multispectral Scanner Data of Different Spatial Resolutions. Major Professor: Roger M. Hoffer.

The 43 microradian angular instantaneous-field-of-view (IFOV) of the Thematic Mapper (TM) will provide a linear spatial resolution of approximately 30 meters from a nominal orbital altitude of 700 kilometers. The activities reported here have been focused on developing an understanding of the relationship between the properties of the imaged scene, the spatial resolution of the system with which the scene is imaged, and the characteristics of the resulting data. Specifically, the objectives of this investigation were : 1) to compare the "pure field" classification accuracies obtained with data of four different spatial resolutions, using a per-point Gaussian maximum likelihood (GML) classifier, and 2) to compare the "pure field" classification accuracies obtained with data of 30 meter spatial resolution using the per-point GML classifier with accuracies achieved using a per-field classifier (i.e., the LARSYS *SECHO, "Supervised Extraction and Classification of Homogeneous Objects", classifier).

The data were obtained on May 2, 1979 with the NASA NS-001 Thematic Mapper Simulator (TMS) over an area in northeastern South Carolina from a height above ground of 19,500 feet. The 2.5 milliradian angular IFOV of the TMS resulted in a nominal 15 meter linear spatial resolution at nadir for the original TMS data. Data

sets of three different spatial resolutions (30 x 30 meter, 45 x 45 meter, and 60 x 75 meter) were computed from the original 15 x 15 meter TMS data. Data of each resolution were classified with a conventional per-point GML classifier. The 30 meter spatial resolution data was then classified with the *SECHO classifier. The classification accuracies were assessed with both training areas and test areas based on agreement with cover class identifications determined from aerial photographs and site visits. The percentage of pixels correctly classified for data of each resolution and with each classifier were compared using the Newman-Kuels' Range Test on the arcsin transformed proportions.

The results were :

1) the use of successively lower (from 15 x 15 meter to 60 x 75 meter) spatial resolution data resulted in higher overall classification accuracies;

2) in areas where the cover classes occupy relatively small contiguous areas, decreases in spatial resolution beyond 45 x 45 meters failed to result in higher "field-center pixel" classification accuracies;

3) statistically ($a = 0.10$) higher classification accuracies were achieved using 60 x 75 meter, as opposed to higher, spatial resolution data in cover classes (eg., forest cover classes) associated with relatively high levels of spectral variability across adjacent pixels;

4) differences in classification accuracies achieved with data of different spatial resolution were not significant ($a = 0.10$) for cover classes with relatively low levels of spectral variability across adjacent pixels (i.e., pasture, crops, bare soil, or water);

5) statistically (a = 0.10) higher classification accuracies were achieved using the *SECHO classifier with 30 meter spatial resolution data, than were achieved using the per-point GML classifier;

6) the largest increases in classification accuracies were achieved with the *SECHO classifier in cover classes associated with relatively high levels of spectral variability across adjacent pixels; and

7) the difference in classification accuracy observed for training pixels as compared to test pixels was much greater than the differences due to spatial resolution of the data, or the classifier employed.

Perhaps most importantly, these results indicate that, in order to make best use of the 30 meter spatial resolution data of the Thematic Mapper, more efforts will need to be focused on the development and refinement of classifiers which employ patterns of spectral variability in the spatial domain.

CHAPTER 1

INTRODUCTION

In forest inventories and surveys the need to classify areas to a detailed level of community composition and stand structure often exists. Landsat data has provided the remote sensing community with a first look at employing spacecraft imagery for natural resource inventory and monitoring. Landsat data enables land cover classifications to be obtained at accuracy levels compatible with many applications. These, however, are generally restricted to fairly low levels of detail. Landsat data usually does not provide adequate classification results for more detailed levels of cover classification. Experience with large scale, high resolution aircraft photography has left many applications scientists with the impression that similar improvements in classification detail and accuracy can be achieved with higher resolution MSS data than is provided with the current Landsat MSS. While there is little doubt that increased spatial resolution data will facilitate visual interpretation of the imagery, the impact on computer-based cover classification is not well known.

This study investigates forest cover type classification accuracy achieved using data of different spatial resolutions. The classification accuracies achieved with the conventional per-point Gaussian maximum likelihood classifier are compared to the accuracies achieved with a compound decision classifier (ie., the supervised ECHO ("Extraction and Classification of Homogeneous Objects") classifier). The characteristics of the data and the class densities (used in training the classifier) are also examined relative to spatial resolution. Information regarding these characteristics are expected to provide a better understanding of the relationship between spatial resolution and classification accuracy.

Much attention has been given to the task of providing a precise theoretical and operational definition of spatial resolution for MSS systems, with considerable ensuing debate and controversy. While the provision of such a definition is beyond the scope of this study, a brief review of some of the work and considerations given this topic will clarify some of the relationships between characteristics of the scene, the scanner system, the resulting data, and the processing techniques employed in converting the data to useful information. Exact values for the spatial resolution of MSS data rely on the operational definition of resolution and are, strictly speaking, not available. Therefore, nominal figures will be used throughout. The term "spatial resolution" will be used in reference to the area on the ground represented by a single picture element (pixel), that is, the area on the ground represented by a single response level vector. Increasing or higher resolution will refer to a decrease in the area on

the ground represented by the pixel. Decreasing or lower resolution will refer to an increase in the area on the ground represented by the pixel.

Objectives

There are two primary objectives of this study.

(1) The hypothesis that per-point classification using four different spatial resolutions result in classification performances which are equal will be tested. The hypotheses can be expressed as :

H0 : P(15m) = P(30m) = P(45m) = P(75m)

H1 : not all performances are equal.

The presence of any trends in classification accuracy associated with resolution will be tested through the use of the an analysis of variance sensitive to rank orders. This will provide a test for the significance of any apparent trends in the classification accuracies. The differences in classification accuracy across spatial resolution for the various cover classes are examined in order to better understand the possible affect of the spectral variability associated with the cover classes.

(2) The classification performance of 30 meter resolution data using a per-point classifier will be compared to performances obtained by employing a per-field classification approach. The hypotheses can be expressed as :

H0 : P(30m,p) = P(30m,f)

H1 : $P(30m,p) < P(30m,f)$

Two sub-objectives of the study are :

(1) to explore the differences, if any, in the within cover class variance and the within spectral class variance associated with each resolution studied, and

(2) to explore the correlation between response levels of spatially proximal pixels within each of the different resolutions.

CHAPTER 2

LITERATURE REVIEW

Spatial Resolution

A conceptual definition for spatial resolution was provided earlier to establish a basis on which subsequent discussion could be conducted. Operationally and theoretically, however, resolution has proven to be a nebulous subject which has received much attention from physicists and engineers in the field of optics. While the problem of spatial resolution for MSS systems is different from that for photographic systems, the majority of the work has been concerned with the latter. A review of some of the work conducted with respect to resolution in the field of photo-optics will provide much insight into the nature and complexity of the resolution of MSS systems.

Resolution, in photography and telescopy, has been used in reference to the "minimum separation between two objects for which the images appear distinct and separate" (Rosenberg, 1971). This separation can either be expressed as a distance between the images of the objects or as the angle subtending the two objects from the point of observation. Operationally, resolution has been defined for

photographic systems by the number of line pairs per millimeter "that are just discernable by the human eye looking at the image of a particular standardized bar target of particular standardized contrast under particular specified conditions of illumination and magnification" (Rosenberg, 1971). Figure 2.1 is an example of such a test target. The highly specific nature of the conditions under which this measure of resolution is obtained makes it misleading in the context of applications for which such conditions rarely, if ever, exist. Resolution, so determined, will vary depending on the shape of the object, object-to-background contrast, location and orientation of the object in the image, exposure, degree of development, angle and amount of illumination, etc., (Rosenberg, 1971; Noffsinger, 1970A; Welch, 1971). Work conducted in spacecraft altitude photography by Atkinson and Jones (1963) established the importance of atmospheric turbulence, and the height of the turbulent layer, as another factor determining the resolution of imagery from orbit altitudes. Other approaches to the problem have been developed in response to the above limitations. Among these other approaches are Rayleigh's, Sparrow's, Conrady's, and Dawe's criteria ; all of which have met with similar objections (Noffsinger, 1970A).

The approach which has received much attention, and has demonstrated advantages over the other criteria, is the application of the modulation transfer function (MTF). The modulation transfer

function is basically a relationship between image contrast and the spatial frequency of the image (1). Noffsinger (1970B) describes the MTF, graphically, as a "plot of spatial frequency versus the ratio of image to object modulations, which are normalized to unity at zero spatial frequency". The image to object modulation is the ratio of the relative amplitude of the exitance at the object surface (the "object") to the relative amplitude of the log-exposure equal to the photographic emulsion density (the "image"). The advantages and nature of the modulation transfer function are best made apparent by the method through which it is obtained, therefore the procedure will be presented here.

The spatial variation in reflectance associated with the bar target presented in Figure 2.1, can be thought of as a gate function, with percent reflectance varying as a function of distance (Figure 2.2 is a plot of percent reflectance versus distance for the bar target of Figure 2.1). The bar target thus provides a target of distinct edges, one side of the edge having a very high reflectance (generally about 80%), and the other having a very low reflectance (generally about 5%; see Welch, 1971). The theory of MTF analysis is based on the amplitude modulations for targets which vary in reflectance in a sinusoidal manner with respect to distance (Welch, 1971). Figure 2.3 is the percent reflectance versus distance for a test target, the bars of

---

(1) Contrast is defined as the change in the density with respect to the change in the log-exposure (Zwick, 1966). Spatial frequency can be thought of as the number of patterns per unit distance, and is generally expressed in cycles per millimeter (Zwick, 1966; Welch, 1971).

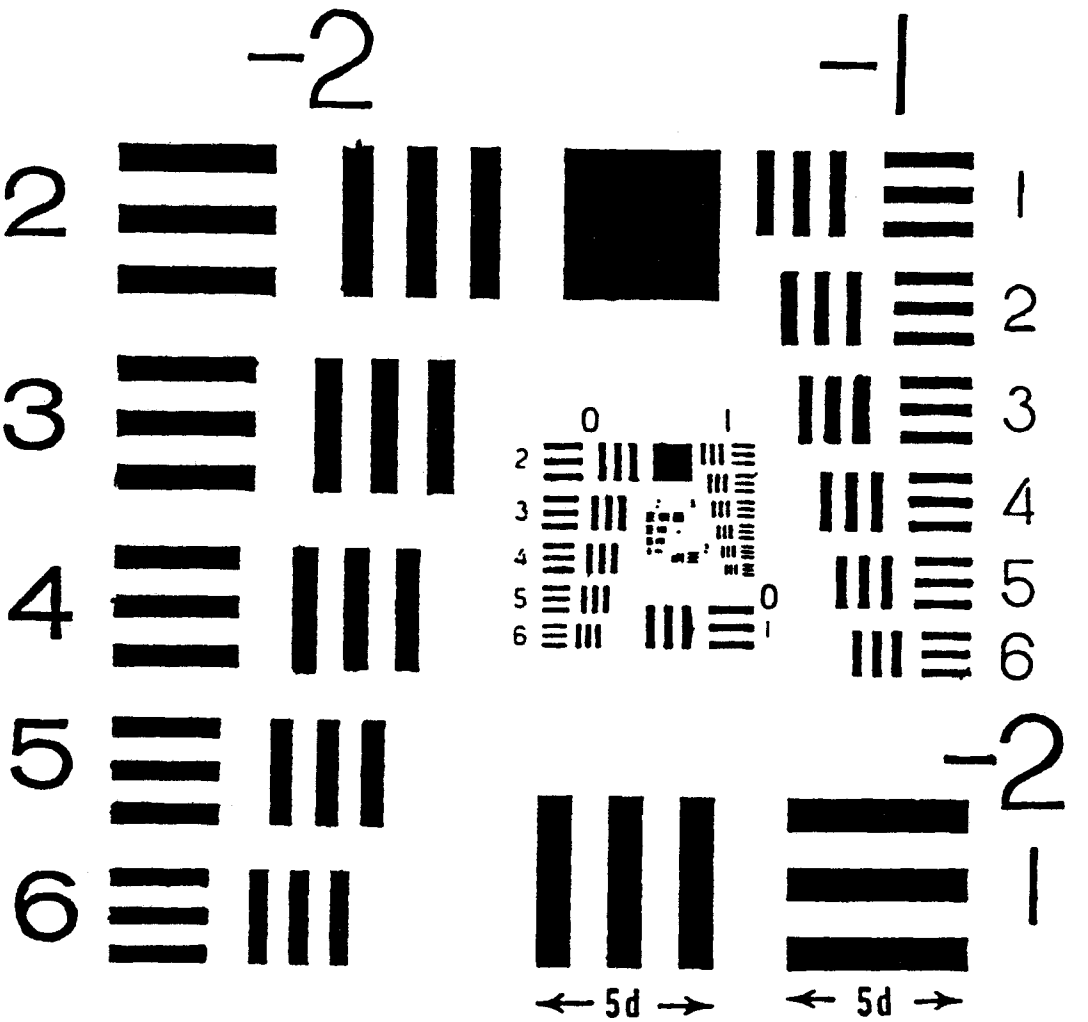

Figure 2.1 Standardized Resolving Power Test Target (from Todd and Zakia, 1969).

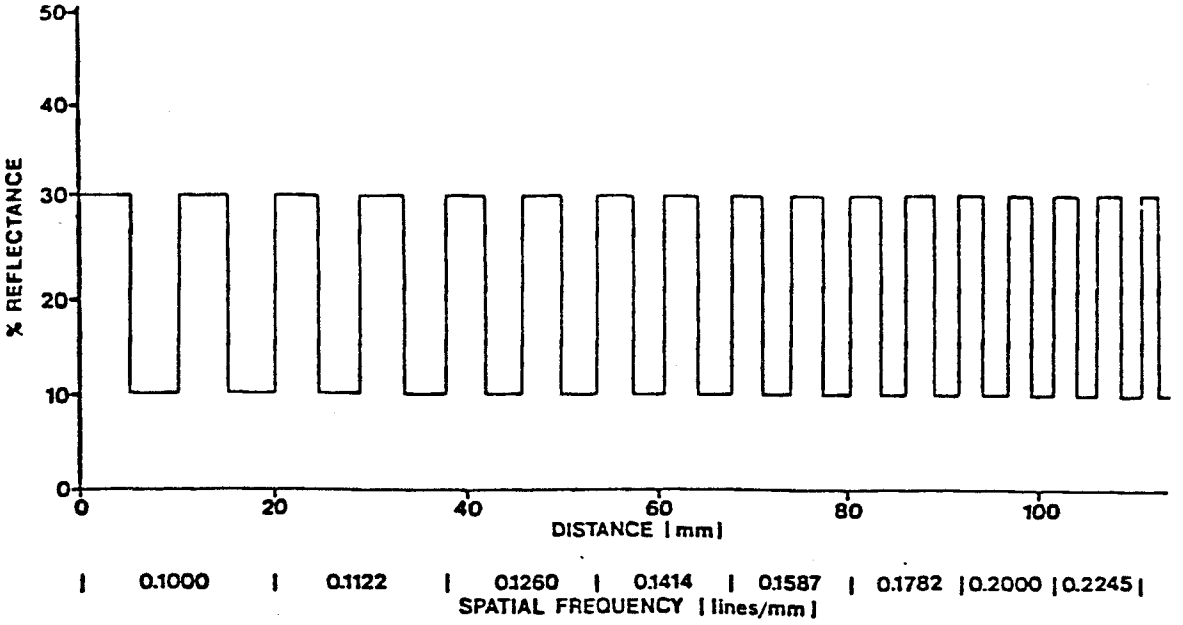

Figure 2.2 The Variation in Reflectance Associated with a Standard Resolving Power Test Target.

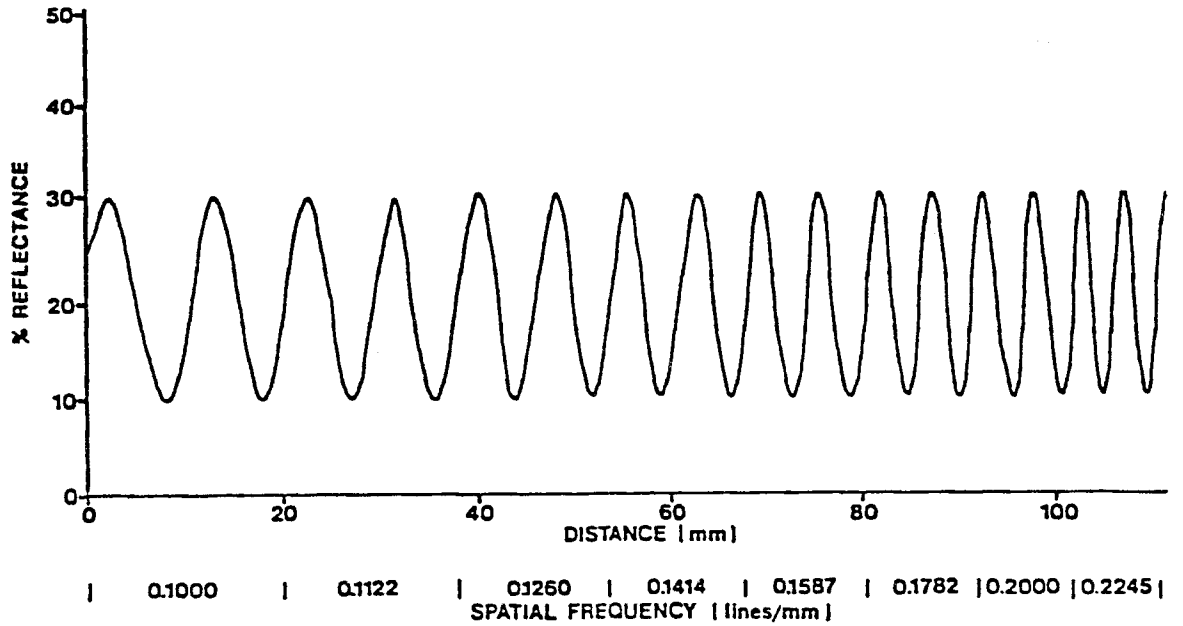

Figure 2.3 The Variation in Reflectance Associated with a Test Target of Sinusoidally Varying Reflectance of Increasing Frequency in the Spatial Domain.

which do not possess distinct boundaries. The test target employed in MTF analysis provides a closer approximation to "real world" situations, in that few boundaries are accurately represented by the gate function characterizing the bar target of Figure 2.2 and rarely, if ever, does the target-to-background contrast have a ratio of 1:16. Slater (1975) discussed procedues for determing the resolution of photographic systems with a range of test target contrasts of 1:1000 to 1:1.6.

A bar target of sinusoidally varying amplitudes of percent reflectance is imaged with the photographic system to be tested (2). The photographic negative is then scanned with a spot or line scanning densitometer. The image is scanned normal to the orientation of the bars. Since the amplitudes recorded for each spatial frequency (ie., for each set of bars having a different spacing) are measured relative to the density of the negative, these amplitudes are generally converted to exposure. This is achieved through the use of the relationship shown in the sensitometric curve (Figure 2.4) between density and log-exposure. This conversion renders the amplitudes independent of image processing and image contrast (Todd and Zakia, 1969). The resulting maximum and minimum amplitudes of exposure are then used to compute the modulation transfer factor for each spatial frequency component by :

$$MT(f) = (I(max) - I(min))/(I(max) + I(min))$$

---

(2) This is generally done at several levels of focus to determine the out-of-focus effects for the system, and at various viewing angles to determine off-axis resolution characteristics.

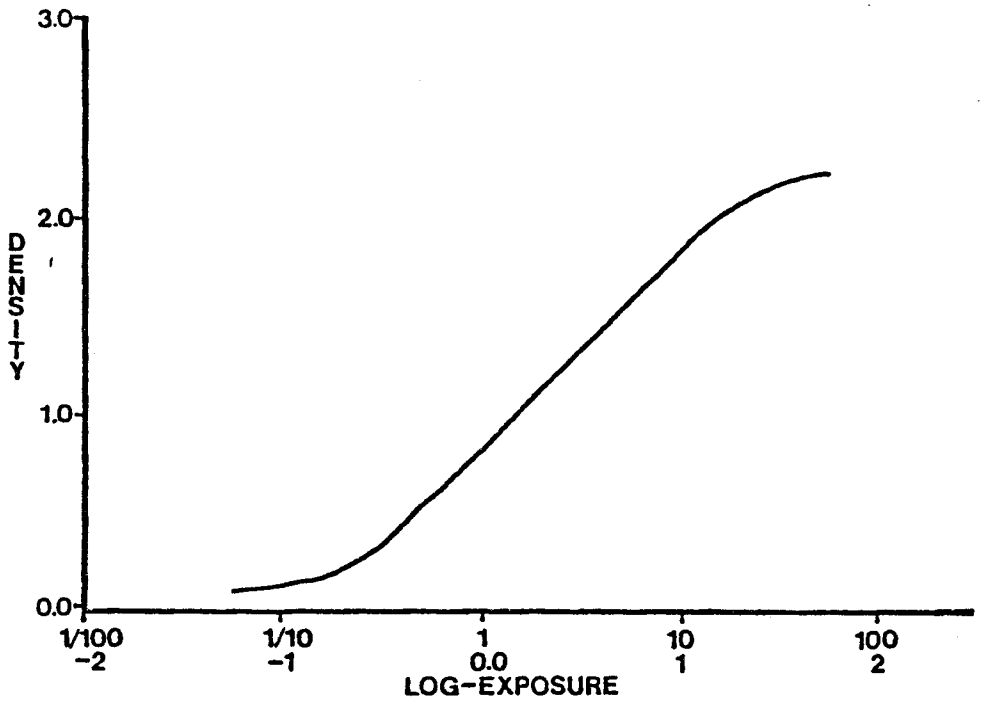

Figure 2.4 Sensitometric Curve. Exposure ($ergs \cdot cm^{-2}$) is defined by $E = It$, where I = illumination or irradiance ($erg \cdot sec^{-1} \cdot cm^{-2}$), and t = time(s). Density is defined as log-Opacity, where opacity is the capacity of a material to resist the transmission of light. Opacity is the inverse of the transmittance (see Cretcher and Reed, 1968).

where :

MT(f) = the modulation transfer factor for frequency (f),
I(max) and I(min) are the maximum and minimum exposure values (respectively) obtained from the transformed densitometer trace.

The modulation transfer factor is then plotted against the corresponding spatial frequency (as shown in Figure 2.5) which is, graphically, the modulation transfer function. The plot is normalized by multiplying all transfer factors by the reciprocal of the transfer factor of the lowest spatial frequency, thus the highest modulation is generally 1.

The elegance of the MTF arises from it's mathematical identity. It is the modulated amplitude of each frequency component of the scene. From communication theory, any signal can be represented by a sum of mutually orthogonal functions (Lathi, 1968). The first period of the gate function of Figure 2.2, for example, can be approximated by summing over a set of sine functions of various frequencies and amplitudes, as shown in Figure 2.6. The sum of sine functions multiplied by their corresponding amplitudes constitutes a trigonometric Fourier series. The Fourier series is an infinite series, the arguements of which are the frequency components, and the coefficients of the arguements are the amplitudes of their respective

---

(3) There are many texts covering the theory and mathematics of the Fourier transform. A particularly tractable coverage is provided in Communication Systems , by B.P. Lathi. Other texts include Principles

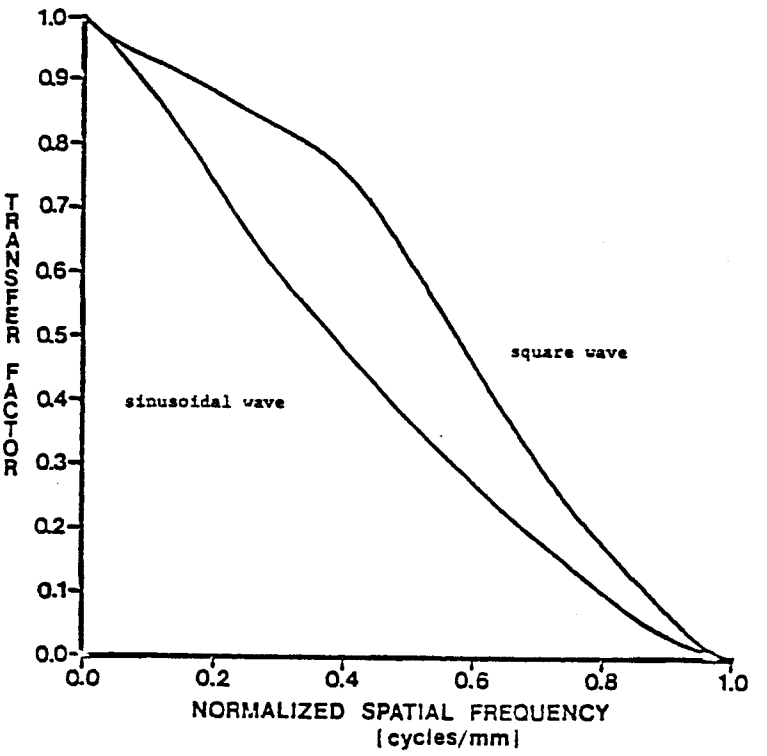

Figure 2.5 Modulation Transfer Function for a Target which Varies in Reflectance According to a Sinsoidal Wave Function and According to a Square Wave Function. (Slater, 1975).

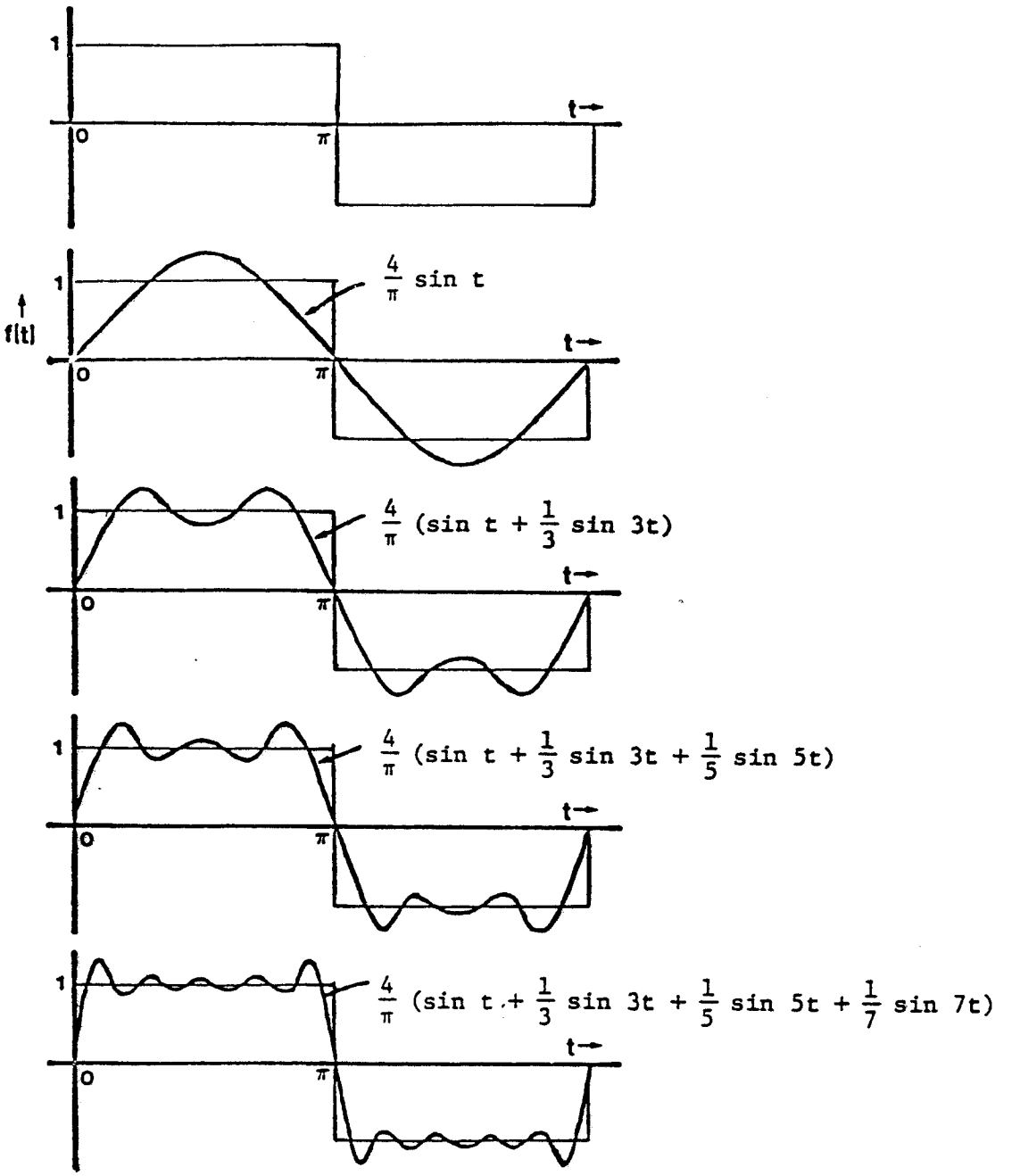

Figure 2.6 Estimation of a Square Wave Function with Trigonometric Fourier Series of an Increasing Number of Frequencies.

frequency components (3). An electrical signal is a representation of a variation in current amplitude in the time domain, x(t). The Fourier transform of the electrical signal is a representation of variation in current amplitude in the frequency domain. The original electrical signal can be obtained by the inverse Fourier transform of its representation in the frequency domain. Similarly, the modulation transfer function is a representation of the amplitude of electromagnetic energy reflected by the object, modulated in the imaging process, represented in terms of the frequency domain. The inverse Fourier transform is the image modulated amplitude in the spatial domain, which is the point spread function for two dimensions and the line spread function for one dimension (Slater, 1975; Noffsinger, 1970B). That is, we can obtain the density function which represents the spatial "spread" of irradiance from a point source or a line source of light, as represented in the image, from the inverse Fourier transform of the modulation transfer function of the imaging system. We can now integrate the line spread function to obtain the edge trace (4), which will provide information regarding the "sharpness" of the image (Noffsinger, 1970A).

Perhaps the primary advantage of approaching resolution in this fashion is that the resolution characteristics of an entire imaging system (ie., the atmosphere, the platform motion, imaging optics, film,

---

of Communication : Systems, Modulations, and Noise , by R.E. Zeimer and W.H. Tranter, and Applied Time Series Analysis , by Otnes and Enochson.
(4) An edge trace is the level of exposure at each point along a line perpendicular to some edge (the boundary between two surfaces of different reflectances) in an image, generally obtained with a scanning densitometer.

and developing techniques) can be obtained by multiplying the MTF of each individual component, provided certain assumptions are met. Thus the resolution resulting from the combination of any set of imaging components can be determined from knowledge about the MTF of each individual component, instead of having to determine a single value under a specific set of conditions for each possible combination.

Noffsinger (1970B) provides a very appealing verification of this "cascading" capability using the convolution integral in the spatial domain. Shelton (1967) used the convolution integral to determine the combined effect of the point source distribution and the point spread function of the imaging system used. Interpretation of the MTF through the use of threshold modulations, which provide a relationship between "just resolvable" spatial frequencies at different levels of contrast, is presented by Scott (1964) and Welch (1971). Zwick (1966) used the resolving power of the human eye (about 0.1 mm or 5 cycles/mm at a distance of 25 cm) to evaluate the MTF of imagery for different anticipated applications. Zimmerman (1966) demonstrated the relationship between the MTF and other commonly used criteria for determining resolution. Slater and Schowengerdt (1972) offered a means of applying the MTF to multispectral scanner systems.

The representation of resolution with the MTF also provides a means of determining the combined effect of the characteristics of reflected radiation and the optical system (including the atmosphere) on the spatial characteristics of the resulting image. Most earth surface features of interest in remote sensing, at illumination angles under which sensing systems commonly operate, reflect radiation in a

diffuse manner. While few materials approach truely Lambertian surfaces in their reflective properties (ie., the reflected radiation is constant independent of the angle of view and the angle of illumination), the reflected radiation is largely diffuse (Higham, Wilkinson, and Kahn, 1973). This property results in a continuous distribution of radiation from a discrete source as a function of the distance from the source. That is, the edge trace of a discrete source would possess a definite slope excluding the effect of any optical imaging system. Therefore, an edge between two surfaces of different reflectances would have a line spread function of definite width, resulting from the diffuse reflection of incident radiation. The maximum resolution acheived for any given imaging system would, consequently, be less than the convolution of the line spread function, resulting from diffuse reflection, with the spread function of the atmosphere (due to scattering caused by turbulence). Atkinson and Jones (1963) suggested that long focal length systems at spacecraft altitudes, which would otherwise provide very high resolutions, would be limited to a maximum resolution of about 1.3 meters under "good" atmospheric conditions. The maximum achievable resolution would also vary as a function of wavelength, since atmospheric scattering effects vary with respect to wavelength (see section on Response Level Adjustment).

Resolution in Multispectral Scanner Systems

The distinction between the resolution of photographic systems and multispectral scanner systems is basically twofold. Resolution for MSS systems is in reference to the area on the ground represented by a single response level vector (5), rather than the minimum distance between two "just distinguishable" points. Efforts to provide an operational definition for resolution of an MSS system are directed at defining the dimensions of this instantaneously viewed area on the ground, and the two dimensional weighting function representing the relative modulation of exitance for each point in the area. This function is analogous to the point spread function of photographic systems. The resulting spread function is the inverse Fourier transform of the product of the modulation transfer functions of all of the components of the system (NASA, 1973). Figure 2.7 is a schematic representation of the components through which the reflected radiation, and subsequent electrical signal, are modulated in the process of MSS imaging. The "post-optics" set of modulators is the secondary distinction between MSS and photographic systems, when considering resolution.

The most commonly cited measure for spatial resolution is the

---

(5) This area on the ground has been refered to as the "effective instantaneous field-of-view, EIFOV" (NASA, 1973), "ground-projected IFOV" (Slater, 1979), "ground resolution" (Higham, Wilkinson, and Kahn, 1973), and "pixel" (Silva, 1978).

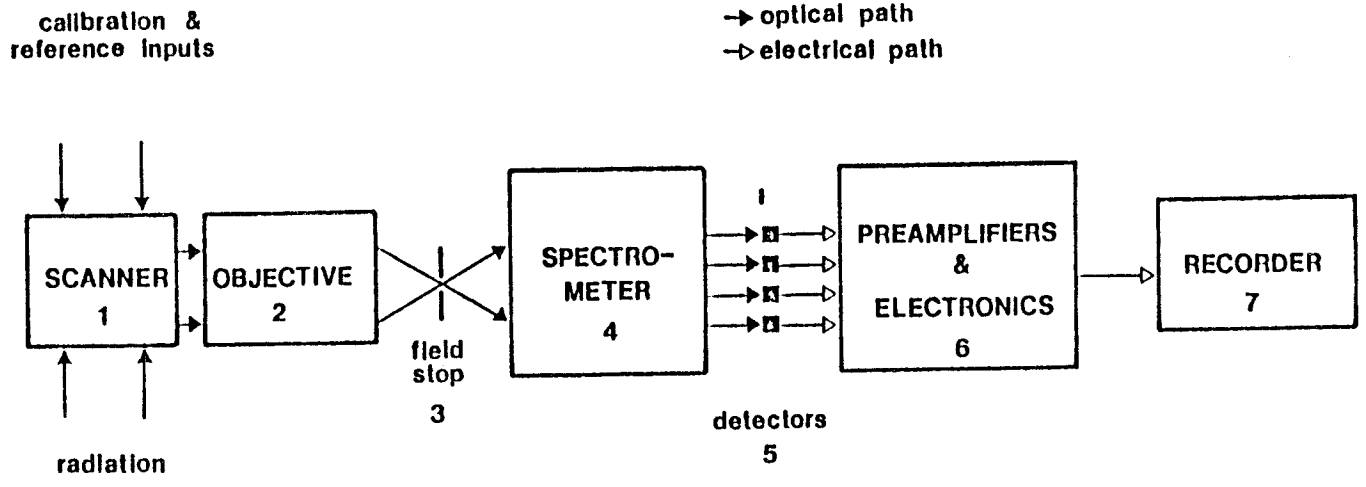

1) usually a scanning mirror
2) usually a paraboloidal mirror
3) defines input field-of-view
4) usually a prism and grating disperser
5) converts radiant energy to electrical energy; at least one per spectral channel
6) digitizes and/or prepares electrical output for storage
7) usually magnetic tape

Figure 2.7 Schematic Diagram of the Components of a Generalized Multispectral Scanner System. (Higham et al., 1973).

instantaneous field-of-view (or angular width of field stop), which is based on the geometry of the system optics (see NASA, 1973; Baker and Scott, 1975; Townshend, 1980). The IFOV is computed by :

$$IFOV = D/f$$

where :

IFOV = instantaneous field-of-view (radians)
D = width of the detector
f = focal length of the collector

The ground projected IFOV is then provided by :

$$Rg = IFOV * H$$

where :

H = height of the imaging system above the earth surface.

This value for the ground projected IFOV alone is not indicative of the area of the ground surface acting as the source of the recorded irradiance measured at the satellite altitude. This area is effectively extended by the point spread function associated with each of the system components.

In an attempt to provide the remote sensing community with a standard definition for resolution, NASA (1973) stated that "the effective IFOV for a raster (sample data) system will be defined as

the RMS sum of the IFOV of the nonsampled system and the distance between samples". The effective instantaneous field of view (EIFOV) would then be provided by :

$$EIFOV = ((IFOV^{**}2 + D^{**}2)/2)^{**}0.5$$

and would result in an EIFOV smaller than the IFOV for distances between samples which are less than the width of the IFOV. This implies that oversampling increases the spatial resolution of the scanner system.

Slater (1979), while recognizing that the purpose of the oversampling (1.4 samples per IFOV) in Landsat data was to improve the spatial resolution of the imagery, states that the value obtained from the swath width divided by the number of samples per swath width (185590 meters/3183 samples = 58.3 meters per sample) " has been misinterpreted by some MSS data users to mean the area on the ground instantaneously sampled by a single detector". He states further, that "according to the system geometry, at any instant the ground-projected IFOV is 76 by 76 meters, ... at the nominal 918.6 km altitude. Neglecting the atmosphere, the output signal from the detector that is recorded on computer compatible tape is proportional to the radiance of this area plus the surrounding area included by the spread function of the optics". A forum (Colvocoresses, Thompson, and Slater, 1980) stimulated by Slater's article, demonstrated the lack of agreement as to the relationship between resolution and other system factors, particularly the frequency at which the analog signal is sampled in the digitization process (6). Thompson provided a series of electronic

signals depicting the degradation of an ideal target through the system to the stage of analog signal output. He states that "sampling 1.4 times per IFOV does not improve resolution, but it does improve the information content of the data". That is, the area on the ground represented by a single recorded response level vector is unaffected by the sampling frequency, but the higher sampling frequency does provide more information about the amplitude variations of the analog signal. Townshend (1980) compiled a table demonstrating the range of values published in reference to the resolution of the current Landsat MSS. These values range from 66 meters, for the half cycle of the point spread function, to 135 meters, for the full cycle of the point spread function. Slater's (1979) concluding remarks provide an appropriate summary of the complexities involved in specifying the spatial resolution for a MSS system. He states :

> "to determine the spatial resolution and radiometric response of the Thematic Mapper, we have to know the system geometry, the profile of the point spread function of the system and it's variation with wavelength and field angle, the variation in responsivity across the area of each detector, the in-track and across-track sampling intervals, and the effect of electronic filtering of the signal from each detector."

---

(6) Other factors discussed which affect the resolution are : the rise and fall times (9 microseconds) of the three-pole low-pass Butterworth filter through which the output signal passes, the effect of the image being scanned over the detector, and the angular diameter (33 microradians) of the point spread function of the MSS.

Previous Work

Investigations of the relationship between the spatial resolution of MSS data and computer-based classification performance indicate that lower classification accuracies are to be expected when employing higher spatial resolution data (Kan and Ball, 1974; Sadowski and Sarno, 1976; Clark and Bryant, 1977; Landgrebe, Biehl, and Simmons, 1977). This relationship appears to be dependent on the variability of the spectral classes associated with each particular cover class and the resultant degree of overlap or statistical similarity among the spectral classes (i.e., the set of class densities parametrically representing the spectral classes). The relationship is also very dependent on the training techniques and the characteristics of the algorithm employed in the classification.

Kan and Ball (1974) conducted a theoretical and empirical evaluation of classification accuracies resulting from data of three different spatial resolutions. The theoretical work focused on the covariance matricies of cover classes associated with the data of different resolutions. They stated that for two data sets A and B, where each data element of B represented the same area on the ground represented by a k-by-k number of elements of data set A, the means and covariance matricies of A and B would have the following relationship:

$$\mu_A = \mu_B$$

$$C_A = C_B$$

where :

μ_A and μ_B are the mean vectors of the j(th) cover class for the data set A and B, respectively.

C_A and C_B are the covariance matrices of the j(th) cover class of data sets A and B, respectively.

They employed this relationship between the covariance matricies to predict classification accuracies using transformed divergence (7). The relationship indicated for the covariance matricies is actually an upper limit and ignores the effect of the spatial correlation of response levels demonstrated by Kettig and Landgrebe (1975), Mobasseri, et al., (1978), and Tubbs and Coberly (1978). This contrast in covariance matricies from data sets of different resolution is further reduced when the spectral classes are produced by a cluster analysis of groups of fields, or areas, of the same cover class. Clustering the data provides a means by which the within cover class variance can be reduced to a greater extent than that achieved by reducing the spatial resolution. The lower variance is due to the fact that clustering the data groups the response level vectors according to their spectral similarity. A group of pixels representing a contiguous area on the ground will not necessarily be assigned to the same cluster class.

---

(7) Transformed divergence is a statistical distance measure which employs the mean vectors and covariance matricies of the spectral classes to compute the "separability" among the class densities used to train the classifier. Provided certain assumptions are met, transformed divergence can be used to estimate probability of correct classification (see: Swain and King, 1973; Swain, Robertson, and Wacker, 1971; Wacker and Landgrebe, 1972; Latty and Hoffer, 1980).

Therefore, pixels of a higher spatial resolution corresponding to the ground area represented by a single pixel of a lower resolution will not necessarily be assigned to the same cluster class (Phillips, 1973).

Kan and Ball (1974) also conducted an empirical evaluation for data representing three different spatial resolutions (8). A supervised selection approach which provided one spectral class for each cover class was implemented to develop training statistics. The resulting "pairwise" classification accuracies were generally found to be higher for the coarser resolutions.

Sadowski and Sarno (1976) examined classification accuracies for 2 meter resolution data collected over a forested area in Texas, degraded to simulate 4, 8, 16, 32, and 64 meter spatial resolutions. Using training classes provided by a supervised selection approach and a per-point maximum likelihood classifier, they observed an increase in classification accuracy with decreasing spatial resolutions. Overall classification accuracies (based on test data) for each resolution varied according to the bases on which the cover classes were defined. Table 2.1 provides the accuracies by class criteria.

Sadowski and Sarno (1976) also conducted an accuracy assessment which involved boundary pixels. They found that probability of correct classification (PCC) for the coarser resolution data depends to a large degree on whether the accuracy assessment technique includes or excludes boundary pixels. Classification estimates are generally lower

---

(8) Original aircraft scanner (Bendix 24 channel MSS) data of a nominal resolution of 8 meters were degraded to provide data of approximately 16 meter and 24 meter resolutions.

Table 2.1 Classification Performance for each Resolution Determined for each Cover Class Criterion using Test Areas Exclusive of Boundary Pixels (from Sadowski and Sarno, 1976).

	Spatial Resolution						
	$(2M)^2$	$(4M)^2$	$(8M)^2$	$(16M)^2$	$(32M)^2$	$(64M)^{2*}$	% of Total Area
Hierarchy: Condition Class							
Conifer Regen. (2.3)	49.9	54.8	59.3	64.6	71.4	78.6	37.3
Loblolly-Imm. (2.5)	26.3	32.3	39.1	49.6	56.8	---	3.8
Loblolly-Mature (2.6)	19.7	19.2	20.9	26.6	19.4	31.0	13.8
Shortleaf-Imm. (1.3)	33.3	24.2	23.8	22.7	31.6	39.5	29.6
Shortleaf-Mature (1.4)	40.8	54.4	57.2	63.3	73.0	82.1	15.4
Overall	38.5	40.0	42.4	46.2	52.2	59.9	
Hierarchy: Growth Stage							
Conifer Regen. (2.3)	49.9	54.8	59.3	64.6	71.4	78.6	37.3
Imm. Sawtimber	50.7	45.0	48.6	50.2	53.5	40.2	33.5
Mature Sawtimber	40.9	46.5	47.5	52.6	54.2	59.3	29.2
Overall	47.5	49.1	52.3	56.3	60.7	61.9	
Hierarchy: Cover Type							
Conifer Regen. (2.3)	49.9	54.8	59.3	64.6	71.4	78.6	37.3
Shortleaf Pine	64.4	62.6	60.6	61.6	67.0	80.0	45.1
Loblolly Pine	38.0	41.1	46.0	53.4	42.4	33.3	17.6
Overall	53.9	55.8	57.6	61.1	64.6	71.8	
Hierarchy: Physiognomy							
Conifer Regen. (2.3)	49.9	54.8	59.3	64.6	71.4	78.6	37.3
Pine Sawtimber	82.7	81.5	82.3	84.7	82.8	80.4	62.7
Overall	70.5	71.4	73.6	76.8	78.3	79.6	

* The $(64 \text{ meters})^2$ data set did not contain a signature for Immature Loblolly Pine (2.5).

when boundary pixels are included in the evaluation as compared to estimates obtained without boundary pixels. However, differences in performance estimates between those evaluations including boundary pixels and those excluding boundary pixels are smaller for higher resolution data than they are for lower resolution data. The accuracy estimate provided by the technique including boundary pixels indicated a higher PCC for the 32 meter data as opposed to the 64 meter data for classes based on growth stages and physiognomy.

The lower PCC generally associated with the higher spatial resolution was identified as resulting from the higher variances of the training classes in the higher resolution data. In subsequent work Sadowski and Malila, (1977) and Sadowski, et al., (1977), using large scale color infrared photography (1:4000 scale), identified and developed statistics for spectrally dissimilar components for each of the cover classes. From an area composed of five different cover classes they identified twenty four component spectral classes. To examine the hierarchy of the class separabilities they employed a sequential "signature" merging process based on the pairwise similarities between class densities. The similarity measure used was the average ranking of three criteria; the Bhattacharyya distance, the combined determinant, and the resultant combined trace (9). The sequence in which the class pairs were merged provides insight as to

---

(9) The Bhattacharyya distance is discussed in Wacker and Landgrebe, 1972; Kailath, 1967; Swain and King, 1973; Swain, Robertson, and Wacker, 1971; and Swain, 1978. The combined determinant is a component of the Jeffries - Mattusita distance (Wacker and Landgrebe, 1972) and the resultant combined trace is a component of the divergence measure (Swain and King, 1973).

which spectral classes would be involved most frequently in misclassifications. Confusion, or low separability, between spectral classes of different cover classes increases the probability of error in cover type classification. The first four occurrences of merging involved the shadowed understory classes from the five different cover classes, indicating that the highest relative frequency of misclassification would involve these spectral classes. The confusion between shadowed areas of different cover classes was suggested as being a major factor associated with the lower classification performances achieved with the higher resolution data.

Sadowski and Malila (1977) conducted further work in forest canopy spectral component analysis which lead them to develop a two stage classification approach, using the percent composition by spectral component of a block of pixels, to classify the pixels. Overall classification performances (based on test points) exceeded 80 percent using the two stage technique, as opposed to 40.5 percent for the conventional per-point classification technique. Further work in multi-element rules for classification followed these efforts (Sadowski, et al., 1977).

Classification performance in land use analysis of an urban environment was evaluated by Clark and Bryant (1977) using supervised training techniques and a Baysian per-point classifier. They worked with 15, 30, and 60 meter resolution data sets which were degraded from original 7.5 meter resolution aircraft MSS data. They observed an increase in class variance and a general decrease in classification performance with increasing spatial resolution.

Landgrebe, Biehl, and Simmons (1977) examined classification accuracies obtained using 30, 40, 50, and 60 meter degraded resolutions computed from aircraft MSS data with an original 6 meter resolution. The data were obtained over agricultural areas in Kansas and North Dakota. They observed an increase in classification accuracy as spatial resolution was decreased when performance was evaluated using the conventional in-place, pure pixel evaluation criterion (10). They conducted another performance evaluation using RMS (root mean square) error associated with the area estimates obtained using each spatial resolution (11). Accuracy based on RMS error was found to decrease with decreasing spatial resolution. The differences between resolutions were significant at the 0.05 Alpha level. These evaluations indicate that while in-place classification accuracies increase with decreasing spatial resolution, the accuracy of area estimation decreases with decreasing resolution.

Landgrebe et al., (1977) also investigated the in-place, pure

---

(10) Overall classification accuracies estimated from test fields ranged from about 88% for 30 meter resolution data to about 92% for the 60 meter resolution data.

(11) RMS (root mean square) error is computed by:

$$\varepsilon_{RMS} = \left[\frac{\sum_{i=1}^{n} (P_i - P_i')^2}{n} \right]^{\frac{1}{2}}$$

where :

P_i = percent of the area classified as class i by the computer-based classification.

P_i' = percent of the area in class i estimated from ground reference data.

N = number of information classes from ground reference data.

pixel classification peformance obtained using a classifier which uses the variance of spectral response in conjunction with the mean spectral response level from a cell of pixels in the assignment of a class label to the pixels of the cell (12). Classification performance was found to be very similar to those obtained with the per-point classifier, however, a noticable difference was observed between the two classifiers for the higher spatial resolution data.

The results obtained by Landgrebe et al., are of particular value in the context of the spectral variability associated with forested areas. Forested areas tend to have more spectral variability (a component of what photo interpreters refer to as "texture") than do agricultural areas, and would therefore be expected to result in greater differences between classification accuracies achieved with and without information as to the variability of the spectral response.

A study by Thomson et al., (1976) indicated that the difference in classification accuracy, based on RMS error, among different spatial resolutions was dependent on field size. In areas of small field sizes (i.e., 1-10 hectares), area estimations provided by coarse resolution data were much less accurate than estimates provided by higher spatial resolution data. The difference in accuracy of area estimation was found to decrease with an increase in average field size and tended to level off with fields of 80-120 hectares in size.

Morgenstern et al., (1977) conducted a study examining

---

(12) The classifier is referred to as the ECHO ("Extraction and Classification of Homogeneous Objects") Classifier (see: Kettig and Landgrebe, 1975; Kast and Davis, 1977).

classification performance with respect to field size and data resolution using a mensurational criterion (e.g., the RMS error). This study confirmed the previous results of Thomson et al., (1976) and Landgrebe et al., (1977). Morgenstern et al., concluded, "the trend to improved proportion estimation accuracy at finer spatial resolution ... is felt to be primarily because relatively fewer boundary pixels would occur for data at the finer spatial resolutions".

To summarize, the studies conducted to date consistently indicate several points.

(1) Classification performance based on in-place classification accuracy of pure pixels decreases with increasing or finer spatial resolution when a per-point classifier is employed. This relationship between classification performance and spatial resolution is considered to be due to the larger within class variance, and consequent higher statistical similarity between spectral classes of different cover classes, associated with the finer resolutions.

(2) Classification performance based on RMS error (i.e., a mensuration criterion) improves with higher spatial resolution when a per-point classifier is employed. This relationship is considered to be due to the greater relative frequency of boundary pixels for coarser resolution data. The relative frequency of boundary pixels for any given spatial resolution is escalated for areas of smaller field sizes.

(3) The difference between classification accuracies across different spatial resolutions tends to be greater for forested areas than for agricultural areas. This is believed to be due to the greater spectral variability of forested areas as opposed to that of

agricultural areas. A component of this spectral variability is analogous to what photo interpreters refer to as "texture".

(4) Improvements in classification performance, based on the in-place, pure pixel criterion, appear obtainable through the use of classifiers which employ the spatial variability of spectral response in the decision logic of class assignments.

Classifiers

The classifier is basically that part of the entire data processing sequence which ascribes class labels (and perhaps probabilities or some other measure) to the pixels being classified. The characteristics of the algorithm employed in the classifier determine how the data will be used in the process of label assignment. The relationship between the data and the components of the scene are the bases on which classifier algorithms are structured. Any algorithm which more fully exploits the relationships between the data and the components of the scene would be expected to more accurately identify the components of the scene. The two approaches examined here belong to two broad categories of classifiers. The per-point category employs information from a single vector in the process of assigning a label to that vector. The per-field category employs information from a cell of spatially adjacent spectral response vectors in the process of assigning the labels to the members of the cell (13).

---

(13) The per-field category is actually a specific form of "sample" classifier. Approaches which classify groups of pixels which are not necessarily spatially adjacent are addressed under the more general term, "sample" classifiers (Wacker and Landgrebe, 1971; Wacker and Landgrebe, 1972).

Per-point Gaussian Maximum Likelihood (GML) Classifier

The per-point GML classifier is a widely used classifier in remote sensing applications. The per-point approach is based on the assumption that the pixel is a random observation. The degree to which the properties of the data deviate from this condition is the degree to which the per-point classifier ignores other sources of information about the scene. The GML classifier employs the measured reflectance characteristics of each cover class, ωj, for all classes ($j = 1,...,m$) to identify any given spectral response measurement, X, as belonging to one of the "m" cover classes. The quantification of detected irradiance returned to the altitude of the scanner platform provides the spectral response measurement. The detection of irradiance in "n" different portions of the electro-magnetic spectrum provides a n-dimensioned vector representing the projected ground area. The expected error rate in classifying the response vectors is minimized by selecting the most probable class label in the context of the available information. By taking a sample of pixels from areas representing each cover class, the mean vector and covariance matrix for each cover class can be estimated. These are then used to estimate the probability density functions representing the distributions of each cover class in terms of the spectral response measurements. The Baye's optimal GML approach allows the use of a priori probabilties of class occurrences in conjunction with the estimated PDF's. These a priori probabilities may or may not be available.

Two further assumptions are made in order to employ the GML classifier. The n-variate spectral response vector is assumed to be absolutely continuous, in order to represent the spectral classes with the estimated probability density functions (PDF's). Since the electrical signal resulting from the irradiation of the detectors is quantified to a word length of generally six to eight bits (resulting in only 68 to 256 response levels, respectively), the response vector is not a continuous variable. The degree of this deviation from continuity, however, does not appear to disrupt the performance of the GML approach (Swain, 1978).

The distribution of the response vectors associated with each cover class is also assumed to be multivariate normal (MVN). This is rarely the case, since most cover classes exist in nature in a wide range of conditions and therefore result in variable spectral characteristics (see Hoffer, 1978; Stoner, 1979; Wooley, 1971; Kumar and Silva, 1974). This problem is usually rectified by "clustering" the response level vectors into MVN distributed "spectral classes". Cluster analysis basically subdivides the sample into sub-samples, the members of which are determined by their mutual spectral similarity (see Swain, 1972; Duda and Hart, 1973; Phillips, 1973; Swain,

---

(14) The cluster analysis of LARSYS *CLUSTER employs an assignment criteria based on the minimum Euclidean distance between each pixel and the "iterated" mean. This assumes equal within class variances in each channel or waveband employed. The deviation from equality among these variances results in spectral classes with larger variances in those channels which would otherwise display relatively small variances. This problem is demonstrated in the work on quantification level by Bartolucci and de Castro (1979), and work in relative scale of different data types by Anuta and Chu (1979). An iterative estimation

1978)(14). The result of cluster analysis is that the "m" cover classes are now represented by a set of "p" spectral classes, where p > m in almost every case (rarely does p = m). Clustering is conducted to provide classes with "unimodal" distributions which do not deviate substantially from the normal distribution.

The assumption of normality now being met by the sample distributions, and assuming a sufficient quantification level (i.e., word length) of the response vector to allow representation of the spectral classes by their estimated PDF's, the decision rule for vector classification is :

Decide the response vector Xi belongs to the spectral class $\omega'j$, if and only if :

$$p(\omega'_j \mid X) \quad p(\omega'_j \mid X)$$

for all i = 1,...,j-1,j+1,...,p.

Where :

$p(\omega'_j \mid X)$ = the conditional probability of the occurrence of the j(th) spectral class, given the occurrence of the response vector X (see Appendix A for a more detailed mathematical formulation).

Note : This rule is a general formulation of the more commonly encountered presentation of each cover class as being represented by a single spectral class (Swain, 1972; Swain, 1978).

A problem arises when a single spectral class represents two or more individual cover classes, or when two spectral classes of different cover classes are so similar that they cannot be reliably

---

of relative weights for each channel, with which to conduct the next "macro" iteration, is needed to explore ways to improve this step of the analysis.

discriminated. This condition was one of the reasons provided by Sadowski and Sarno (1976) for the low classification accuracies achieved with the per-point classification of high spatial resolution data over forested areas. Measured levels of irradiance returned from the shadowed areas between tree crowns were very similar for all forested cover classes. Therefore, the assignment of the correct cover class label to any given single pixel, will depend on what area (e.g., shadow, ground cover, illuminated crown, etc.) within the cover class the response level represents. The problem can be thought of as an interaction effect of resolution and structural similarities between different cover classes. These structural similarities often result in spectral similarities, as exemplified by forested cover classes (15). of similar structure, when the distances across the objects (or simply areas of differing reflectances) composing the cover classes are large relative to the ground resolution of the scanner system, the separability among spectral classes of different cover classes is expected to decrease. This spatial frequency of spectral variability is a form of information, but its influence in the context of per-point classification is that of noise (Landgrebe, 1978). The attempt to make use of the information in the spatial frequency of the spectral

---

(15) Structural similarities refer to the similarities in the spatial distribution of spectrally different areas within the cover class. The occurrence of gaps between the crowns of trees in forested areas, for example, constitutes a structural similarity between different forest cover classes. Structural similarities may result in spectral similarities, depending on solar elevation. For azimuthal solar angles of zero, the degree of spectral similarity resulting from the gaps between the tree crowns would be greatest for zenith solar angles greater than the arctan of the tree height divided by the gap width.

variability inherent in the scene is the potential advantage of the per-field classifiers.

Per-Field Classification

The entire idea of converting spatially discrete response levels to cover class information is premised on the size of the cover class as being larger than the size of the pixel. Data from a cell of pixels (ie., a group of spatially adjacent pixels) can be effectively employed in classifying the pixels where the cover class is much larger than the pixel. The relationship between adjacent pixels can be formalized as the conditional probability, $p(\omega j(x,y)|\omega j(x-0,y-1))$, of observing cover class ωj at the pixel coordinates of (x,y), given the occurrence of ωj at the coordinates (x-0,y-1). The higher this probability is relative to its compliment, the more appropriate is the per-field approach. Kettig and Landgrebe (1975) demonstrated this statistical dependence through the use of the "spatial correlation" of spectral response. The level of correlation between response vectors from adjacent pixels was developed from samples within various cover classes. This spatial correlation coefficient tends to be higher for cover classes which demonstrate small amounts of "texture" (e.g., corn). The coefficient drops off very rapidly for cover classes with higher levels of texture (e.g., forested areas). They also demonstrated that the coefficients for adjacent pixels in the across track dimension were consistently larger than those in the along track dimension. Subsequent work by Mobasseri, et al., (1978) confirmed these results. Theoretically, the across track spatial correlation would tend to be greater in

circumstances where the signal digitization sampling rate is greater than the scan rate, thereby resulting in adjacent pixel overlap. The across-track pixel overlap in Landsat data is approximately 28 percent, according to Slater (1979). While the applicability of the per-field approach is dependent on the cover class being much larger than the pixel, the advantage of per-field classification is premised on the spatial frequency of spectral variability within a cover class being lower than the spatial frequency of pixels. From the previous discussion on spatial resolution, it should be apparent that the spatial frequency of pixels is an expression of the spatial resolution. In fact, employing coarser resolutions is merely the use of a per-field classifier where the averaged response level of the cell (i.e., the spatially adjacent set of pixels) is used in classifying the pixels of the cell (16). A considerable amount of potentially useful information is being ignored by such a technique.

The classification of pixels through the per-field approach involves two tasks. The first task is defining the fields, or blocks, of data in the scene which contain a single cover class. This step of the process is often refered to as "image partitioning" (Robertson, 1973; Robertson, et al., 1973; Wacker and Landgrebe, 1972). The second task is to classify the field of pixels.

---

(16) Recall, another very important variable affected by the spatial resolution of the MSS system is the signal-to-noise ratio (S/N). This was considered to be a major determinant in the classification accuracies across the different resolutions examined by Landgrebe, et. al., (1976). This work involved data from a predominantly agricultural scene, where the within class spatial frequency of spectral variability is rather low. For a presentation of the system components of S/N see NASA (1973), Silva (1978), and Slater (1975).

Image Partitioning. Kettig and Landgrebe (1973) distinguished between two groups of algorithms employed in the image partitioning phase. The "boundary seeking" approach generally locates partition boundaries through the use of gradient analysis, Laplacian operators, digital filters, or some related technique (Gupta and Wintz, 1973). Most boundary seeking algorithms do not guarantee closed boundaries, and therefore fail to provide well defined samples. The second group is often refered to as "object seeking". These are designed on the premise that objects, or areas of the same cover class identity, express a higher level of spectral homogeneity than do areas containing a boundary. Object seeking algorithms have been treated by Robertson, et al., (1973) as being one of two types. "Conjunctive" algorithms are those which begin with a small object and combine or annex adjacent areas which display a certain level of statistical similarity. "Disjunctive" algorithms begin with a large object and subdivides it until each partitioned area satisfies some level of spectral homogeneity.

Object seeking algorithms are often the prefered approach, since they provide a closed boundary and, therefore, a defined sample or field. However, the dependence on a homogeneity criterion restricts the application to those cases where the tonal variability associated with any given cover class is less than the tonal variability associated with a boundary between any pair, or set, of cover classes. A considerable effort has been focused on developing classification techniques using measurements and characteristics of tonal variability

associated with the various cover classes. An excellent review of some of this work is provided by Haralick (1979). He categorized the work into eight subdivisions : autocorrelation functions, optical transforms, digital transforms, textural edgeness, structural elements, spatial gray tone cooccurrence probabilities, gray tone run lengths, and autoregressive models. In the classification of forested areas, the utility of computations based on the level and nature of tonal variability is well demonstrated by the work of Triendl (1972), Herzog and Rathja (1973), Haralick and Shanmugam (1974), and Iisaka (1979). Wiersma and Landgrebe (1976) conducted a comparative evaluation of cover classification accuracies achieved with four different textural measurements and the ECHO classifier (which employs the conjunctive, object seeking approach). Their results indicated that ECHO resulted in somewhat higher classification accuracies than any of the four texture measures examined. The study employed Landsat data with a nominal spatial resolution of 79 meters. The "cost" of using homogeneity thresholds in terms of classification accuracy and detail when higher spatial resolution data is employed remains in question. The use of homogeneity thresholds may well limit the use of the level and spatial frequency of tonal variability in per-field classification.

Other approaches to image partitioning have been developed. One such approach involves the clustering of spatially weighted response vectors (Kauth, et al., 1977). By spatially weighting the response vector with the line-column coordinates of each pixel, the probability of neighboring pixels to be assigned to the same class is greatly enhanced. Kast and Davis (1977) recognized the potential application of this approach to image partitioning for subsequent sample

classification. Wacker (1969) examined another similar clustering approach.

Classifying the Fields. Once the image has been partitioned into fields of a single identity, the fields must be classified. Wacker (1971) and Wacker and Landgrebe (1972) provide an extensive survey of the "minimum distance" (MD) classifiers. These are based on some measure of statistical distance, or measure of dissimilarity, between probability density functions. The estimated PDF of the field being classified is compared to the PDF of each spectral class representing each of the cover classes. The spectral class with which the field is most similar is the class to which the field is assigned. A problem with the MD approach is that in order to estimate the multivariate PDF, the number of observations provided by the field must be greater than the dimensionality of the observation. That is, the number of pixels in the "field" must be greater than the number of wavebands employed in the analysis. While the computation of the covariance mathematically requires at least as many observations as wavebands, the number of observations to provide a reliable estimate of the covariance increases exponentially with the number of wavebands. This restriction often prohibits the use of the MD approach to per-field classification. This is the well known problem of dimensionality (see Duda and Hart, 1973).

An extension of the GML approach is presented by Kettig and Landgrebe (1975) for use in classification of the partitioned fields.

The relationship to the GML classifier can be seen from the following expression :

$$p(X|\omega_j) = \frac{1}{2\pi^{d/2}|C_j|^{d/2}} \exp\left(-\tfrac{1}{2} \sum_{j=1}^{n} (X_j - \mu_i)C_i^{-1}(X_j - \mu_i)^T\right)$$

Where :

X_j = the j(th) pixel of the field,
μ_i = the mean of the i(th) spectral class,
C_i = the covariance matrix of the i(th) spectral class.

The class to which the field is assigned is that class for which $p(X|\omega'j)$ is greatest. Where "n" equals one, the rule simplifies to the per-point classifier. This provides a test which can be used even if the homogeneity test is failed, and the pixels of the cell are to be classified individually. While the above extension of the GML classifier does not employ the covariance associated with the cell in classifying the cell pixels, it is sensitive to the spectral distribution of the cell. The practical advantage is that there are no cell size restrictions on the GML computation. The disadvantage is that it does not provide discrimination between cells of equal means but different covariances.

The ECHO Classifier : the Supervised Mode

The supervised ECHO classifier is used in this study to examine relative classification performances achieved with a per-field approach compared to those achieved with a per-point approach. The particular means of image partitioning, and subsequent field classification,

employed in ECHO are provided as a basis for understanding the results.

The image is partitioned by first testing whether a cell of pixels is homogeneous. In the supervised mode this involves computing a statistic, Qj(Y), and comparing it to some threshold, where :

$$Q_j(Y) = \text{tr}\left(C_j^{-1} \sum_{i=1}^{m} Y_i Y_i^T\right) - 2M_j^T C_j^{-1} \sum_{i=1}^{m} Y_i + m \cdot M_j^T C_j^{-1} M_j$$

where :

C_j = the covariance matrix of the j(th) spectral class.
M_j = the mean vector of the j(th) spectral class.
Y_i = the i(th) response vector in the cell being tested.
m = the number of vectors in the cell being tested.

The cell is considered homogeneous if Qj(Y) < c, where c is the prespecified threshold. The homogeneity statistic, Qj(Y), is multivariate in that it reflects the property of the cell in all channels, but it does not require the computation of the covariance of the cell. Therefore, the statistic does not suffer cell size constraints resulting from the dimensionality problem. This homogeneity test not only rejects those cells which are not homogeneous, but also rejects those cells which do not resemble the spectral classes provided by the training data. This statistic (Kettig and Landgrebe, 1975B) also has the distribution function P(Qj(Y) > c W'j), which is chi-square distributed with "mn" degrees of freedom (16). This provides a basis for selecting a value for the homogeneity threshold, c.

---

(16) Recall from equation 3.2, m = the number of vectors in the cell, and n = the number of wavebands in the measurement vector.

If the cell is found not to be homogeneous then each pixel of the cell is classified individually. If the cell is found to be homogeneous it is then compared, in a serial fashion, to the adjacent cells for possible annexation. That is, the cell is annexed to the first adjacent cell, or field, to which it bears a certain minimum level of similarity. The "similarity" is computed by the "likelihood ratio" (Kettig and Landgrebe, 1975B), Λ, where :

$$\Lambda = \frac{\max_i p(X|w_i') \; p(Y|w_i')}{\max_i p(X|w_i') \; \max_i p(Y|w_j')}$$

where :

max $p(X|w'i)$ = the probability of observing the vectors of cell X, given spectral class w'i, for which the probability is maximum relative to all w'k, k = 1,...,p.

$p(Y|w'i)$ = the probability of observing the vectors of cell Y, given spectral class w'i.

max $p(Y|w'j)$ = the probability of observing the vectors of cell Y, given spectral class w'j, for which the probability is maximum relative to all w'k, k = 1,...,p.

The two cells are annexed in the event $\Lambda \geq T$, for some specified threshold, T. It should be apparent, max $\Lambda = 1$, and is obtained where $j = i$. While Λ is a multivariate statistic, it avoids the dimensionality problem relative to cell size, since the covariance is provided by the spectral classes. The computation of Λ requires an exhaustive search among all spectral classes for the maximum probabilities for each cell.

This criterion, as does the homogeneity criterion, employs the

covariance of the spectral classes. The criterion, therefore, assumes a certain level of resemblance between the potential cells and the spectral classes. This feature may well disturb the partitioning process, depending on the degree to which the training data represents the area to be classified. The cell is annexed to the first cell or field for which $\Lambda \geq T$. A superior performance in this phase of the partitioning would be expected from a criterion where the criterion is "max Λ, given $\Lambda \geq T$" is used in annexing adjacent cells or fields. A flow chart depicting the image partitioning phase of the algorithm is presented in Figure 2.8. Once the individual fields have been established, they are classified.

The minimum distance classifiers employ the covariance of each field in classifying the field. The extended GML approach, however, does not use these covariances. The covariance of a cell or field is a multispectral component of the "texture" associated with the cell or field. In Haralick's terms (1979) it is but one of many measures of "tonal primatives" (i.e., some attribute characterizing the variation in tonal values associated with a set of pixels). The other major component is the "spatial organization of tonal variation in the set of pixels" (Haralick, 1979; see also Crowley, 1976). It may therefore be more appropriate to think of the ECHO/extended GML classifier as being more robust in the context of spectral variability than the per-point classifier, as opposed to actually using that spectral variability.

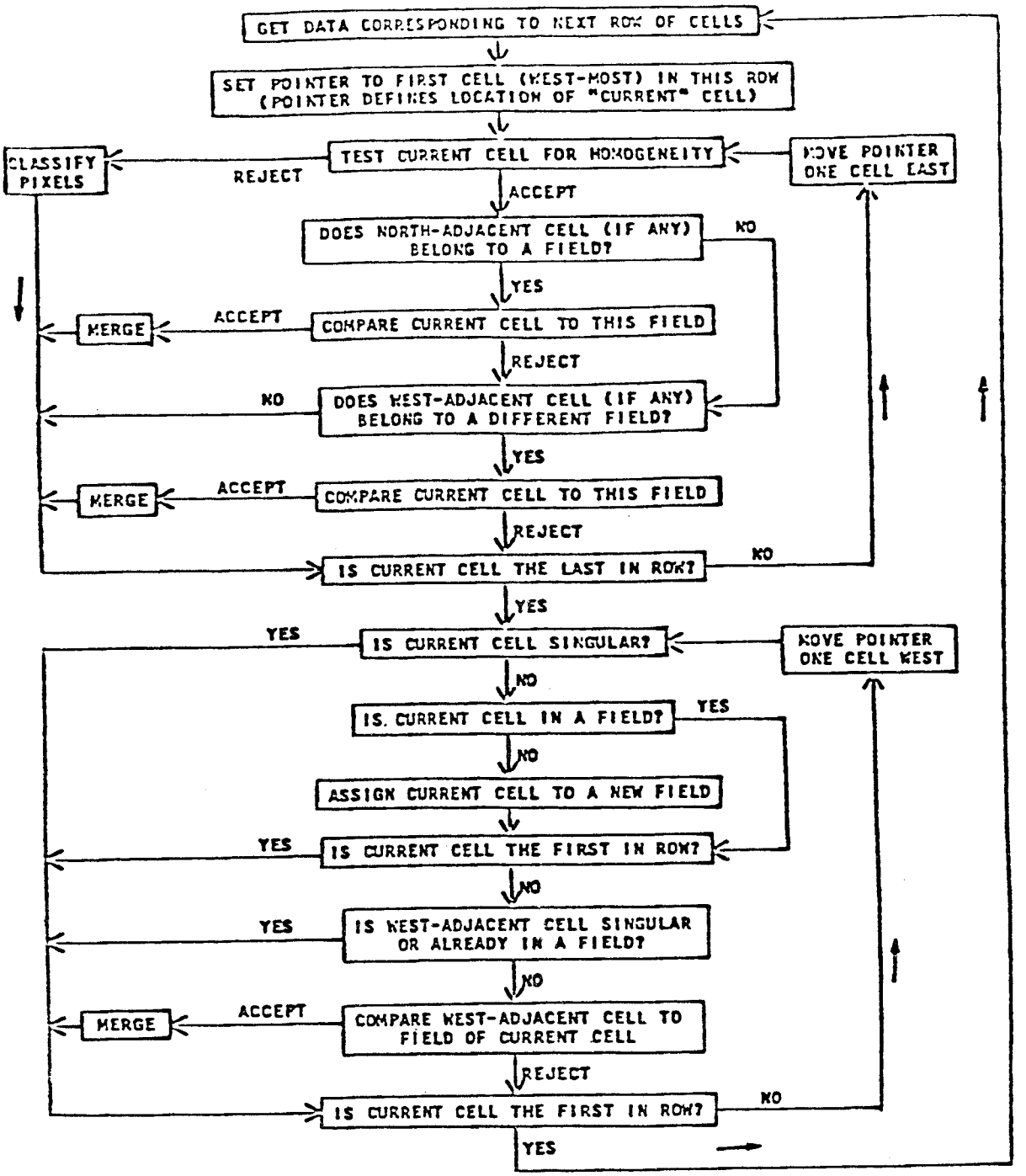

Figure 2.8 Flow Chart for the Image Partitioning Phase of the ECHO Classifier (Kettig and Landgrebe, 1975A).

CHAPTER 3

METHODS AND MATERIALS

Study Site Description

The study site is an approximately 186,000 acre area in central eastern South Carolina, situated on the escarpment between the Piedmont plateau and the coastal plain. The geographical location of the study site and the orientation of the flight lines are shown in Figure 3.1. The area changes from a heavily disected region of steep topographic relief in the north to a river bottom area of gently sloping terrain in the south. The soils of the northern area are deeply disected acid clays of low permeability. These grade into loamy sediments in the river bottom area to the south. Higher sand fractions characterize the upland soils of the south. The geomorphological diversity of the area provides environments resulting in a wide variety of vegetation cover classes. This same diversity of environmental factors also provides a wide range of conditions under which the various cover classes occur, resulting in a considerable variability of spectral characteristics associated with each cover class. These complexities make the area a prime choice for testing various remote sensing techniques employed in

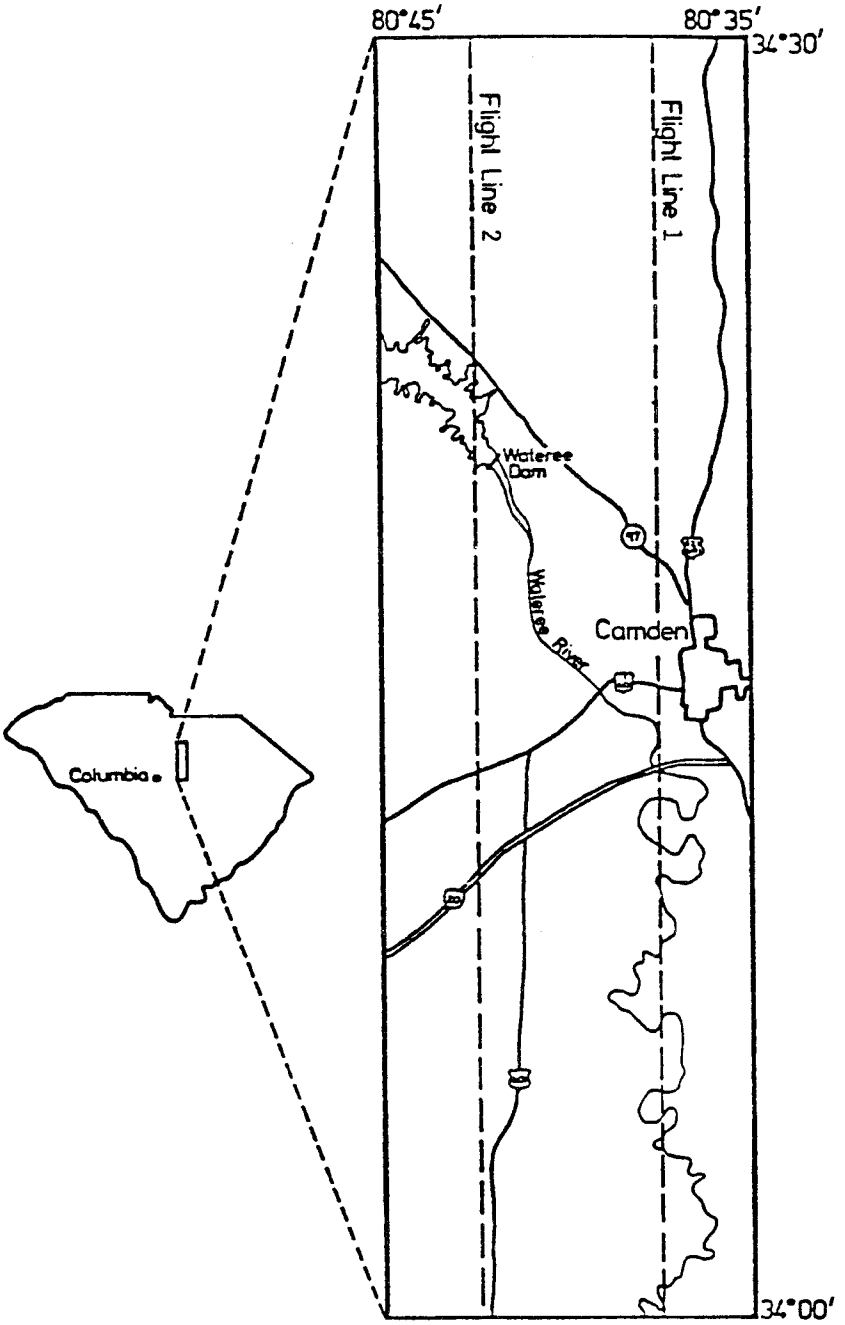

Figure 3.1 Geographical Location of the Study Site and the Position of the May 2, 1979 Flight Lines.

ground cover classification for land-use and plant cover type mapping. The site was selected by the U.S. Forest Service as a prime candidate for testing various remote sensing techniques for potential use in various phases of forest inventories.

The southeastern portion of the study area contains cover classes which occupy much larger contiguous areas than does the area to the north. This difference is well illustrated in the two aerial photographs contained in Figure 3.2. In the southeastern region, the flat to very gently rolling topography provides a minimum of environmental variability with the result that single cover classes occupy large contiguous areas. The exception is water tupelo which requires a narrow range of water fluctuation levels and therefore occupies rather restricted areas. The major cover classes of the southern area are bare soil, pasture, crops, pine, pine-hardwood mix, old age hardwood, second growth hardwood, water tupelo, clearcut areas, marsh vegetation and water. The bare soil areas are generally associated with agricultural activities or occupy areas in the more recent clearcuts. Areas in crops are associated with a wide variety of ground cover conditions, ranging from primarily bare soil to closed crop canopies, depending on the amount of time since planting. Similarly, the clearcut areas vary in ground cover condition depending on the length of the period since cutting. Areas of saturated soil and standing water in some of the clearcuts increase the diversity of spectral characteristics associated with that information class. A considerable diversity in age classes exist for the pine and pine-hardwood mix with a consequent range in canopy closures. Most of the

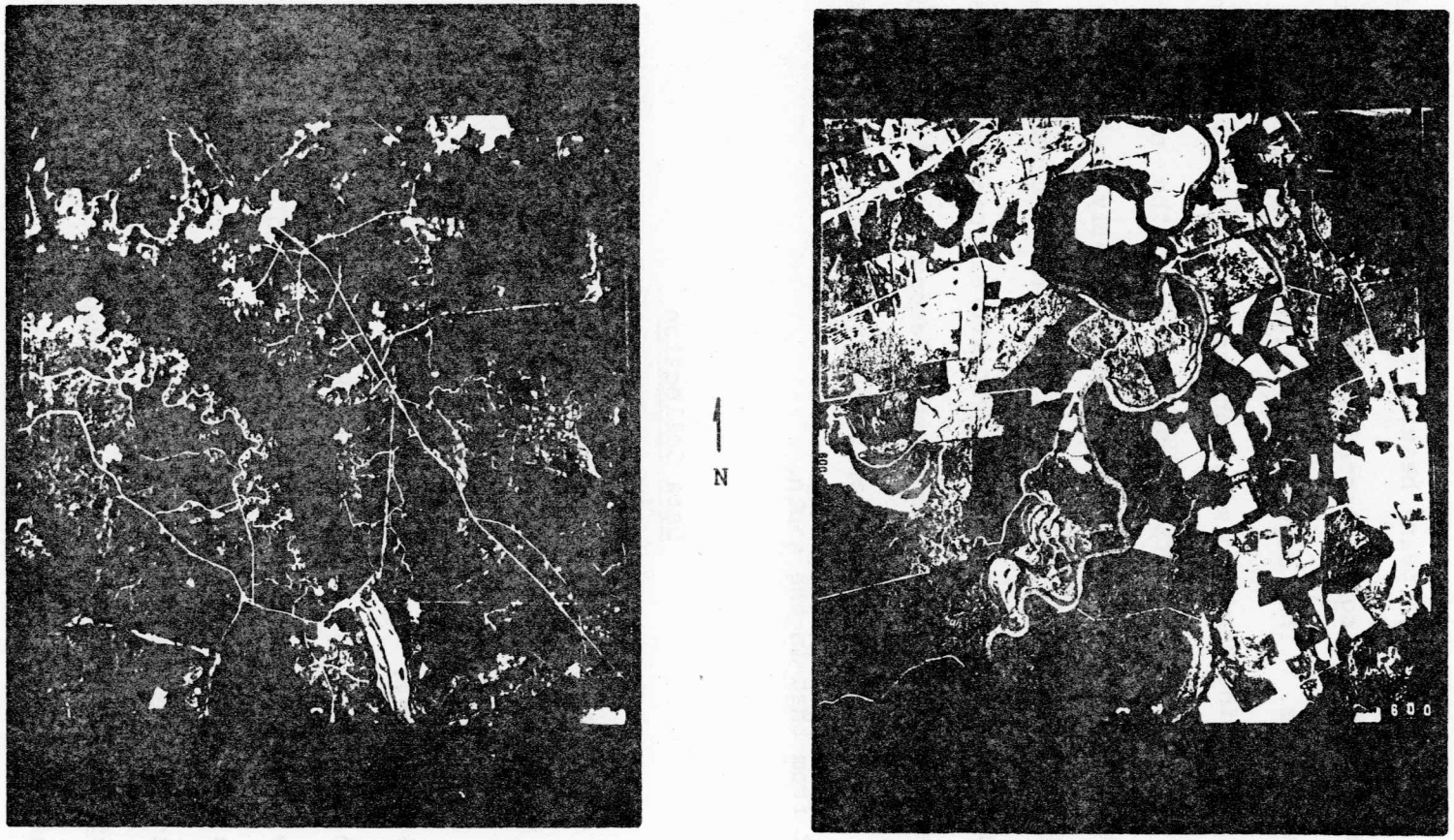

northwestern region
(CAM2N)

southeastern region
(CAM1S)

Figure 3.2 Reproduced Aerial Photography of the Two Major Regions in the Study Area. The images illustrate, the relative sizes of the contiguous areas occupied by individual cover classes for the two areas. Approximate Scale = 1:114,000.

area occupied by water in the test site is contained in the Wateree River, which is not much more than a Landsat pixel in width.

The northern area, being heavily disected and of relatively steep topography, contains cover classes which do not generally occupy large contiguous areas. The major cover classes are bare soil, crops, pasture, pine, pine-hardwood mix, hardwood, clearcut, water, and urban. The pine areas vary in crown closure more in the north than in the southeastern region. The hardwoods are generally restricted to narrow gully bottoms. Areas in crop and pasture are generally very small due to the size of areas suitable for agricultural practices. Most of the surface area in water is in the Wateree Reservoir, therefore providing a ratio of the frequencies of boundary-to-nonboundary pixels very different from that in the south.

Data Collection

The data employed in this study were collected by the NASA NS-001 Thematic Mapper Simulator (TMS) on May 2, 1979. The TMS data were obtained in mid-morning from an average height above ground of 19,500 feet (5,944 meters). Three flight lines were flown in a south to north direction. Color and color infrared photographs were taken at the same time the scanner data were obtained. Table 3.1 contains the specifications of the aerial photography. Table 3.2 provides a comparison of the characteristics of the NS-001 TMS system with the characteristics of the proposed Thematic Mapper (TM). The photographs and documented observations of ground conditions from two visits to the study area provided the ground reference data for the study. Only two

Table 3.1 Aerial Photography Specifications.

Flight line	Run time	Altitude (kft) MSL	Altitude (kft) MGD	Line miles	Ground speed
1	5 min	20	19.5	30	240 knots
2	5 min	20	19.5	30	240 knots
3	3 min	20	19.5	15	240 knots

Film type	Camera type	Filter #1	Filter #2	Shutter speed	Factor	ASA	Focal length	Forward lap	Side lap	Roll #
2443(CIR)	Zeiss	12	36AV	1/200	2	80	6"	65%	15%	14
S0397(C)	Zeiss	2A	36AV	1/400	2	160	6"	65%	15%	15

Table 3.2 Specifications of the NS-001 Multispectral Scanner System as compared to that of the Proposed Thematic Mapper System.

NS-001 Multispectral Scanner[1]				Proposed Thematic Mapper[2]			
Channel	Bandwidth (μm)	Low Level Input ($W \cdot CM^{-2} \cdot SR^{-1}$)	NEΔρ	Channel	Bandwidth (μm)	Low Level Input ($W \cdot CM^{-2} \cdot SR^{-1}$)	NEΔρ
1	0.45-0.52	8.7×10^{-6}	0.5%	1	0.45-0.52	2.8×10^{-4}	0.8%
2	0.52-0.60	6.8×10^{-6}	0.5%	2	0.52-0.60	2.4×10^{-4}	0.5%
3	0.63-0.69	5.0×10^{-6}	0.5%	3	0.63-0.69	1.3×10^{-4}	0.5%
4	0.76-0.90	4.4×10^{-6}	0.5%	4	0.76-0.90	1.6×10^{-4}	0.5%
5	1.00-1.30	6.0×10^{-6}	1.0%				
6	1.55-1.75	6.2×10^{-6}	1.0%	5	1.55-1.75	8.0×10^{-5}	1.0%
7[3]	2.08-2.35	4.7×10^{-5}	2.0%	6	2.08-2.35	5.0×10^{-5}	2.4%
8	10.4-12.5	NA	NEΔT=0.25°K	7	10.4-12.5	300°K	NEΔT=0.5°K

[1] Data was obtained from the "Operations Manual, NS-001 Multispectral Scanner," NASA; JSC-12715, April 1977.

[2] Data was obtained from Salomonson, 1978.

[3] Channel 7 (2.08-2.35 μm) was not operational at the time of the mission; all subsequent references to "channel 7" refer to the 10.4-12.5 μm waveband.

sections of the three flight lines were actually employed in this investigation, on behalf of time limitations. The third flight line was flown to provide an alternate data set in the event of cloud coverage over the preferred study site.

Data Preprocessing

The variation in viewing angle (i.e., +/- 50 degrees from nadir) inherent in low altitude scanner data, results in geometric distortions in the original data which hamper determining in-place location and area estimation. Changes in viewing angle relative to the angle of radiant energy incident on the scene can be a major source of variance in the recorded spectral response levels. The presence of both of these data characteristics due to variable viewing angle indicated the need for data adjustments prior to attempting to employ the data in experiments involving computer-based classification techniques. Internal calibration was not conducted due to the lack of information as to whether such calibration was previously conducted.

Geometric Adjustment

The objectives of the geometric adjustment activities were :

(1) to produce a data set which corresponded geometrically to the aerial photography and U.S.G.S. maps of the area, in order to facilitate the identification of training and test areas, and

(2) to provide a data set which will allow accurate area estimates from pixel summations.

The criteria used in evaluating the level of residual geometric

distortions remaining in the adjusted image were :

(1) consistency of scale in each dimension everywhere in the data set, and

(2) equivalency of scale between the two dimensions (ie., a fixed distance on the ground, represented by a determinable number of lines in the data, is to be represented by an equal number of columns).

The instantaneous field-of-view (IFOV) of the scanner, the average height above ground of the aircraft, and the change in scan angle corresponding to the analog signal sampling interval were employed to model the geometry resulting from the variable viewing angle. This provided a means of adjusting for the across-track distortions in the original image.

The nominal spatial resolution (the on-ground dimension of the pixel at nadir) for the NS-001 TMS flown at an altitude of 5944 meters is approximately 15 meters. The along-track scale of the imagery at nadir, relative to the nominal spatial resolution, was determined from control points located on the imagery and a 1:62500 scale U.S.G.S. map. The ground distance between the control points along the component parallel to the flight line (perpendicular to the scan lines) was determined from measurements made on the imagery and map. The ground distance divided by the number of scan lines between the two points yielded an average along-track distance per scan line of approximately 7.6 meters (17). The nominal spatial resolution divided by the average

---

(17) Fourteen different pairs of control points located along the flight line as near to the nadir as possible were employed to obtain the average distance per scan line.

along-track distance per scan line provides the scan rate. Scan rate values greater than one are overscan rates. Scan rates less than one are underscan rates. This data set had a scan rate of approximately two. To adjust for this source of distortion in the imagery, every other scan line was omitted as a part of the geometric adjustment algorithm. While overscan in an image provides an opportunity to improve data quality by averaging pixels of adjacent scan lines, an overscan of two is not sufficient for achieving these improvements.

The geometry of the image resulting from a variation in viewing angle (O) is related to the change in pixel dimension as f(O). The nominal pixel dimension at nadir is given by :

$$D(n) = A * IFOV$$

where :

D(n) = nominal pixel dimension at nadir
A = altitude of the scanner platform above the ground at nadir
IFOV = instantaneous field-of-view of the scanner (mrad)

The nominal pixel dimension at the scan angle (O) is then given by :

$$D(O) = (A * \sec O) * IFOV$$

The reduction in scale of the image with increases in the viewing angle is due to the fact that larger areas on the ground are being represented by a fewer number of pixels. Figure 3.3 is a dot matrix image showing the geometric characteristics of the original, or unadjusted, data set. The geometric adjustment algorithm also reversed the data line sequence to provide a data set with a line-column orientation corresponding to the compass coordinates. Figure 3.4 was

*

Figure 3.3 A Dot Matrix of a Portion of the Original, Unadjusted NS-001 MSS Data, Channel 5 (1.00-1.30 μm).

*Vertical line signifies the nadir column.

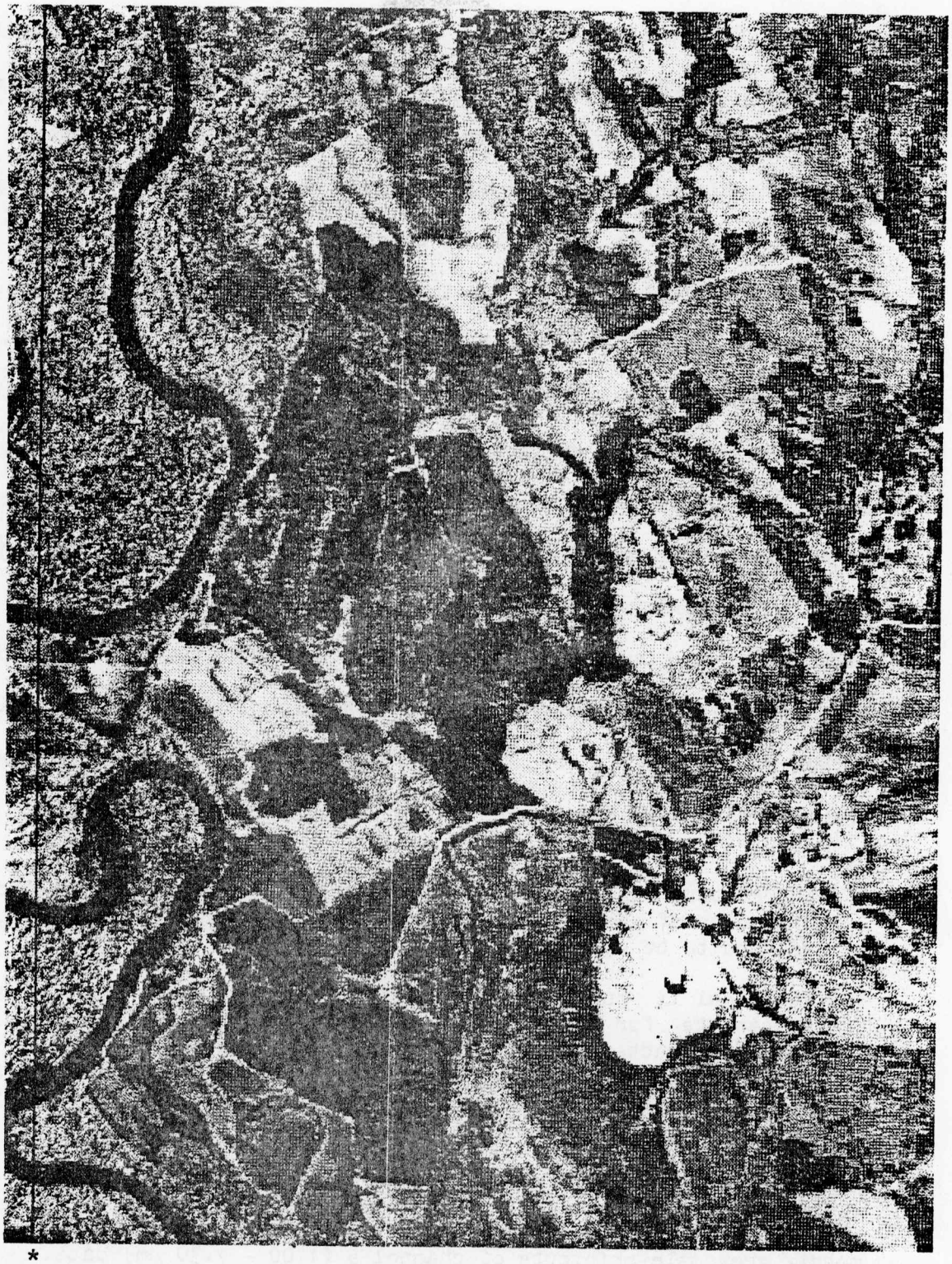

*

Figure 3.4 A Dot Matrix of a Portion of the Geometrically Adjusted NS-001 MSS Data, Channel 5 (1.00-1.30 μm).

*Vertical line signifies the nadir column.

generated from the geometrically adjusted data set (18). It should be apparent, by comparing Figures 3.3 and 3.4, that visually separable units become increasingly compressed in the across-track dimension with increasing distance from the nadir column in the image of the original data, as compared to the adjusted data.

The above relationship was implimented in a FORTRAN program which computes the dimensions for all pixels in a line of data. The nominal pixel dimension at nadir is then compared to the pixel dimension for each scan angle (O), which is sequentially incremented in units of the IFOV. The program constructs an array which supervises the duplication of response level vectors for the construction of each line of adjusted data. The geometry of all lines are assumed to be equivalent. The flow chart in Figure 3.5 demonstrates the functional behavior of the geometric adjustment algorithm (19). The algorithm was inserted in the DUPSUP subroutine in the LARSYS *DUPLICATERUN module. The general characteristics of the geometric adjustment routine are :

(1) The routine is based on a model which defines the location and dimension of each pixel, for each line in the data (the lines are assumed to be equivalent).

(2) The model is purely deterministic. There was no attempt made to compensate for the stochastic variations in the geometry (ie., image characteristics resulting from random roll, pitch, yaw, change in altitude of the aircraft, fluctuations in the rate of mirror oscillation, or variations in the ground speed of the aircraft).

---

(18) The images for both Figures 3.3 and 3.4 were produced as dot matrix greyscale printouts of channel 5 (1.00 - 1.30 um) data.
(19) A one-time computation of the supervisor array and indexing of a do-loop with the values of the array is the actual design of the program, but such a flow chart would not display the design of the algorithm with respect to the geometry of the original data.

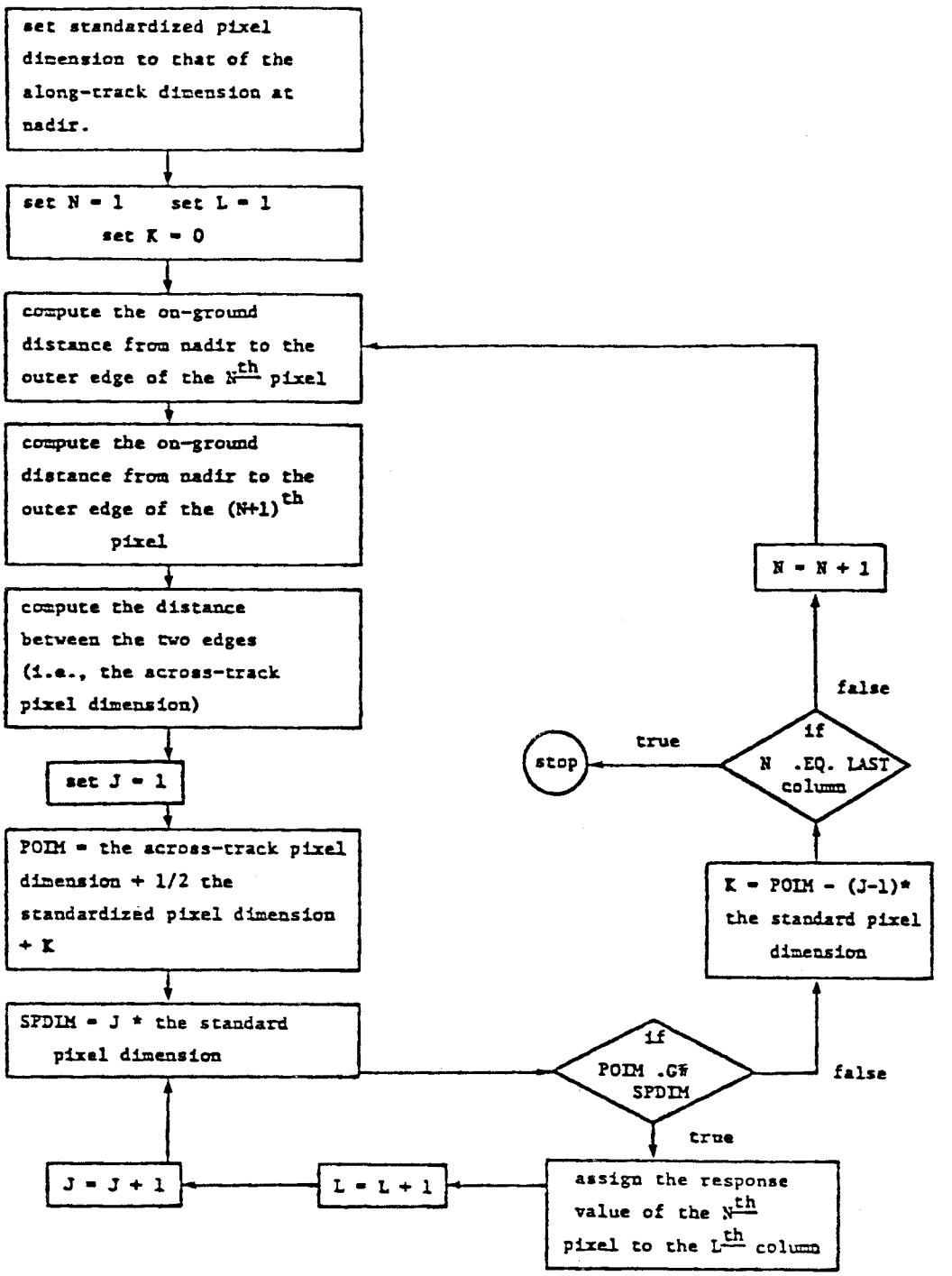

Figure 3.5 Flow Chart for the Geometric Adjustment Algorithm.

(3) The data set was truncated at the +/- 35 degree viewing angle (see Radiometric Adjustment for discussion).

(4) No data within the set defined by the bounding viewing angles were omitted.

The consistency of scale in each dimension, and the equivalency of scale between dimensions (ie., the along-track and the across-track dimensions) was evaluated by superimposing control points located on a 1:62500 scale U.S.G.S. map onto the adjusted imagery using a Zoom Transfer Scope. The coincidence of all control points indicated that the acceptance criteria were met. The data sets selected for analysis were then geometrically adjusted with the above technique.

Response Level Adjustment

The potential need for some degree of response level adjustment was evidenced by an along-track band of high reflectance across different cover types in the dot matrix imagery. The decision to adjust the response level was based on :

(1) classification results are dependent on the amount of variance in the response level associated with cover type differences;

(2) plots of the data and regression analysis employing response levels averaged over lines, by column, by channel, indicated a strong trend with respect to column (see Figure 3.6); and

(3) changes in reflectance associated with changes in viewing angle are considered sufficient to obscure reflectances otherwise correlated with cover type.

The objective in adjusting the response level of the data was to remove, or reduce to an acceptable level, the variance in response

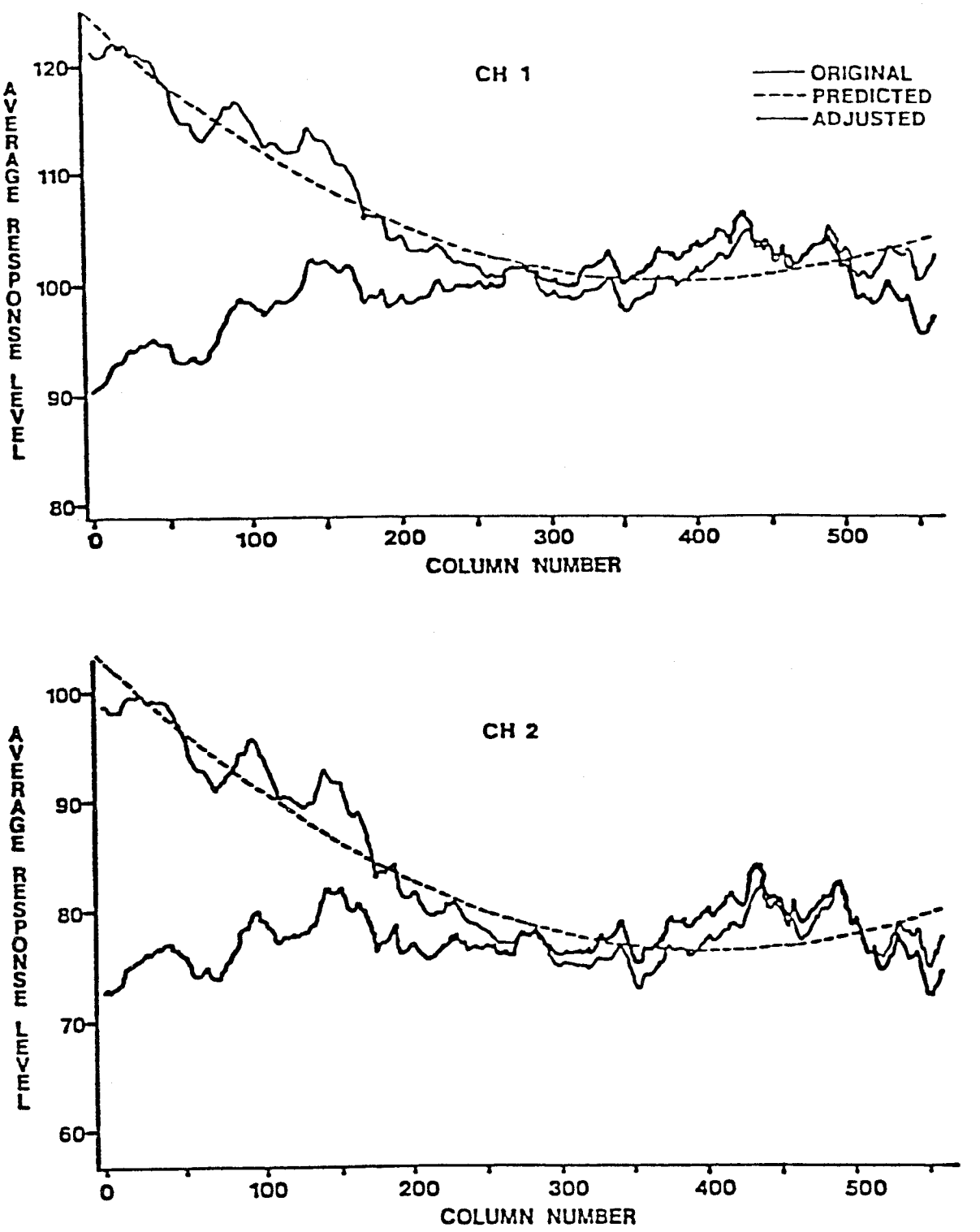

Figure 3.6 Response Level by Column for the Original Data, the Adjusted Data, and the Prediction Function for Channels 1 (0.45-0.52 μm), 2 (0.52-0.60 μm), 3 (0.63-0.69 μm), 4 (0.76-0.90 μm), 5 (1.00-1.30 μm), 6 (1.55-1.75 μm), 7 (10.40-12.50 μm).

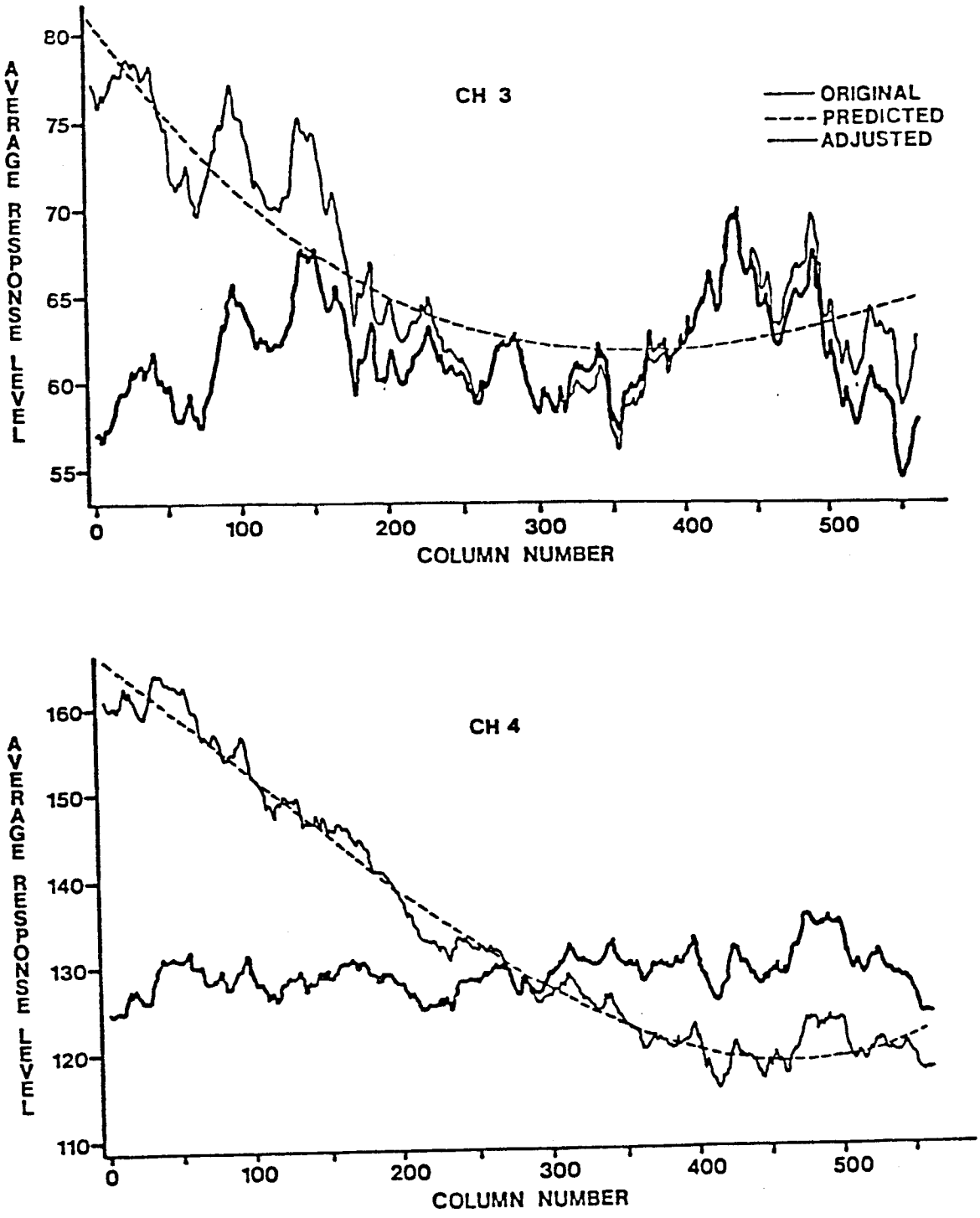

Figure 3.6 Continued.

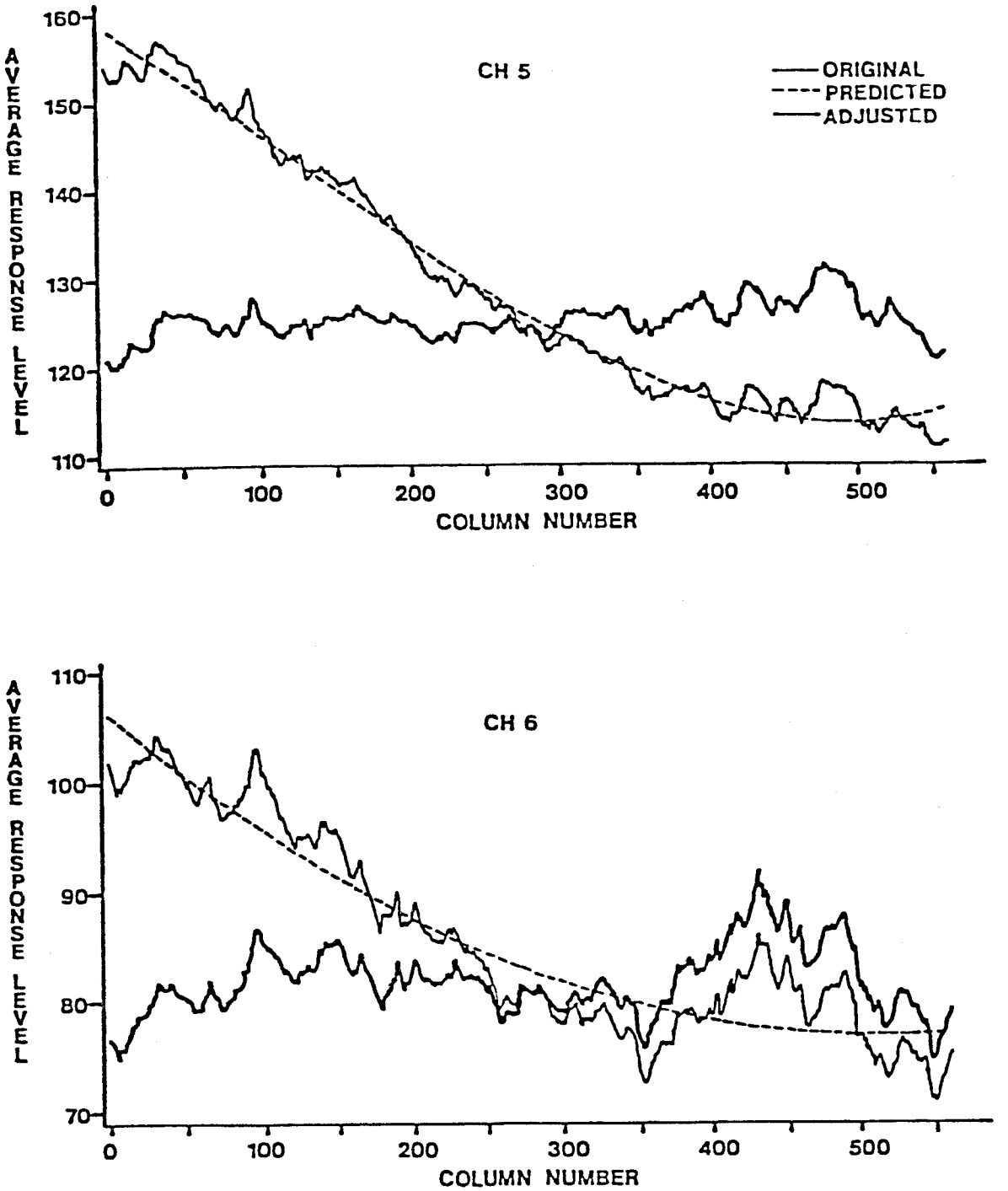

Figure 3.6 Continued.

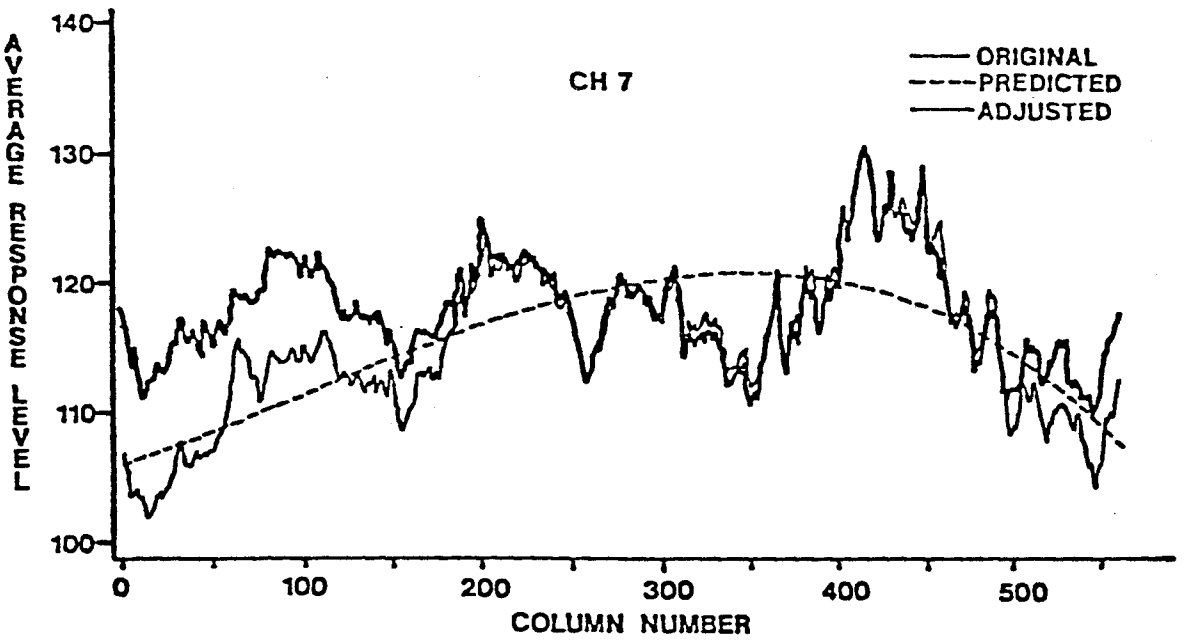

Figure 3.6 Continued.

level extraneous to cover type. Variance extraneous to cover class, increases the within class variance. This would tend to decrease separabilty of the class densities and therefore decrease classification performance (Swain and King, 1973). Figure 3.7 provides a summary of the response level adjustment method employed in this study.

A linear multiple regression analysis was employed to explore the viewing angle effect on recorded response levels. Four areas in the data set which appeared to have no across-track stratification of cover type were identified. Modifications were then made to TRAXEQ, a subroutine called by the LARSYS *TRANSFERDATA module, in order to compute the mean response level by column for each channel, over all scan lines in the designated blocks. The average response level by column was computed over a total of 2237 lines of data in the original TMS data. This was considered a sufficient number of lines to "remove" the variation in response level due to cover type. The graphs in Figure 3.6, however, indicate that a considerable variation due to some variable other than viewing angle is present in the computed averages. A regression analysis was then run using first, second, and third degree polynomials. A separate regression was run on each channel. The regression equations used were :

$$Y(ij) = B(0j) + B(1j)X + e(ij)$$

$$Y(ij) = B(0j) + B(1j)X + B(2j)X*X + e(ij)$$

$$Y(ij) = B(0j) + B(1j)X + B(2j)X*X + B(3j)X*X*X + e(ij)$$

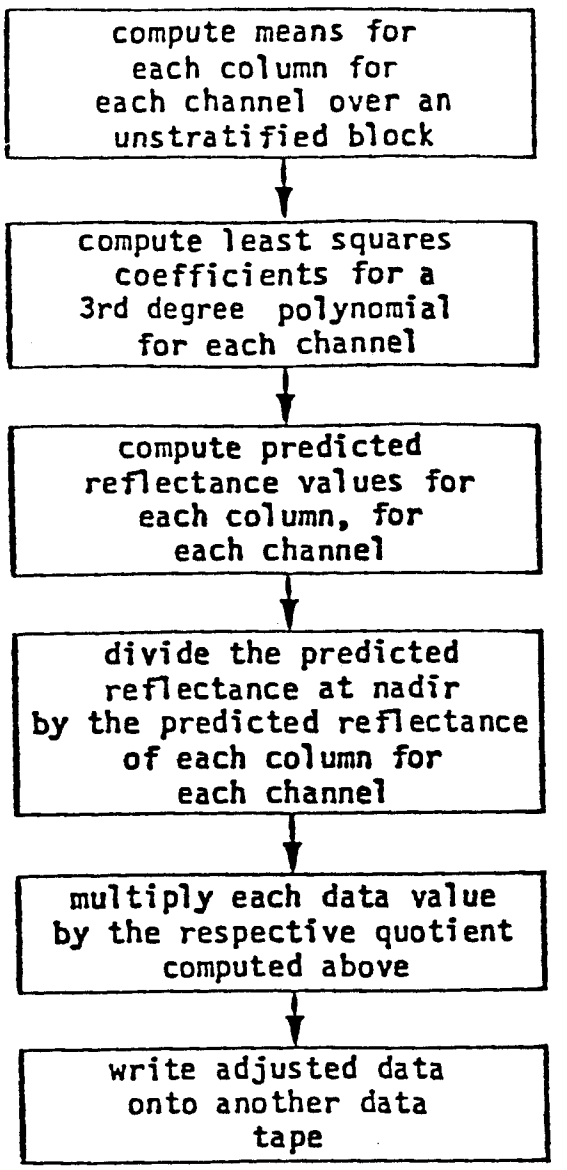

Figure 3.7 Flow Chart for the Response Level Adjustment Algorithm.

where :

Y(ij) = predicted response level of the i(th) column, of the j(th) channel

X = column ; 1,...,560

Assuming the areas from which the data were obtained to conduct the analysis had cover types randomly distributed over the area, such that each column had a nearly equivalent fraction composed of each cover type, then the averaging of response level over all lines in each column would, according to the theory behind the analysis of variance, remove the variance associated with the cover type factor. Any variance in response level between columns should be a function of the column factor, or some covariate (ie., viewing angle). The areas were, by visual inspection, unstratified in the along-track dimension, and were considered to provide a sufficient approximation to the above condition. Therefore, the amount of variance accounted for by the regression model (ie., the MSR) is the expected variance due to variation in viewing angle over an assumed constant cover type.

The empirical nature of this model, and the fact that it is provided by the data for which it will be used to adjust, leaves in question to what degree the various sources of variance will actually be "backed out" of the data. It would be preferred to use some deterministic model which employs the relationship between the angle of observation and the angle of incident solar energy, to develop the adjustment function. Models of this sort have received much attention and have warranted merit, but they require knowledge of the precise

location of the sun, atmospheric turbidity for computation of the diffuse component, and assumptions regarding the distribution and isotropic properties of the reflective surfaces over the area of interest. Due to these constraints the empirical model was deemed more appropriate.

Prior to actually conducting a response level adjustment of the data, the potential components of this source of variance were examined to provide information regarding the expected shape of this prediction function. The major components of this source of variation are thought to be :

(1) an interaction between cover type and viewing angle with respect to angle of illumination (or, for the most part, solar angle), and

(2) atmospheric affects.

The interaction between cover type and viewing angle results in changes in recorded response level due primarily to changes in the total area illuminated versus the area in shadow within the pixel (Anuta and Strahorn, 1973). The area in illumination is at a maximum when the light reflecting surface is viewed along the path of incoming radiation (ie., when the viewing angle is coincident with the zenith solar angle). This orientation has been refered to by some investigators as the "hot spot" (Suits, 1972; Colwell, 1974). As the viewing angle is gradually reduced (ie., shifting the viewing orientation toward nadir), the relative area in illumination versus shadow decreases and the response level, therefore, decreases. The rate of this change with respect to changes in viewing angle approaches zero near nadir. However, as the viewing angle is increased (ie.,

shifting the viewing orientation further from the nadir, away from coincidence with the solar zenith angle), the relative area in illumination versus shadow does not change, since areas in shadow will continue to lie beyond the reflecting object from the point of view of the scanner. With regards to this consideration, the actual mean reflectance by column appears consistent with theory.

The relationship between mean response level by column and the relative area in illumination versus the area in shadow is actually an interaction effect with cover types. The change in relative area in illumination versus shadow is dependent on a vertically nonequivalent distribution of the actual reflecting surfaces. This component of the viewing angle effect is less for vertically equivalent reflecting surfaces, such as bare soil, than for vertically nonequivalent surfaces, as are found in forested or otherwise vegetated cover types. While this variability involves cover type differences, it results in a greater variance in response level <u>within</u> particular cover types when the azimuthal solar angle is zero, and therefore needs to be removed or reduced.

It is of interest to note that this change in reflectance with viewing angle and solar angle is directly proportional to the cosine of the azimuthal angle (i.e., the angle separating the plane of propagation from the plane of observation). Figure 3.8 displays this relationship and schematically defines the terms. This within cover type source of variance is therefore greatest when (Ψ) equals zero (i.e., the planes are coincident) and smallest when (Ψ) equals 90 degrees. Since the vertical heterogeneity of the reflecting surface

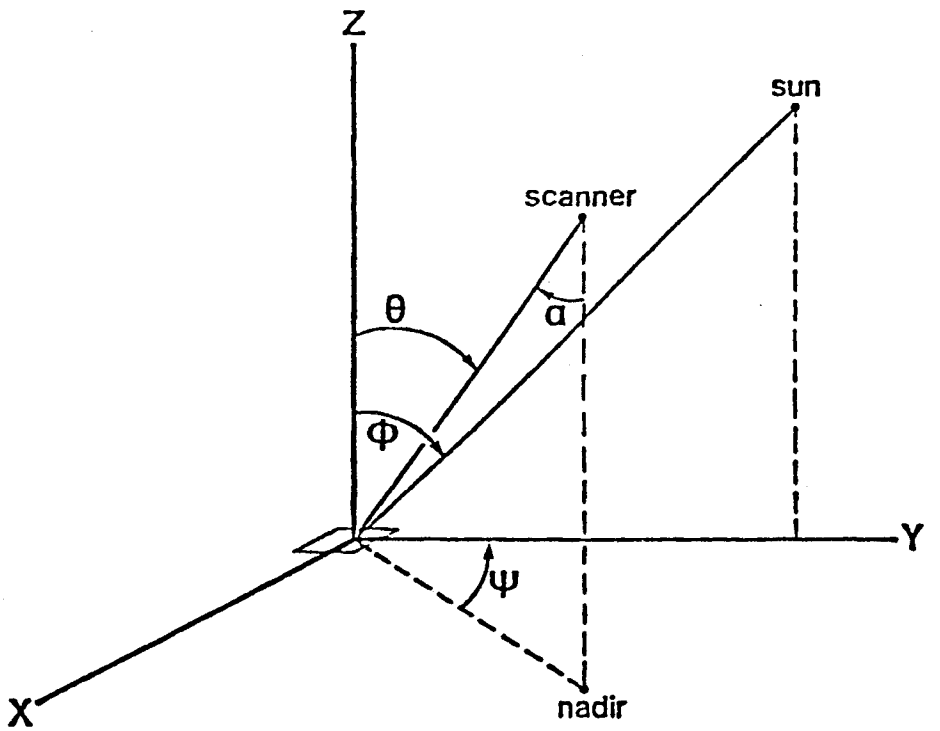

Figure 3.8 Schematic Diagram of the Angular Relationships between the Illumination Source, the Reflecting Surface, and the Location of the Scanner. An arbitrary pixel is centered at the origin. The zenith solar angle is represented by Φ; the viewing angle is represented by α; and the azimuthal solar angle, the angle between the plane of propagation (defined by the sun, the origin, and the y-axis) and the plane along which the surface is scanned (defined by the scanner, the origin, and nadir), is represented by Ψ. The zenith viewing angle is represented by Θ, ($\Theta = \alpha$).

differs for different cover types, this source of variance may actually assist in classification efforts when the plane of propagation is separated from the plane of observation by an angle of 90 degrees. While this area is in need of attention it is beyond the scope of this study.

A second component of the viewing angle source of variance is primarily an atmospheric affect. The following discussion is greatly simplified, as its inclusion here is primarily for purposes of understanding the relationships which result in the overall shape of the response level function across varying view angles.

Radiant energy passing through a segment of the atmosphere has a probability of colliding with atmospheric constituents dependent on the density of the gas molecules and larger suspended particles in the segment considered (Kondratyev, 1969; Jurica, 1973). Collision with atmospheric constituents results in either scattering or absorption. Absorption is fairly invariant to changes in viewing angle with respect to solar illumination angle, except for the small increase in the probability of absorption due to the increased optical thickness of the atmosphere consequent to larger viewing angles. This factor is considered negligible in the range of illumination angles in which remote sensor data is obtained.

Scattering, however, is highly variant with respect to view angles. For both Rayleigh and Mie scattering, the principal component of the scattered light is along the axis of transmission. Rayleigh scattering, or molecular scattering, of visible light, has equal backward and forward components which are approximately twice that of

the sideward components (Kondratyev, 1969). Figure 3.9 is an illustration of the relative distribution of scattered light for all potential directions. Mie scattering is very similar except the forward scattering is predominant over backward scattering, which is dominant over sideward scattering (Jurica, 1973). These relationships result in greater amounts of light being scattered into the transmission path than away from this path. Hence, when viewing is along the transmission path the recorded response level is greater relative to that of other viewing angles with respect to the illumination angle. This would suggest a dampened cosine function with the peak amplitude centered on the column corresponding to the viewing angle coincident with the zenith solar angle.

In the context of the above considerations, the empirical model was regarded appropriate. Existing LARSYS programs were then modified to produce the response level adjusted data sets. This basically involved inserting code which computed a normalizing multiplier for each column, for each channel. Data values from each line in each channel were then multiplied by the respective normalizing multiplier for each particular column. The product was then read onto magnetic tape (20). The normalizing multiplier is the quotient of the predicted

---

(20) The format in which these tapes were constructed complies with the MIST format specifications as they appear in the LARSYS documentation.

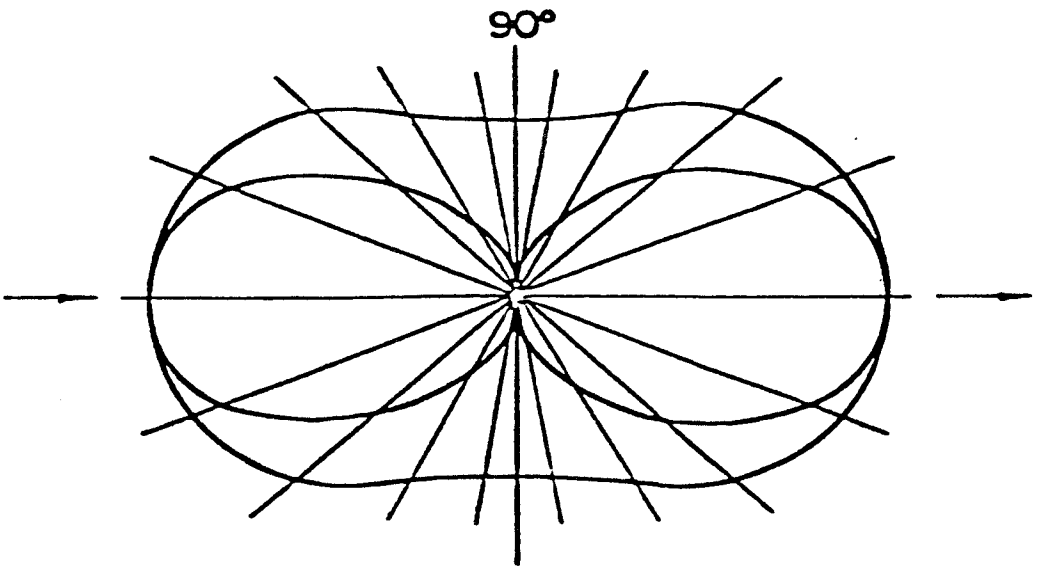

Figure 3.9 Schematic Diagram of Rayleigh Scattering Probability Density Function. The probabilities of scattering a photon in any of all possible directions, given the direction of incidence is indicated. The horizontal axis is the axis of incidence (Kondratyev, K. Ya, 1969).

response level at nadir and the predicted response level for each column. The normalizing multiplier is computed by :

$$NM(ij) = Y(in) / Y(ij)$$

where :

NM(ij) = the normalization multiplier of the j(th) column of the i(th) channel.

Y(in) = predicted response level at nadir for the i(th) channel.

Y(ij) = predicted response level of the j(th) column of the i(th) channel.

A qualitative evaluation of the response level adjustment procedure is provided by comparing the images contained in Figures 3.10 and 3.11. Figure 3.10 is a dot matrix greyscale image of Channel 5 (1.00-1.30 um) of a portion of the geometrically adjusted data prior to conducting the response level adjustment. Figure 3.11 is a dot matrix greyscale image of the same area after the data has been response level adjusted (Channel 5). Visual inspection of the two images should make apparent the reduction in across-track (by column) variation in response level in the adjusted data set as compared to the unadjusted data set.

Spatial Resolution Degradation

Due to the 2.5 milliradian IFOV of the NS-001 multispectral scanner and the 5944 meter (19,500 feet) average height above ground, the original data has a nominal spatial resolution at nadir of approximately 15 meters. Neighboring pixels were averaged together to

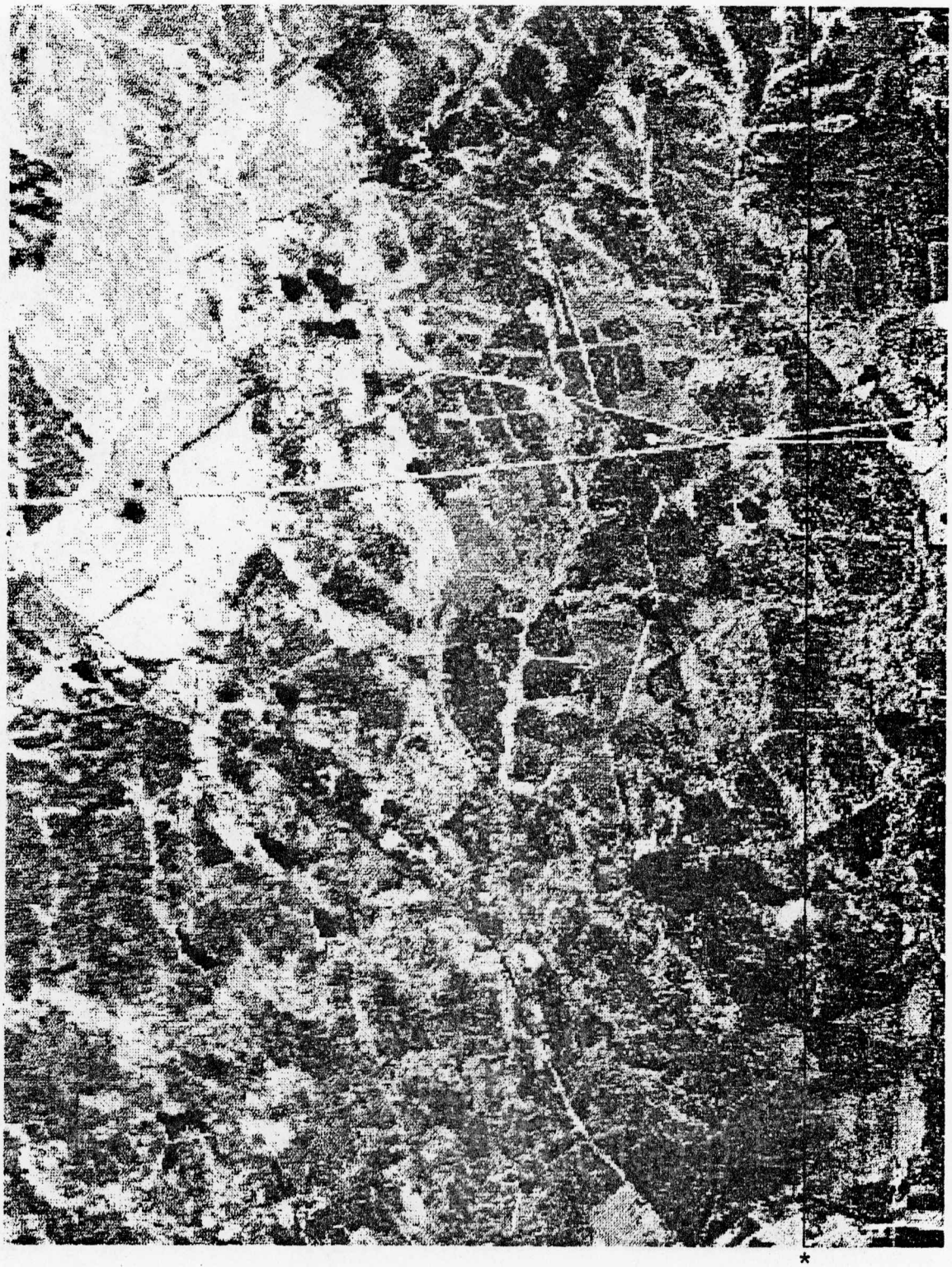

*

Figure 3.10 A Dot Matrix of a Portion of the Geometrically Adjusted Data prior to Adjustment of the Response Level, Channel 5 (1.00–1.30 μm).

*Vertical line signifies the nadir column.

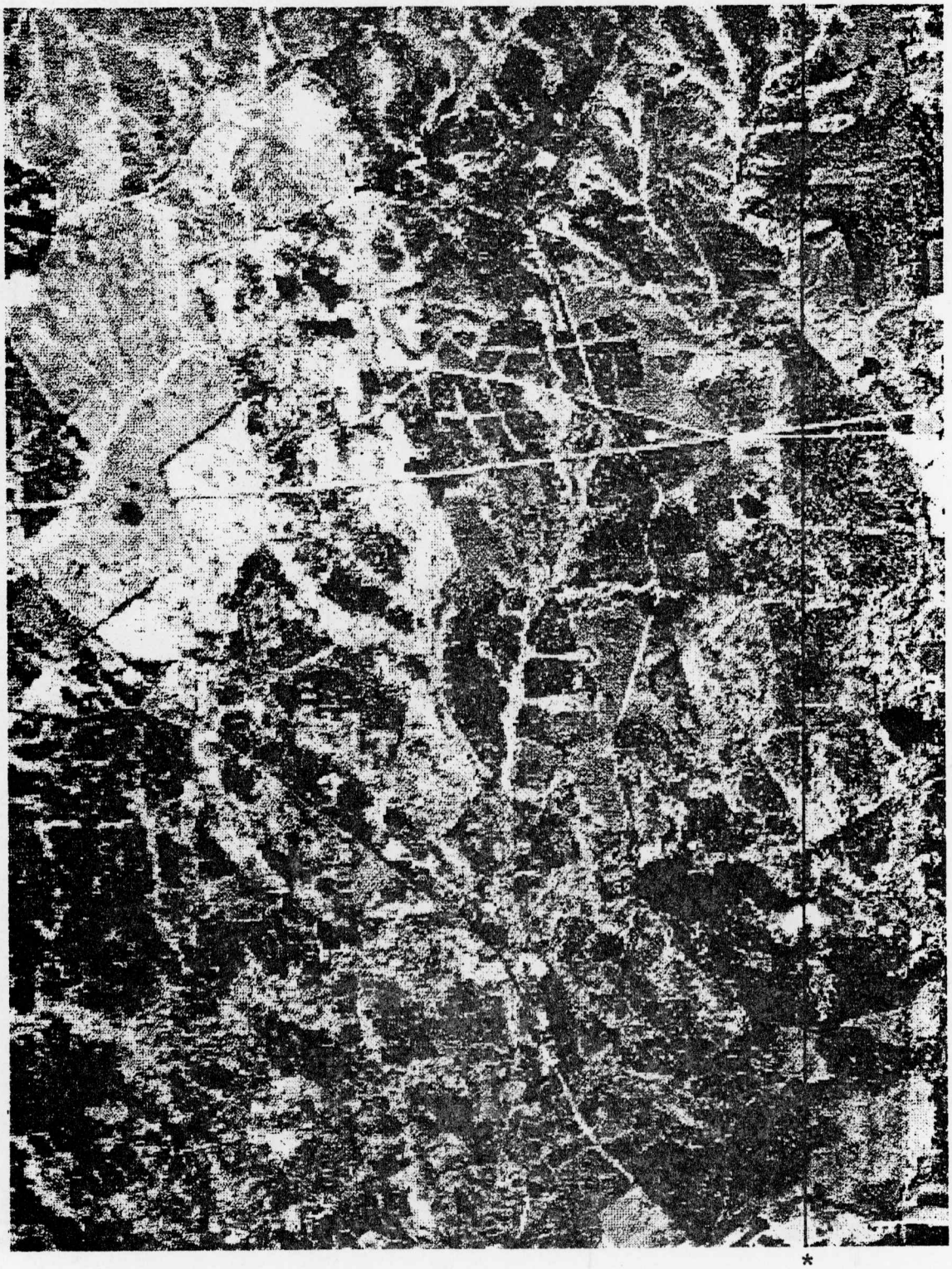

*

Figure 3.11 A Dot Matrix of a Portion of the Geometrically Adjusted and Response Level Adjusted NS-001 MSS Data, Channel 5 (1.00-1.30 m).

*Vertical line signifies the nadir column.

provide data sets of approximately 30 x 30 meters (corresponding to the proposed Thematic Mapper), 45 x 45 meters, and 60 x 75 meters (corresponding to the current Landsat data (21)). A separate tape file was constructed for each resolution from each flight line segment. Figures 3.12, 3.13, 3.14, and 3.15 are photographs of the dot matrix greyscale imagery (Channel 5) of a portion of the data of each spatial resolution. No weights were used in the averaging of neighboring pixels, as would be required to simulate the point spread function resulting from the optics of the scanner systems from which each of the data sets would actually be provided. Weights were not used due to the small number of pixels employed in any particular averaging, and would therefore fail to satisfy the continuity requirement of the function.

Similarly, there was no attempt made to simulate the signal-to-noise ratio (S/N), which would generally characterize each resolution. This investigation is concerned primarily with the characteristics of the data and the resulting classification performances due primarily to the area on the earth surface represented by a single pixel. The preferred approach would be to select a range of S/N values and construct a data set corresponding to each pairwise combination of spatial resolutions and S/N levels. Comparisons between classification accuracies achieved from each of these data sets would provide information on the relative effect of decreasing S/N (which is generally consequent to increasing spatial resolution, see NASA, 1973;

---

(21) Recall that the Landsat MSS has a nominal spatial resolution at nadir of 79 by 79 meters (Slater,1979). The 60 by 75 meter data set is subsequently referred to as "80 meter" data, implying a resolution approximating that of the Landsat MSS.

Figure 3.12 A Dot Matrix Greyscale Image of a Portion of the 15 Meter Spatial Resolution Data, Channel 5 (1.00-1.30 μm).

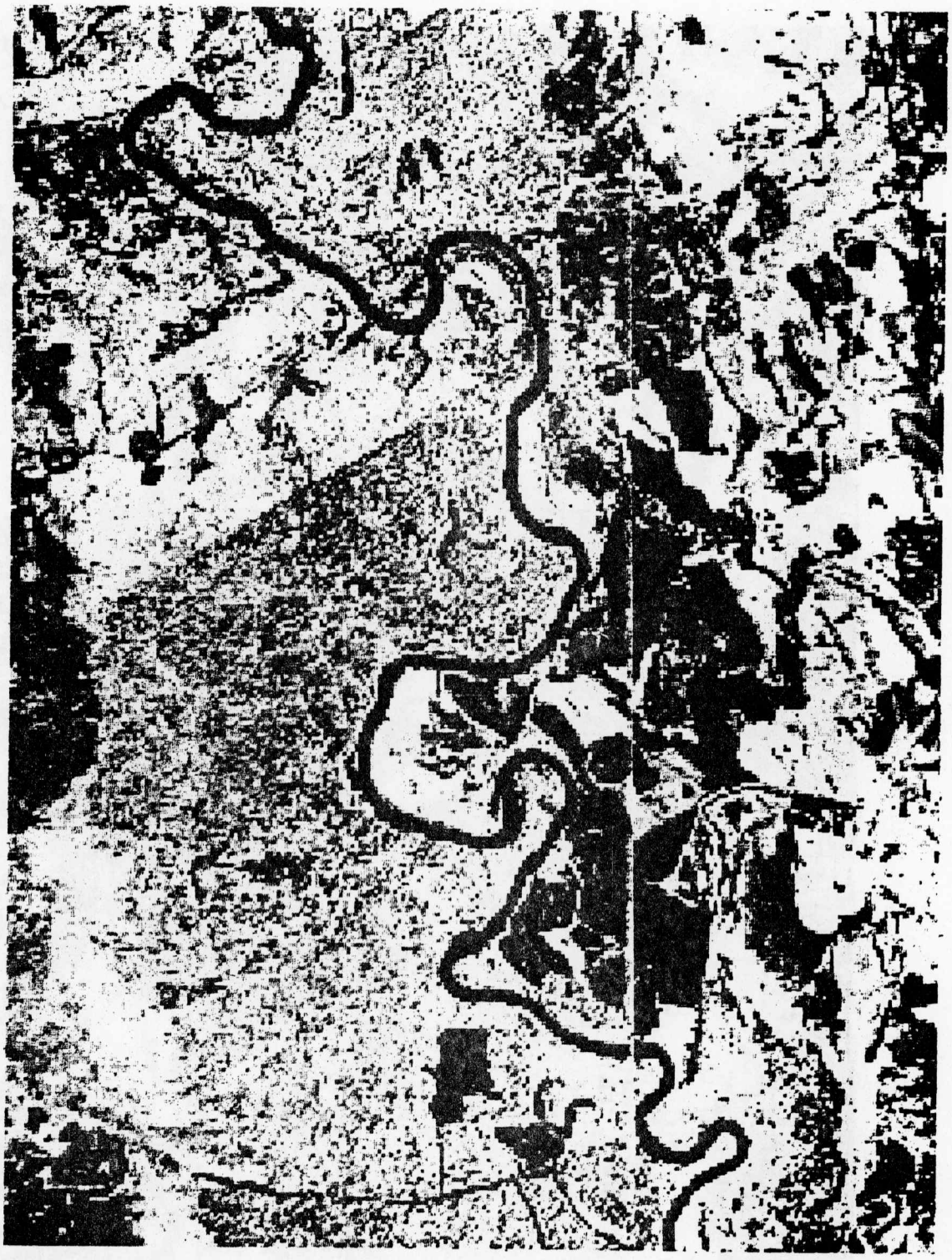

Figure 3.13 A Dot Matrix Greyscale Image of a Portion of the 30 Meter Spatial Resolution Data, Channel 5 (1.00-1.30 μm).

Figure 3.14 A Dot Matrix Greyscale Image of a Portion of the 45 Meter Spatial Resolution Data, Channel 5 (1.00-1.30 μm).

Figure 3.15 A Dot Matrix Greyscale Image of a Portion of the 80 Meter Spatial Resolution Data, Channel 5(1.00-1.30 μm).

and Silva, 1978) and increasing the spatial frequency of spectral sampling relative to the spatial frequency of areas of differing reflectances (which is also a direct consequence of increasing spatial resolution). The limited time and funding, however, did not permit such an extensive investigation.

Development of Training Statistics

Training statistics were developed independently for the two areas examined in the study site. An independent analysis approach was considered most appropriate since the areas differed considerably with respect to cover class composition, and due to a break in data continuity (the two areas were recorded and digitized independently). To facilitate further discussion, the area in the southern portion will be referred to as CAM1S (i.e., data of the Camden area, flight line 1, Southern section), and the area in the northern portion of the study area will be referred to as CAM2N (Camden area, flight line 2, Northern section).

Training statistics for the southeastern flight line were provided by a supervised clustering approach. Two 512 x 512 blocks of the 15 meter spatial resolution data were displayed on a COMTAL Vision One/20 using data of channels 3, 4, and 5 (0.63-0.69 µm, 0.73-0.90 µm, and 1.00-1.30 µm, respectively). Areas representing each of the eleven cover classes referred to in the test site description were identified using the digital imagery and the 1:40,000 color infrared aerial photographs. The line-column coordinates were recorded for later mapping into the MIST (multispectral image storage tape) coordinates.

FORTRAN programs were written to map the line-column coordinates of the 15 meter spatial resolution COMTAL image into the 15, 30, 45, and 80 meter spatial resolution coordinates of the MIST. Non-integer quotients resulting from the transformations are rounded up for the first line and first column and rounded down for the last line and last column of each training field. This provision avoids the inclusion of cover class boundaries in the coarser resolution training fields. The reduction in sample sizes for the coarser resolutions is regarded as a natural consequence associated with coarser resolution data and, therefore, no effort was made to compensate this effect by providing a proportionately greater number of training fields for the coarser resolutions. The relatively low number of pixels employed in developing training statistics for the coarser spatial resolution data may well result in such an approach being inferior to other training techniques previously found well suited for Landsat resolution data (22). Imposing the, perhaps inferior, supervised clustering technique

---

(22) Fleming (1977) examined several training techniques and found an unsupervised clustering approach ("multicluster blocks") particularly well suited for developing training statistics in using Landsat data. In this approach the analyst locates several blocks in the data. Each block contains a multiple of cover classes and cover class conditions. The blocks are selected with the intention of representing all of the cover classes, and the variation of their conditions, contained in the area to be classified. The blocks are then clustered independently, or in groups, depending on the size of the blocks and the dimension restrictions associated with the clustering program. The analyst then identifies the cover class corresponding to each cluster class. Employing such a "multicluster blocks" technique with high resolution aircraft data was expected to result in pixels from different cover classes being clustered into common cluster classes due to spectral similarities among areas within the different cover classes. A pilot clustering of blocks of data containing several cover classes confirmed this expectation.

on data of lower spatial resolutions may well result in classification accuracies which are lower than would otherwise be achieved, but adding another variable to the classification accuracy comparisons would have similarly obfuscated the results.

The fields were grouped by cover class and each group for each resolution was clustered separately (23). A description of the major cover classes of CAM1S, and the corresponding number of spectral classes specified in the cluster analysis of each cover class, is provided in Table 3.3. All seven channels were used without in-band calibration. The means and variances, by channel, are provided for each spectral class in Appendix B. The cluster analysis resulted in a total of thirty-three spectral classes representing the eleven cover classes of CAM1S. Table 3.4 provides the number of pixels clustered into each spectral class, for the data of each spatial resolution. Pooling and deleting of cluster classes was avoided where possible to avoid introducing different analyst effects in the spectral classes associated with the data of each spatial resolution. One spectral class of water for the 45 meter data was deleted from the training statistics of CAM1S, due to an insufficient number of pixels to compute the covariances. The pair-wise separabilities of the spectral classes were examined across cover class, within each resolution. Based on the class separabilities, the spectral classes were considered appropriate for classification purposes.

---

(23) The convergence parameter was set to 98.5 percent, which means the percent of pixels which are not reassigned in the last iteration of pixel assignment to the nearest (Euclidean distance) mean is not less than 98.5 (Phillips, 1973).

Table 3.3 Description of each of the Major Cover Classes and the Number of Spectral Classes Representing each Cover Class for CAMIS.

Cover Class	Number of Spectral Classes	Description of Cover Class
Tupe	3	Water tupelo; generally restricted to narrow ox-bow lakes and other areas of inundated soils.
Mveg	2	Misc. shrubs and small trees; located on saturated and inundated soils.
Crop	4	Row crops and small grain crops in varying stages of development and maturity.
Past	5	Pasture and old fields; plant cover varies from healthy, improved pasture grasses to senescent forbs and invader species.
Soil	3	Bare soil areas associated with agricultural activities; varies in sand, clay, and organic material content as well as moisture content.
Pihd	2	Pine-hardwood mix; generally varies from 35 to 65% hardwood intermixed with pine (determined by visual inspection).
Hdwd	3	Old age bottom-land hardwood; sweet gum is the dominant species, crowns are large, inter-crown gaps are generally deep and result in dark shadowed areas.
Ccut	4	Areas subjected to clearcut forestry practices; ground cover comprised of dry to inundated soils without vegetation, to dense vegetative cover of slash, grasses, shrubs and residual trees. Windrowed slash is common on these areas.
Sghd	3	Second growth hardwood; species composition is highly diverse, crown height and diameter is variable, inter-crown gaps are generally shallow and do not result in dark shadowed areas.
Pine	2	Pine forest areas; the principle species is pine; long-leaf and loblolly are common; age class varies from recently planted (5-10 years) to mature, closed canopy.
Watr	2	Water; primarily associated with the Wateree River (approximately 70-90 meters in width). Other areas comprising the water class are associated with surface mining and open marsh.

Table 3.4 The Number of Pixels in each Spectral Class of each Cover Class by Spatial Resolution for CAMIS.

Cluster Class	Spatial Resolution 15 Meter	30 Meter	45 Meter	80 Meter
Tupe 1	511	139	72	27
Tupe 2	452	104	36	20
Tupe 3	403	99	45	21
Mveg 1	658	158	68	29
Mveg 2	534	136	62	27
Crop 1	598	130	58	28
Crop 2	2887	746	312	152
Crop 3	1003	266	127	65
Crop 4	1227	299	126	54
Past 1	432	112	37	18
Past 2	572	164	70	61
Past 3	1154	296	127	21
Past 4	1233	303	137	68
Past 5	419	104	36	23
Soil 1	765	375	184	83
Soil 2	1919	909	428	187
Soil 3	1366	662	259	114
Pihd 1	246	72	28	16
Pihd 2	1015	242	115	45
Hdwd 1	1159	1319	693	335
Hdwd 2	1846	1701	656	268
Hdwd 3	1043	955	418	189
Ccut 1	771	714	335	157
Ccut 2	1480	1294	582	285
Ccut 3	1414	1445	634	280
Ccut 4	666	732	324	132
Sghd 1	1597	909	428	203
Sghd 2	1979	817	324	139
Sghd 3	757	396	187	93
Pine 1	1244	356	156	85
Pine 2	1946	429	205	72
Watr 1	925	215	*	11
Watr 2	164	39	121	53
Totals	68010	17085	7548	3482
Averages	2060.9	517.7	235.9	105.5

*Spectral class was deleted due to an insufficient number of observations to compute the covariance.

Training statistics were developed for CAM2N by a technique very similar to the one used in CAM1S. The fields in CAM2N, however, were selected in a "directed" manner. A line-column grid was superimposed on the imagery and fields were selected from all cells in the grid where the sizes of the areas occuppied by a single cover class were large enough to provide a "pure field". This modification was implimented as it was expected to result in training statistics which are more representative of the diversity of ground conditions and spectral charasteristics associated with each of the cover classes. The fields were then grouped by cover class, and each group of fields was clustered individually. Table 3.5 provides a brief description of the major cover classes in CAM2N, and the number of spectral classes specified for each cover class in the cluster analysis. The means and variances, by channel, are provided for each spectral class of CAM2N in Appendix B. A spectral class in the urban cover class was deleted from the training statistics of CAM2N for the 45 meter and 80 meter spatial resolutions due to an insufficient number of pixels to compute a 7-variate covariance. Table 3.6 provides the number of pixels clustered into each spectral class using the data of each spatial resolution. The average pair-wise separabilities of the spectral classes were computed and examined. The separability values indicated that the training statistics were appropriate for classifying the area.

The pure fields (required in the supervised clustering approach) are generally much smaller in CAM2N, and therefore contain fewer pixels of each spatial resolution, as compared to the training fields of CAM1S. This is due to the smaller contiguous area occuppied by a

Table 3.5 Description of each of the Major Cover Classes and the Number of Spectral Classes Representing each Cover Class for CAM2N.

Cover Class	Number of Spectral Classes	Description of Cover Class
Watr	2	Water; primarily associated with the Wateree Reservoir. Other areas of the water class are the Wateree River and small impoundments.
Soil	3	Bare soil areas associated with agricultural activities; varies in sand, clay, and organic material content as well as water content.
Hdwd	4	Mixed hardwood species; varying age classes and canopy closures, located primarily in gully bottoms and stream beds.
Pine	4	Pine forest area; almost exclusively slash pine; varying age classes and canopy closures; thinned areas are common.
Past	4	Pasture and old fields; plant cover varies from healthy, improved pasture grasses to senescent forbs and invader species (shrubs are common).
Urbn	3	Urban areas; varies from old residential areas with large lawns and old trees to commercial areas of primarily concrete and asphault.
Ccut	4	Areas subjected to clearcut forestry practices; ground cover comprised of bare dry soil to heavily vegetated areas. Windrowed slash and uncut gully bottoms are common.
Pihd	3	Pine-hardwood mix; generally varies from 35 to 65% hardwood intermixed with pine (determined by visual inspection).
Crop	2	Row crops and small grain crops; generally in earlier stages of development than the crop areas of CAM1S.

Table 3.6 The Number of Pixels in each Spectral Class of each Cover Class by Spatial Resolution for CAM2N.

Cluster Class	Spatial Resolution 15 Meter	30 Meter	45 Meter	80 Meter
Watr 1	365	82	42	27
Watr 2	2015	509	228	102
Soil 1	577	137	49	19
Soil 2	804	206	120	57
Soil 3	900	218	84	39
Hdwd 1	810	444	187	33
Hdwd 2	850	366	158	146
Hdwd 3	1407	733	348	136
Hdwd 4	621	250	92	54
Pine 1	202	58	25	11
Pine 2	1017	247	104	61
Pine 3	1658	393	186	103
Pine 4	1476	414	178	74
Past 1	895	218	100	38
Past 2	692	163	71	35
Past 3	944	226	110	46
Past 4	890	239	104	51
Urbn 1	84	14	6*	4*
Urbn 2	676	146	78	40
Urbn 3	701	203	79	36
Ccut 1	797	196	82	34
Ccut 2	1768	408	176	99
Ccut 3	2449	620	251	115
Ccut 4	1290	383	201	73
Pihd 1	658	140	71	34
Pihd 2	464	138	59	26
Pihd 3	851	233	133	61
Crop 1	475	123	50	25
Crop 2	443	105	52	26
Totals	30746	7784	3476	1643
Averages	1060.2	268.4	124.1	58.7

*Spectral class was deleted due to an insufficient number of observations to compute the covariance. These were not included in the totals.

single cover class in CAM2N as compared to CAM1S. This physiographic difference was previously illustrated in Figure 3.2. This difference is also demonstrated by the average number of pixels per training field in CAM1S as compared to CAM2N. CAM1S has an average of 15.5 pixels per training field for the 80 meter resolution data, while CAM2N has an average of only 6.0 pixels per training field for the 80 meter resolution data. Tables 3.7 and 3.8 contain the number of training fields obtained for each cover class, and the average number of pixels per training field by cover class for each spatial resolution, in CAM1S and CAM2N, respectively. The differences in the average number of pixels per training field between the two flight lines is a good indication of the relative "field" sizes for each area.

Development of Test Pixels

A set of pixels were selected for each section of the study area with which to determine "pure field", in-place classification accuracy independent of the areas used for training the classifier. This was conducted to provide an estimate of the expected classification accuracies achieved with data of each spatial resolution examined. Since the accuracy estimates are obtained in areas selected independently from the training areas, the classification accuracy estimates apply to all pixels of the area classified which satisfy the test pixel selection criteria. A method was developed which provided the test pixels for all four spatial resolutions simultaneously, and which provided a test pixel selection technique which avoids excessive analyst bias.

Table 3.7 The Average Number of Pixels per Training Field for each Spatial Resolution, for each Cover Class in CAM1S.

Cover Class	No. of Training Fields	Spatial Resolution 15 Meter	30 Meter	45 Meter	80 Meter
Soil	35	223.0	55.6	25	11.0
Past	51	75.7	19.4	8.0	3.8
Crop	34	168.6	42.5	18.4	8.9
Pine	16	204.4	50.3	23.1	9.8
Pihd	4	318.2	78.5	35.7	15.2
Hdwd	17	926.2	235.1	104.8	46.6
Sghd	16	557.7	140.1	60.9	28.8
Tupe	17	82.0	20.6	9.1	4.1
Ccut	22	772.0	194.4	85.9	40.7
Mveg	2	596.0	147.0	65.0	28.0
Watr	10	182.7	42.8	20.3	11.1
Total	224	68010	17085	7554	3482
Average	20.4	303.6	76.3	33.7	15.5

Table 3.8 The Average Number of Pixels per Training Field for each Spatial Resolution, for each Cover Class in CAM2N.

Cover Class	No. of Training Fields	Spatial Resolution 15 Meter	30 Meter	45 Meter	80 Meter
Ccut	20	317.5	81.5	35.5	16.0
Crop	15	62.8	15.5	6.8	3.7
Hdwd	72	100.6	25.7	11.2	5.4
Past	37	92.6	22.9	10.4	4.6
Pihd	22	95.3	24.8	12.6	5.9
Pine	66	66.7	17.0	7.6	3.8
Soil	30	81.5	20.1	9.0	4.1
Urbn	4	365.25	90.7	40.7	20.0
Watr	5	476.0	118.2	54.0	25.8
Total	271	30746	7784	3482	1647
Average	30.1	113.45	28.72	12.85	6.08

The method employs a line-column grid which is overlaid on the MSS data using the COMTAL image display. The use of such a grid constitutes a systematic sample based on line-column coordinates, with sampling intervals of approximately 180 meters in the across-track dimension and approximately 450 meters in the along-track dimension. Since the variables being sampled (i.e., cover class and the assigned label) are not considered to vary systematically with respect to the MSS line-column coordinate relative to the sampling interval, the estimates for the mean and variance provided by such a systematic sample are considered unbiased (see Cochran, 1963; especially pages 206-230). The grid was constructed such that candidate pixels located by the grid were mapped precisely between the different spatial resolutions. This provided a means of developing test points for all spatial resolutions simultaneously and avoided any identifications of test pixels in one resolution from involving more than one pixel in a lower resolution. This was achieved with the smallest grid spacing which is integer divisible by the number of original data pixels averaged to compute the data values for each resolution. In the across-track dimension the number of pixels averaged together were 2, 3, and 4. Therefore, the smallest number for which each resolution provides an integer quotient is 12. In the along-track dimension the number of pixels averaged together were 2, 3, and 5, resulting in 30 being the smallest value with an integer quotient. The grid spacing was therefore 12 columns by 30 lines. A FORTRAN program (GRID.FTN) was modified to generate the grid for display on the COMTAL. The areas specified by the grid and associated with each resolution (the

"candidate test pixels") were identified using channels 3, 4, and 5 of the 15 meter spatial resolution data and the 1:40,000 color infrared aerial photographs. Only those candidate test pixels which contained a single cover class, and which the analyst could locate and identify with a high level of confidence, were recorded as suitable test pixels. The test pixels were then mapped into the MIST coordinates of each resolution.

Test pixels for both CAM1S and CAM2N were generated through the use of this technique. Again, the relatively small contiguous area occupied by a single cover class in CAM2N resulted in a substantially smaller number of candidate test pixels. The grid spacing used provided 1428 possible test pixels for each flight line. In the context of the anticipated frequency at which candidate test pixels would fail the inclusion criteria, this candidate test pixel sample size was considered sufficient to provide sensitive tests for classification accuracy comparisons. The total number of acceptable test pixels in CAM1S was 523, but in CAM2N only 376 pixels satisfied the conditions required of text pixels.

No attempt was made to determine what component of the cover class was actually contained in the higher spatial resolution pixel. Such efforts were considered spurious, since the interest is concerned primarily with the classification performance achieved with the data of various spatial resolutions relative to cover type mapping. While it is recognized that the cover classes defined for any particular classification effort greatly affect the classification performance achieved, the cover classes were selected on the basis of their

informational value relative to commonly encountered applications. In the context of this evaluation, any erroneous classification among cover classes arising due to ground cover similarities over a small area on the ground are considered valid errors. For example, clearcut areas which have areas in grass may be confused with pasture. While this misclassification is reasonable, the outcome is regarded as an error.

CHAPTER 4

RESULTS AND DISCUSSION

Introduction

This investigation was conducted in two separate phases using data from two different areas. The following discussion is therefore divided into two major sections based on area or flight line. The comparison of classification accuracies achieved with the per-point Gaussian maximum likelihood (GML) classifier using data of the four different spatial resolutions is followed by the comparison of classification accuracies achieved with the per-point GML classifier and the per-field *SECHO (supervised ECHO) classifier using the 30 meter spatial resolution data. Subsections contain discussion of classification accuracy estimates based on training field pixels followed by estimates based on test pixels.

Flight Line CAM1S

Per-Point GML Classification Using Data of Different Spatial Resolutions

Evaluation Using Training Field Pixels. Classification accuracy estimates based on training field pixels provides a "first look" at expected classification performance. High classification accuracies of the training field pixels informs the analyst that the spectral classes are generally :

1) statistically separable,

2) represent no more that one cover class, and

3) correspond to "natural" regions of concentration, in the measurement space, associated with the spectral characteristics of each of the cover classes in the training fields.

The overall classification accuracies achieved with the per-point GML classifier using data of each of the four spatial resolutions are illustrated in Figure 4.1 (1). The differences between the overall classification accuracies achieved with the data of each spatial

---

(1) Overall percent correct classification is computed by:

$$PCC = \frac{\sum_{i=1}^{n} (P'_i - P_i)}{n}$$

where:

P_i = number of pixels classified as the i(th) cover class which have been identified by the analyst as the i(th) cover class.
P'_i = the total number of pixels employed in the evaluation, identified by the analyst as the i(th) cover class.

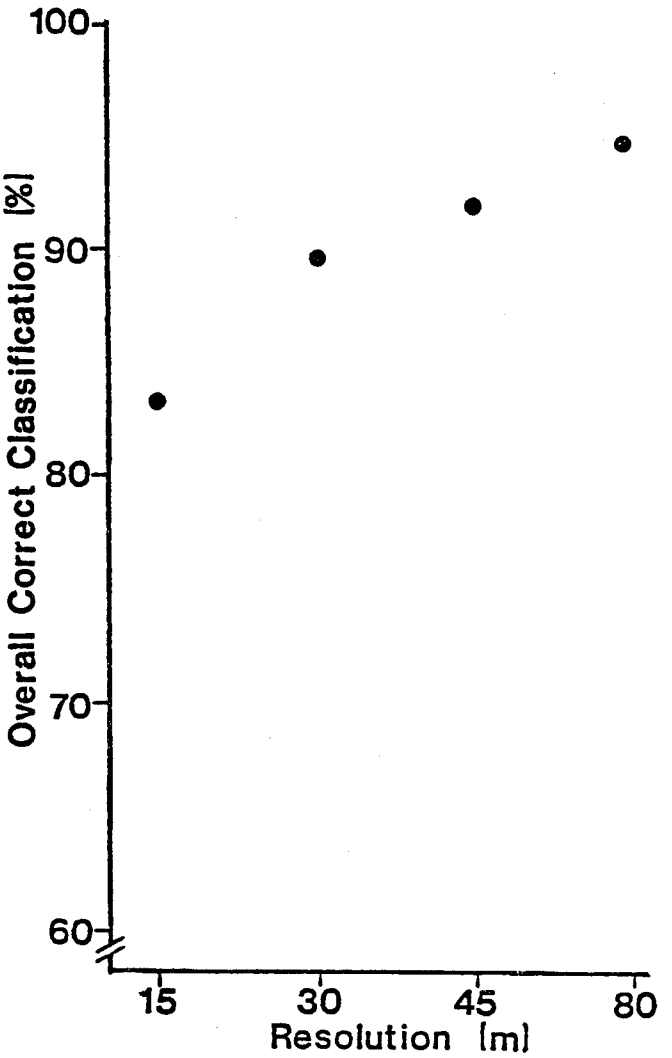

Figure 4.1 Overall Percent Correct Classification of Training Field Pixels by Spatial Resolution (Per-Point GML Classifier, CAM1S).

resolution were found to be significant at the a = 0.10 level of confidence (2). These results indicate that overall percent correct classification (PCC) tends to increase with decreasing spatial resolution. That is, as the size of the area on the ground corresponding to a single pixel increases, overall classification accuracy is expected to increase.

The training field pixel classification accuracies achieved for each cover class with the per-point GML classifier using data of each spatial resolution are illustrated by the response surface in Figure 4.2 (3). The slope of the lines connecting the PCC levels across different spatial resolutions represents the rate of change of PCC with respect to spatial resolution for each cover class. The lines connecting the PCC levels across the various cover classes have no

---

(2) This test for significant differences between levels of percent correct classification used the Newman-Keuls' range test employing the arcsin transformation of the percent of correctly classified pixels (see Appendix C for a presentation of the test for significant differences).

(3) Conventionally, results have been evaluated only on the basis of the relative rate of omission. Instances of omission are the non-diagonal row elements of the error matrix. Omission is of primary interest to those concerned with the likelihood of an area "known" to be of the i(th) cover class being classified as some other cover class. The commission error is equally a part of the error frequency associated with a classification. Commission error is represented by the non-diagonal column elements of the error matrix. This index of error is of interest to those concerned with the likelihood of an area being classified as the i(th) cover class when acutally the area is in some other cover class. Both of these forms of misclassification constitute a legitimate error. The problem of providing a meaningful index for evaluating a classification arises when the evaluation is conducted by cover class, since the use of either measure will result in the same computed "overall" classification performance. The problem is most crucial when the two error components are poorly correlated, which is often the case. Attention is needed for determining a meaningful combination of the two error components.

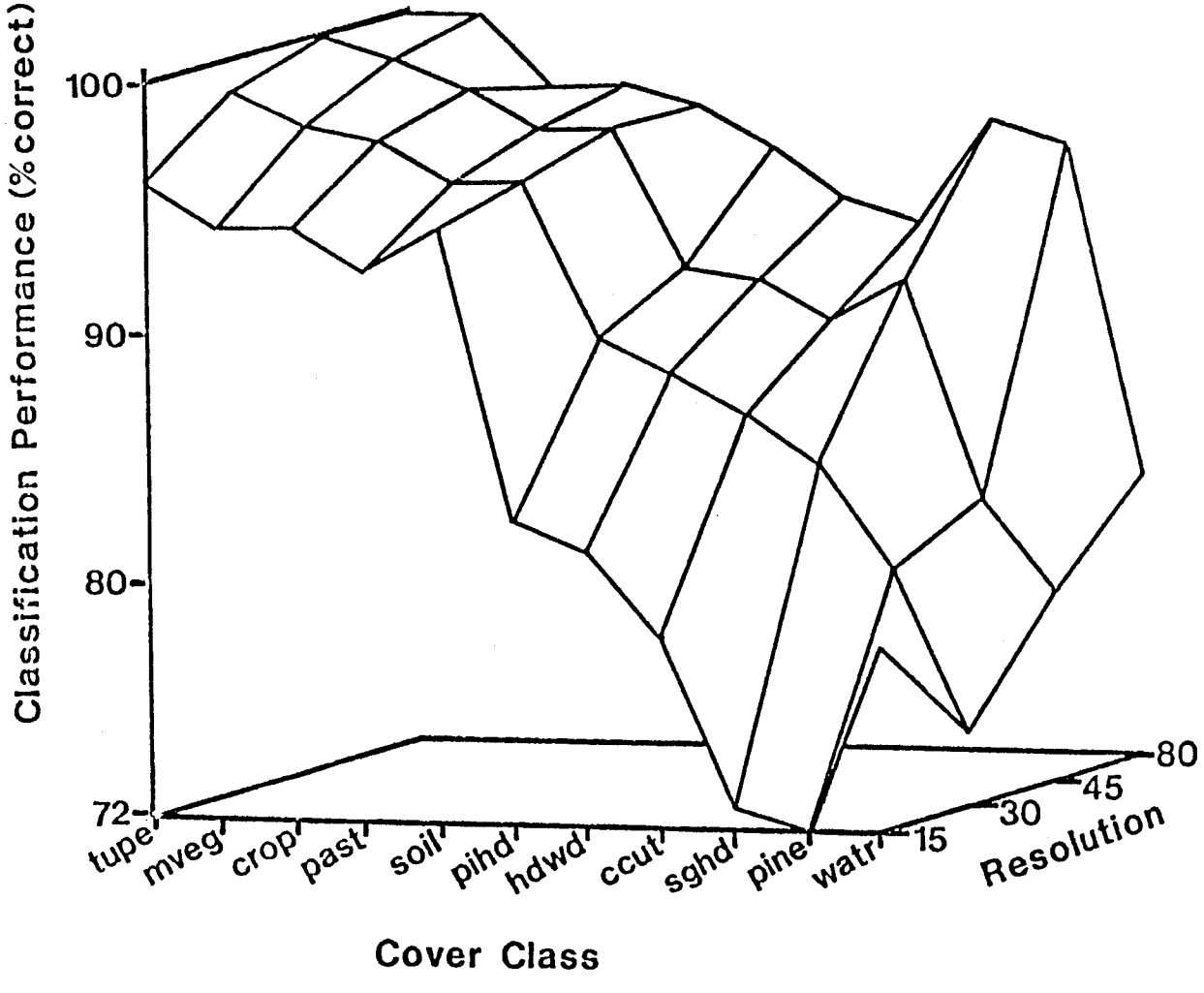

Figure 4.2 Response Surface in Percent Correct Classification by Cover Class, for each Spatial Resolution (Training Field Pixels, Per-Point GML Classifier, CAM1S).

implied importance, but are included to illustrate the relative levels among the various cover classes. The statistical evaluation of the differences in PCC achieved within each cover class, across spatial resolution, is presented in Table 4.1. The PCC levels achieved with data of each spatial resolution were not statistically ($a = 0.10$) different for water tupelo, marsh vegetation, crop, pasture, bare soil, or pine-hardwood mix. The PCC levels achieved with data of each resolution were statistically different for pine, old age hardwood, second growth hardwood, and clearcut areas.

The irregular classification accuracies associated with the water cover class are believed to be due to the inclusion of the inundated surface mining areas as water. These areas are borrow pits which contain windrowed spoil. The older spoil surfaces are covered with vegetation. The pixels corresponding to these areas are consequently composite measurements of the spatially weighted irradiances associated with each of the ground cover materials actually present. Varying levels of "contamination", of the spectral characteristics of water, with those of another cover class is believed to be the factor responsible for the low classification accuracies achieved for water. The fact that nearly all of the misclassified water pixels were classified as a spectral class representing clearcut areas of inundated soil with standing vegetation tends to confirm the above scenario. It is of interest, however, that classifications conducted with 80 meter spatial resolution data appear to be more robust in the context of these levels of contamination.

The greatest changes in PCC with respect to spatial resolution

Table 4.1 Statistical Evaluation of Classification Performances by Cover Class for each Spatial Resolution (Training Field Pixels, Per-Point GML Classifier, CAMIS).†

Cover Class	Spatial Resolution 15 Meter	30 Meter	45 Meter	80 Meter	Harmonic Mean
Tupe	96.3[a]	98.9[a]	100.0[a]	100.0[a]	182.49
Mveg	94.7[a]	97.6[a]	99.2[a]	100.0[a]	150.64
Crop	94.8[a]	97.1[a]	98.1[a]	97.3[a]	771.28
Past	93.2[a]	95.6[a]	96.6[a]	97.4[a]	503.43
Soil	94.9[a]	95.7[a]	96.7[a]	96.6[a]	1019.80
Pihd	83.7[a]	89.8[b]	91.6[b]	95.1[b]	146.22
Hdwd	82.5[a]	88.5[b]	91.2[c]	93.3[d]	2092.56
Ccut	79.3[a]	87.0[b]	89.7[c]	92.4[d]	2297.24
Sghd	72.9[a]	85.1[b]	91.3[c]	96.3[d]	1183.66
Pine	72.1[a]	81.1[b]	82.9[b]	95.5[c]	420.12
Watr	79.1[ab]	74.8[a]	79.3[ab]	82.9[b]	232.17

†Dissimilar superscripts within each particular cover class denotes a significant difference at the $\alpha = 0.10$ level of confidence based on the Newman-Keuls' range test conducted on the arcsin transformed proportions. The proportions are the relative rates of omission in classification.

occur with the forest cover classes. The differences in PCC among all spatial resolutions were found to be significant at the a = 0.10 confidence level for the old age hardwood, clearcut, second growth hardwood, and pine cover classes. Classification accuracy for these forest cover classes increases with decreasing spatial resolution. While the pine-hardwood mix cover class ranged from 83.7 to 95.9 percent correct classification with 15 meter and 80 meter spatial resolution data, respectively, these differences were not found to be significant at the a = 0.10 level of confidence. The low change in PCC with respect to resolution for water tupelo as compared to that associated with other forest cover classes is probably due to the very distinct spectral characteristics of water tupelo. Areas between the crowns of tupelo, which may be nearly identical in spectral characteristics to the areas between the crowns in other forest cover classes, probably do not affect the average pair-wise statistical separability of tupelo to the extent that the separabilities of other forest cover classes are affected. Pure pixels of between crown gaps (even at the 15 meter spatial resolution) are expected to be very rare for the crown closures commonly found in forest cover classes of this area. Pixels containing the inter-crown gaps (as for pixels in general) represent the spatially weighted averages of the irradiances associated with the regions contained in the pixel. Inter-crown gaps, which have spectral characteristics which are very similar across different forest cover classes, are expected to affect the classification accuracies of those classes which have similar spectral characteristics associated with the crowns, to a greater degree than

those for which the spectral characteristics of the crowns are very different.

The differences between PCC levels achieved with data of the different spatial resolutions, observed for forest cover classes, is believed to be due to the level of spectral variability across neighboring pixels associated with forest cover classes. The irradiance of the tree crowns is different from that of the inter-crown gaps. This results in a variation in spectral response level between adjacent, or neighboring, pixels (4). This source of variation is a component of the within cover class variances associated with each of the cover classes. Cluster analysis reduces this source of variance to some degree but does not remove it entirely. Figure 4.3 illustrates the degree to which the standard deviation of the spectral response associated with each cover class is reduced by clustering the vectors obtained within each of the cover classes. For example, the standard deviation of the spectral response level over all of the training fields of the old age hardwood (channel 4, 80 meter resolution data) is approximately 15 (Figure 4.3A). The standard deviation (channel 4, 80 meter resolution data) averaged over the three cluster classes of old age hardwood is approximately 7 (Figure 4.3B). The within class variance as shown in Figure 4.3 is also reduced by averaging the measured irradiance of adjacent pixels, which is analogous to reducing

---

(4) This variation in spectral response level between adjacent pixels, or areas, is analogous to concept of "texture" in aerial photography. Texture is a major feature in aerial photographic images associated with forest classes. The identification of cover classes through the use of aerial photography relies, to a considerable degree, on the texture associated with the various cover classes.

Figure 4.3 Standard Deviation of Spectral Response Level in each Channel, by Spatial Resolution (15, 30, 45, and 80 meter), for each Cover Class.
A = population defined by cover class identity.
B = population defined by cluster analysis. Standard deviation is the average over the cluster classes representing each cover class.

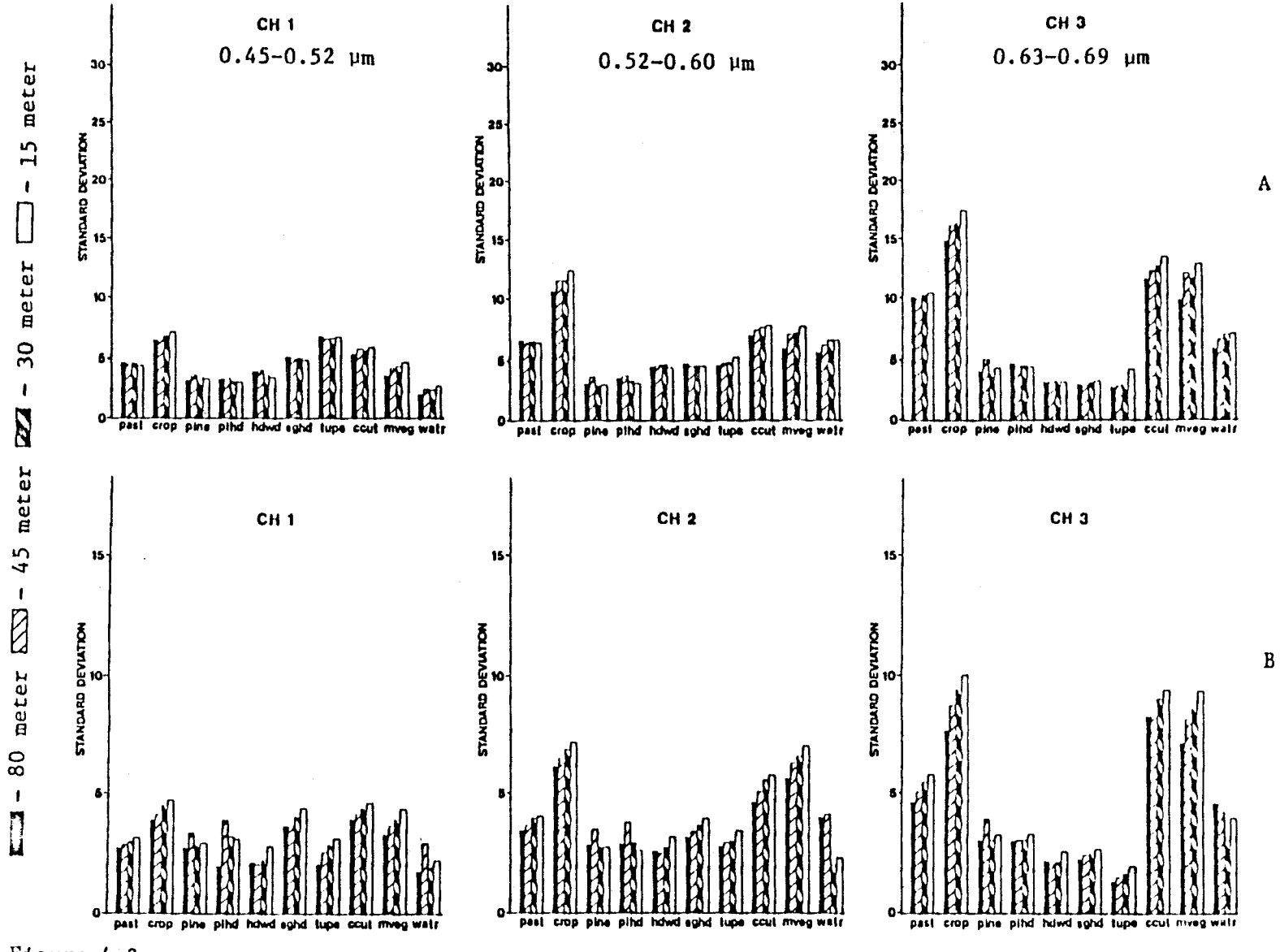
80 meter - 45 meter - 30 meter - 15 meter
CH 1
0.45-0.52 µm
CH 2
0.52-0.60 µm
CH 3
0.63-0.69 µm
STANDARD DEVIATION
past crop pine pihd hdwd sghd lupe ccut mveg watr
A
B

Figure 4.3

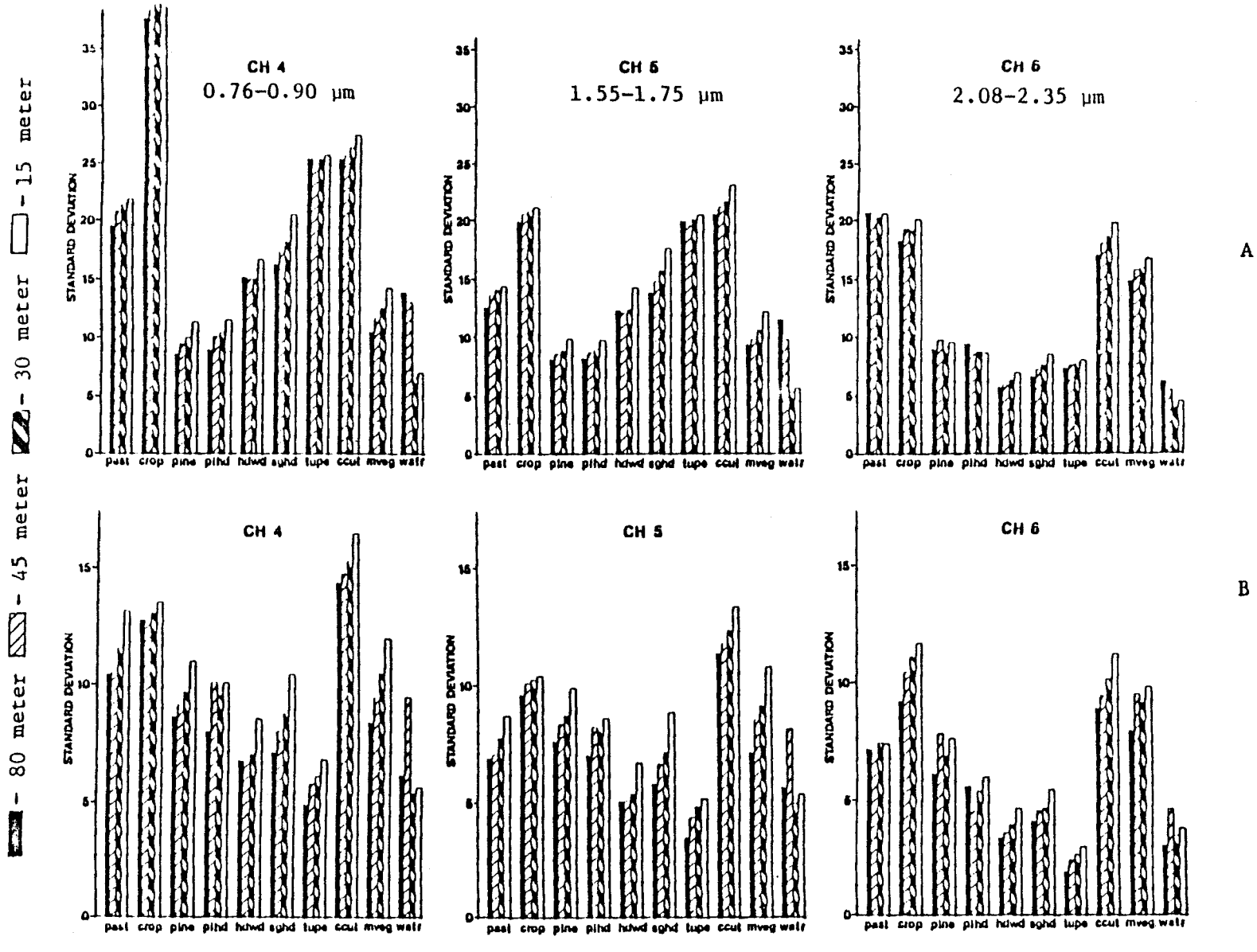

Figure 4.3 (continued)

the spatial resolution of the scanner system with which those measurements are actually obtained. Recall (Chapter 3, Spatial Resolution Degradation), that the averaging of measured irradiances of adjacent pixels is exactly how the different spatial resolutions were simulated. A comparison of the relative standard deviation in spectral response level across data of different spatial resolutions with the relative standard deviation in spectral response levels between "cover class" (Figure 4.3A) and "spectral class" (Figure 4.3B) indicates that clustering reduces cover class variance to a greater degree than reducing the spatial resolution of the scanner system employed. The high variance in crop and pasture is probably due mostly to shot noise in the scanner detectors (5).

The comparison of training field pixel classification results achieved with the per-point GML classifier using data of the four different spatial resolutions indicates that no real differences in PCC are expected between the different spatial resolutions in classifying areas of water tupelo, marsh vegetation, crops, pasture, pine-hardwood mix, and bare soil. However, when classifying old-age hardwood, second growth hardwood, pine and clearcut, higher classification accuracies are expected to be achieved with data of progressively lower spatial resolution (over the range examined here). This inference is based on the relative frequency of omission error using "field-center pixels. The spectral characteristics associated with these forested areas

---

(5) Shot noise is basically current resulting from the thermal instability of the detectors. This source of current variation is largely responsible for the correlation between mean response level and variance (see NASA, 1973; and Silva, 1978).

indicate, further, that higher classification accuracies are expected using the lower resolution data when classifying areas containing cover classes with "large" levels of spectral variability across neighboring pixels. How large this level of spectral variability must be before significant differences in classification accuracies result is not known.

There is some question regarding the sensitivity of the statistical tests provided by the percent correct classifications based on training field pixels. The sensitivity of these statistical tests is dependent on the sample size from which the PCC was obtained. Regarding each pixel in the training field as a sample generally results in a very large sample size. The fact that the harmonic mean of the number of samples divided into a constant (i.e., 821) provides the variance estimate for evaluating the differences between the arcsin transformed proportions makes the issue of 'what constitutes a true sample' most crucial to a proper evaluation of the apparent differences. How this question should be resolved is currently unknown and is in need of much attention.

The results discussed thus far are based on training field pixels and, therefore, are <u>not</u> indicative of the probability of erroneous class assignments for any pixel in the area to be classified. While test pixels, on the average, provide lower classification accuracies than training field pixels, the <u>relative</u> PCC levels of training field pixels achieved with data of different spatial resolutions are not expected to be different from the <u>relative</u> PCC values obtained from test pixels selected independent from the training areas.

Evaluation Using Test Pixels. The evaluation of classification accuracy based on a set of pixels selected independent of the training fields provides an estimate of the probability of erroneously classifying a pixel selected from the entire area classified. The intended inference space of this estimate is the percent correct classification expected for all of the pixels in the area classified. The extent to which the intended inference space is provided by this estimate is determined by the limitations imposed by the test pixel selection criteria.

The overall percent correct classification achieved with the per-point GML classifier using data of each of the four spatial resolutions is illustrated in Figure 4.4. These differences were not found to be significant at the a = 0.10 confidence level (6). The percent correct classification achieved for each cover class using data of the four resolutions is illustrated in the bar chart of Figure 4.5. Table 4.2 summarizes the outcome of the statistical evaluation of these differences. Only the PCC achieved for the old age hardwood and the clearcut cover classes differed significantly (a = 0.10) across spatial resolution (7).

These results indicate that classification accuracies achieved

---

(6) The harmonic mean for this evaluation is 539.26 resulting in a small enough estimated variance ((821/539.26) = 1.5225) to provide what is considered a sufficiently sensitive test for "real" differences.
(7) While the differences across spatial resolution associated with the water cover class are statistically significant, the results for the water class are difficult to interpret due to the reasons cited in the "Training Field Pixel Evaluation" section.

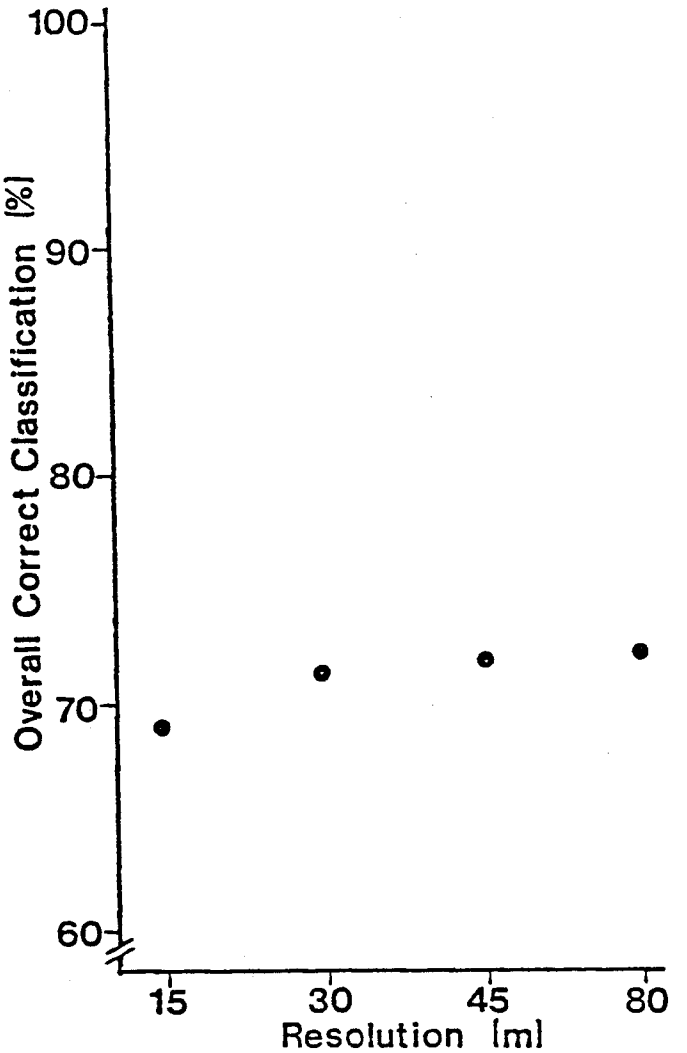

Figure 4.4 Overall Percent Correct Classification of Test Pixels by Spatial Resolution (Per-Point GML Classifier, CAMIS).

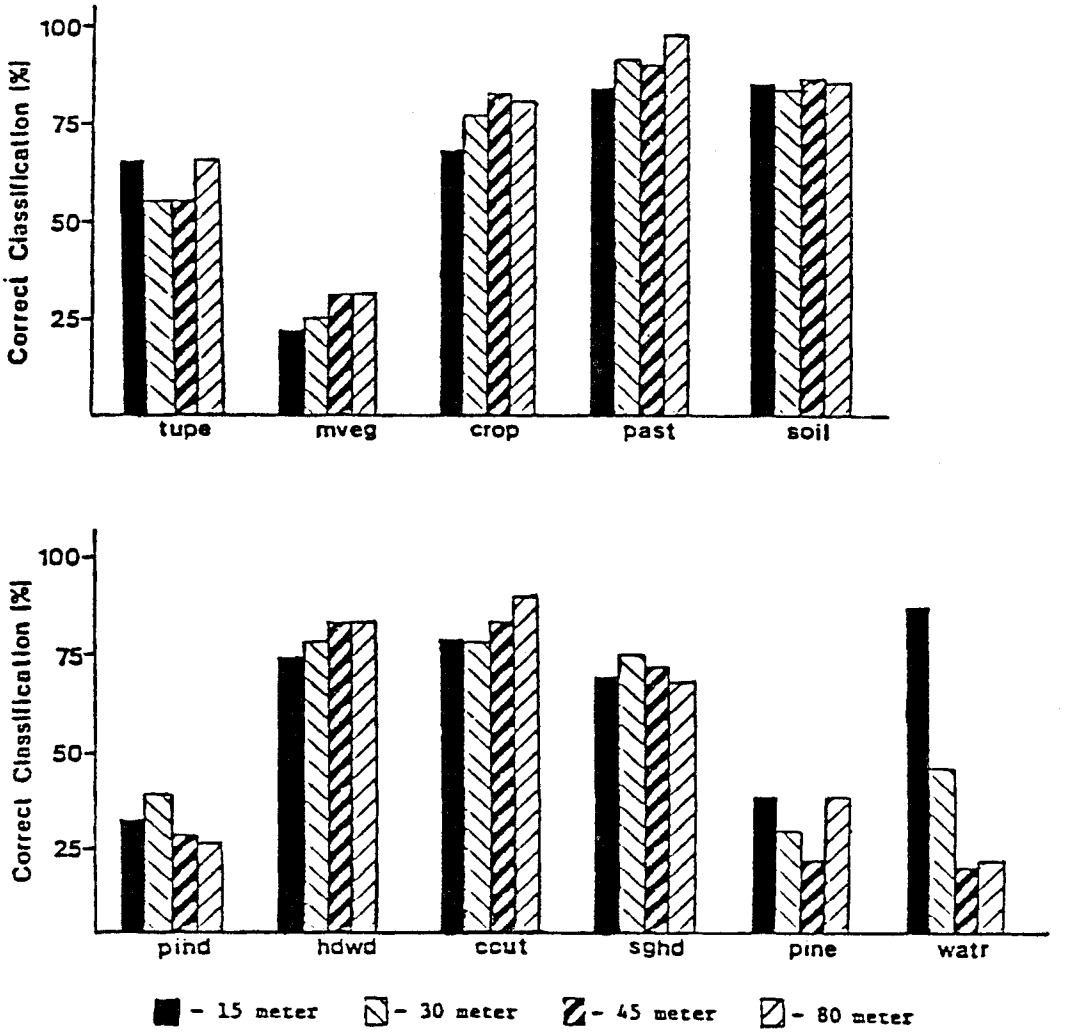

Figure 4.5 The Percent Correct Classification of Test Pixels by Spatial Resolution for each Cover Class (Per-Point GML Classifier, CAMIS).

Table 4.2 Statistical Evaluation of Classification Performances by Cover Class for each Spatial Resolution (Test Pixels, Per-Point GML Classifier, CAMIS).†

Cover Class	Spatial Resolution 15 Meter	30 Meter	45 Meter	80 Meter	Harmonic Mean
Tupe	66.7[a]	55.6[a]	55.6[a]	66.7[a]	9.0
Mveg	21.1[a]	26.3[a]	31.6[a]	31.6[a]	19.0
Crop	69.7[a]	78.8[a]	84.8[a]	82.1[a]	31.86
Past	86.7[a]	92.9[a]	92.3[a]	100.0[a]	13.52
Soil	87.5[a]	85.9[a]	81.7[a]	86.9[a]	62.97
Pihd	29.0[a]	35.5[a]	25.8[a]	22.6[a]	31.00
Hdwd	72.4[a]	77.6[ab]	81.4[b]	81.4[b]	156.00
Ccut	77.5[a]	76.1[a]	81.7[ab]	88.4[b]	70.59
Sghd	66.7[a]	72.4[a]	69.4[a]	65.5[a]	121.49
Pine	36.4[a]	27.3[a]	18.2[a]	36.4[a]	11.00
Watr	85.7[c]	42.9[b]	16.7[a]	18.2[a]	12.86

†Dissimilar superscripts within each particular cover class denotes a significant difference at the $\alpha = 0.10$ level of confidence based on the Newman-Keuls' range test conducted on the arcsin transformed proportions. The proportions are the relative rates of omission in classification.

with the per-point GML classifier are not expected to vary significantly with respect to the spatial resolution of the data employed. However, the sensitivity of the test for significant differences is proportional to the square root of the harmonic mean of the number of test pixels available for each resolution. Table 4.2 also contains the harmonic mean of the sample sizes with which the estimated variance of the transformed proportions are computed. The harmonic means of the number of test pixels for some of the cover classes indicate that an insufficient number of test pixels were available to conduct a meaningful test on the differences between the PCC values achieved using the data of different spatial resolution. It appears that classification evaluations are caught in the quandary of providing a pixel selection technique such that; 1) every pixel included in determining the percent correct classification can be regarded as an observation, or sample, and 2) a sufficient number of observations are provided to conduct a test which is adequately sensitive to test for meaningful differences. In this investigation the problem was further compounded by the restriction of coordinates which could be mapped between data sets of the various spatial resolutions without location errors arising due to arithmetic rounding.

The degree to which the training statistics represent the spectral characteristics and variability associated with each of the cover classes throughout the area classified is a major determinant of the classification accuracies achieved. If the effects of this factor were invariant with respect to spatial resolution then comparisons involving different spatial resolutions theoretically would not be affected. The

differences between the classification accuracies achieved for training field pixels and those achieved for test field pixels indicate that the training statistics for CAM1S are not actually representative of the range of spectral characteristics associated with each cover class throughout the area classified. To what degree this factor interacts with resolution is unknown. Comparing the accuracies tabulated in Table 4.1 with those in Table 4.2 indicates that the degree to which the training statistics represent the range of spectral characteristics associated with their respective cover classes is a more important factor than is the spatial resolution of the data used in conducting the classification. Thus, the trends, or lack thereof, in the PCC across spatial resolution indicated by the test pixel classification results are probably more indicative of the relative importance of representative training statistics as compared to the spatial resolution of the data. However, the differences between the percent of test pixels correctly classified using 15 meter vs. 80 meter spatial resolution data were significant for the old age hardwood and clearcut cover classes. This tends to confirm the inferences based on training field classification comparisons; for cover classes characterized by high levels of spectral variability across adjacent pixels (eg., forest cover classes), higher classification accuracies can generally be realized using low spatial resolution data.

Classification Results Using *SECHO Compared to Results Using the Per-Point GML Classifier

Introduction. The 30 meter spatial resolution data was classified using the *SECHO classifier (see section "The ECHO Classifier : The Supervised Mode") to determine whether improvements in classification accuracies could be achieved through the use of a classifier which was written to accomodate some degree of spectral variability among neighboring pixels. The unfamiliarity of the analyst with the effect of the threshold settings required by the classifier warranted some exploration of how the algorithm behaved over a range of thresholds. Previous work with *SECHO (see Kettig and Landgrebe, 1975A; Kettig and Landgrebe, 1975B; and Kast and Davis, 1977) indicated that a homogeniety threshold of 15q (where q = the number of channels employed) was appropriate for a small number of channels. Recall that higher homogeneity thresholds increase the likelihood that the classifier will regard the pixels of the cell as belonging to a single spectral class. Based on this consideration and the previous work, classifications using the homogeneity thresholds 105, 140, 175, and 210 were conducted. Four values of the annexation threshold were also examined. As previously indicated in Chapter 3, the likelihood that two cells are regarded as belonging to the same spectral class increases with decreasing annexation thresholds. Since the threshold is compared to the logarithm of the computed likelihood ratio, classifications were conducted with a narrow range of annexation thresholds (i.e., 3.0, 4.0, 5.0, and 6.0). Sixteen classifications were conducted using each possible combination of the four homogeneity

and annexation thresholds. The 30 meter spatial resolution data were used in each of these classifications.

Figure 4.6 illustrates the results of these preliminary tests with the *SECHO classifier. The overall percentage of test pixels correctly classified (PCC) is plotted against homogeneity threshold and annexation threshold. The overall PCC by threshold combination displayed by this response surface, appears to vary quite regularly across homogeneity thresholds for each annexation threshold. The general trend of the overall PCC by homogeneity threshold is very similar for each annexation threshold. This provides the analyst some indication that the accuracies achieved with any particular annexation threshold, in the range of values examined here, will increase with lower homogeneity thresholds (at least down to 105). At higher homogeneity thresholds the highest overall PCC appears to be provided by an annexation threshold of 5.0. At the lowest homogeneity threshold examined (i.e., 105) overall PCC was higher for an annexation threshold of 6.0 than that of 5.0. The scale of the percent correct classification (based on test pixels) ranges from 72.5 percent tc 75.0 percent, which implies that within the range of thresholds examined, the supervised ECHO classifier is quite robust; that is, the performance of the classifier is stable over the range of thresholds examined. The point of convexity of the response surface appears to lie somewhere between the homogeneity threshold of zero and 105 and an annexation threshold of greater than 6.0. However, resources did not permit the allocation of further efforts to locating this point of convexity.

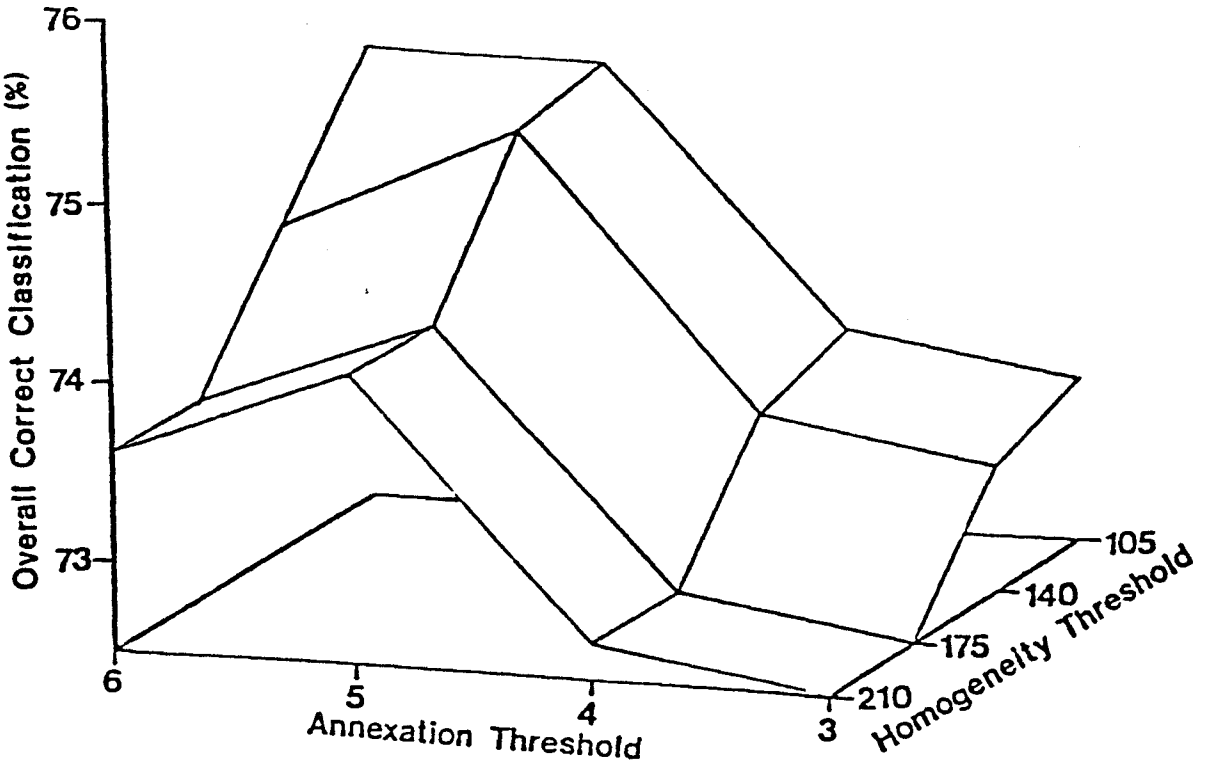

Figure 4.6 Response Surface in Percent Overall Correct Classification, by Homogeneity Threshold, by Annexation Threshold, Obtained with the *SECHO Classifier using the 30 Meter Spatial Resolution Data (CAM1S).

Evaluation Using Training Field Pixels. The overall percent correct classification of training field pixels with the per-point GML classifier (89.3 percent) was found to be significantly lower (a = 0.10) than the overall PCC achieved with the *SECHO classifier (94.1 percent) using the 30 meter spatial resolution data. Figure 4.7 illustrates the PCC achieved with each classifier for each cover class. Table 4.3 provides a summary of the statistical evaluation of the differences between PCC levels achieved with each of the classifiers for each of the cover classes. The PCC achieved with *SECHO was found to be statistically greater (a = 0.10) than that achieved with the per-point GML approach for marsh vegetation, soil, old-age hardwood, clearcut, and second growth hardwood. The PCC achieved with the per-point GML approach was found to be statistically greater than that achieved with *SECHO only for water. This difference is considered to be due to the previously detailed contaminations present in the water Training fields. These results indicate that improvements in overall classification accuracies can be achieved with *SECHO (a per-field classifier) compared to the accuracies achieved with the per-point GML classifier using 30 meter spatial resolution data. Improvements in classification performance are variable when differences are examined on the basis of individual cover classes. Both old age hardwood and clearcut are associated with a considerable level of spectral variability among adjacent pixels. While old age hardwood appears to have a higher degree of spectral variability among adjacent pixels than does second growth hardwood, greater apparent improvements in PCC were

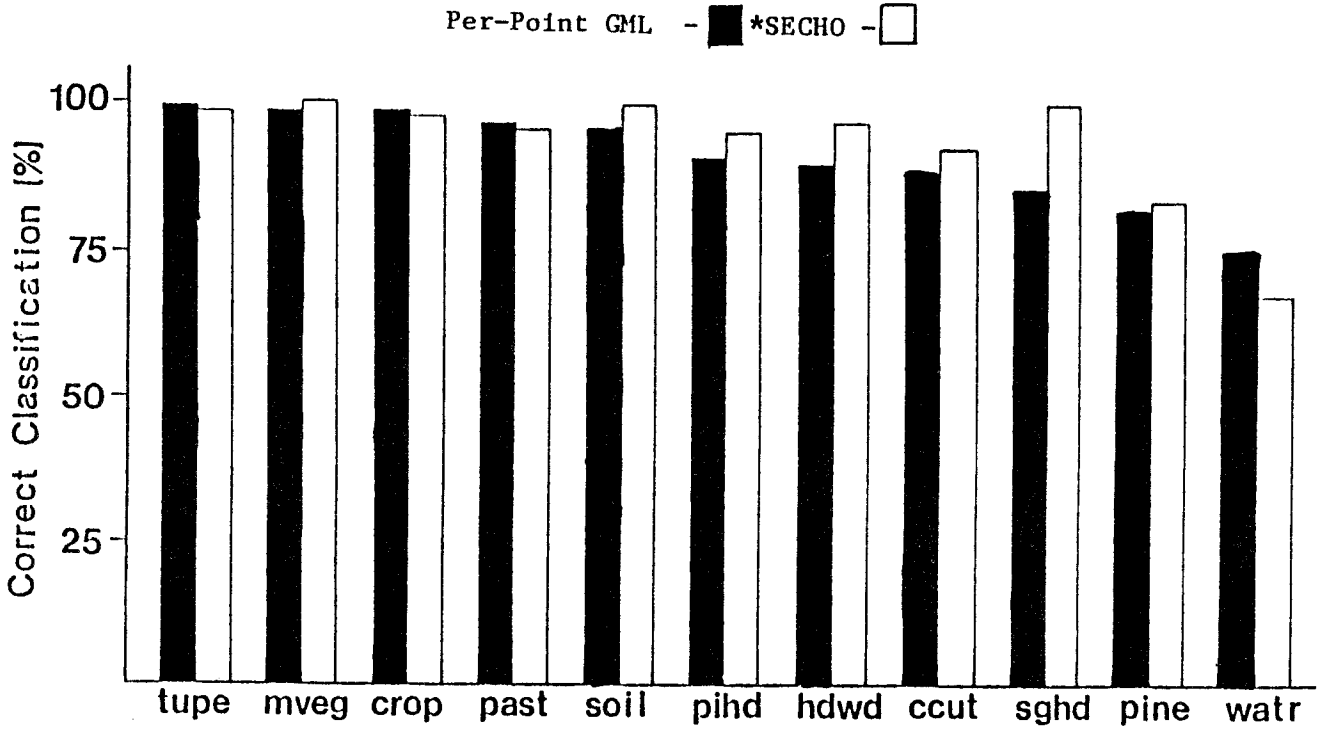

Figure 4.7 Percent Correct Classification by Cover Class Achieved with the *SECHO Classifier as Compared to the Per-Point GML Classifier using 30 Meter Spatial Resolution Data (Training Field Pixels, CAMIS).

Table 4.3 Statistical Evaluation of Classification Performances by Cover Class Achieved with the *SECHO Classifier and the Per-Point GML Classifier using 30 Meter Spatial Resolution Data (Training Field Pixels, CAM1S).†

Cover Class	Classifier: Per-Point GML	Classifier: *SECHO	Harmonic Mean
Tupe	98.9[a]	97.4[a]	350
Mveg	97.6[a]	100.0[b]	294
Crop	97.1[a]	96.6[a]	1445
Past	95.6[a]	94.1[a]	987
Soil	95.7[a]	99.3[b]	1946
Pihd	89.8[a]	93.6[a]	314
Hdwd	88.5[a]	95.5[b]	3997
Ccut	87.0[a]	90.4[b]	4277
Sghd	85.1[a]	99.8[b]	2242
Pine	81.1[a]	82.2[a]	805
Watr	74.8[b]	66.5[a]	428

†Dissimilar superscripts within each particular cover class denotes a significant difference at the $\alpha = 0.10$ level of confidence based on the Newman-Keuls' range test conducted on the arcsin transformed proportions. The proportions are the relative rates of <u>omission</u> in classification.

achieved for the second growth hardwood class than were achieved for old-age hardwood. The properties of the cover classes which are responsible for these improvements with the use of *SECHO are not clearly indicated by the results achieved for each cover class. A comparison of the classification performances for each cover class using some index which combines the omission and commission components of classification "error" may provide more insight regarding the relationship between classification performance, cover class, and classifier.

Evaluation Using Test Pixels. The overall percentage of test pixels correctly classified by the *SECHO classifier (75.0 percent) was statistically greater (a = 0.10) than that achieved with the per-point GML classifier (71.2 percent). These proportions were determined from classifications of 545 text pixels. Figure 4.8 illustrates the test pixel PCC achieved with the *SECHO and the per-point GML classifiers for each cover class. Table 4.4 provides a summary of the statistical evaluation of the differences between the PCC achieved with the two classifiers for each cover class. Only the accuracies achieved for the clearcut class were statistically different between the two classifiers.

The harmonic means of the number of the test pixels available for the evaluation of each classification indicate that an insufficient number of observations were available to adequately assess the apparent differences in PCC levels achieved for several of the cover classes. Comparing the relative PCC levels of second growth hardwood in Table

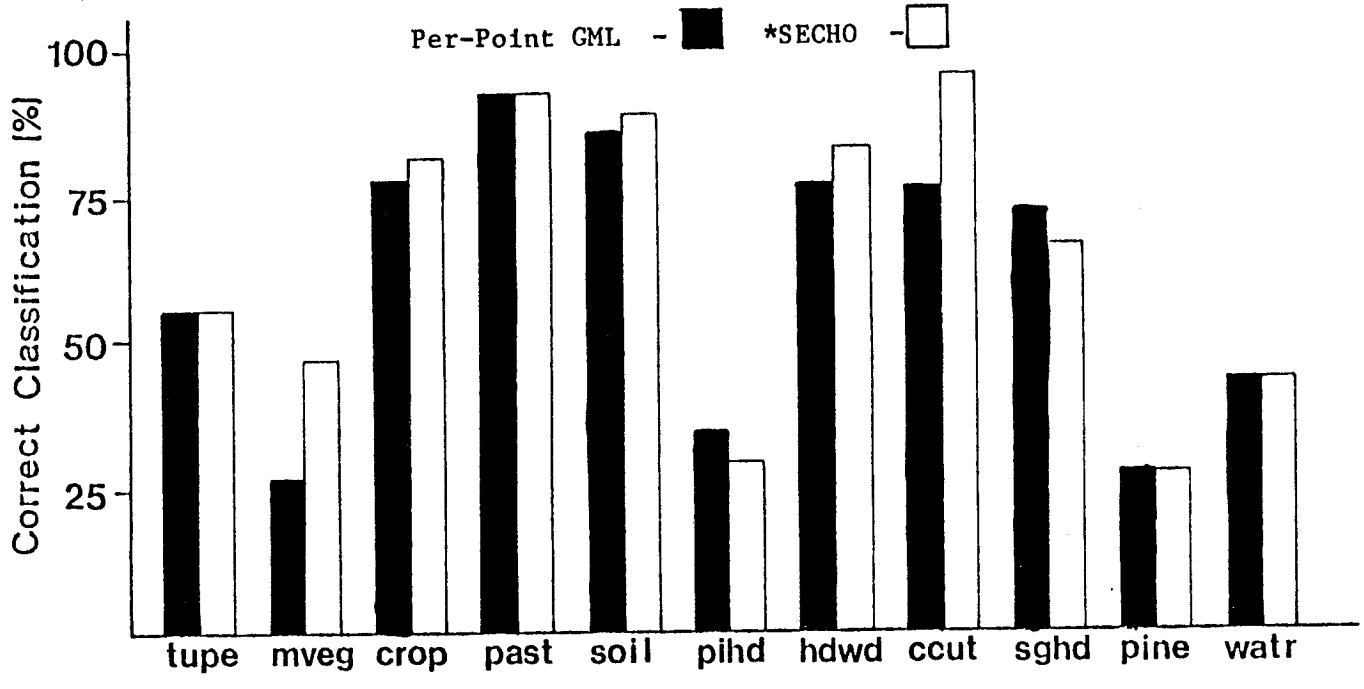

Figure 4.8 Percent Correct Classification by Cover Class Achieved with the *SECHO Classifier as Compared to the Per-Point GML Classifier using 30 Meter Spatial Resolution Data (Test Pixels, CAM1S).

Table 4.4 Statistical Evaluation of Classification Performances by Cover Class Achieved with the *SECHO Classifier and the Per-Point GML Classifier using 30 Meter Spatial Resolution Data (Test Pixels, CAMIS).†

Cover Class	Classifier: Per-Point GML	Classifier: *SECHO	Harmonic Mean
Tupe	55.6[a]	55.6[a]	9
Mveg	26.3[a]	47.4[a]	19
Crop	78.8[a]	81.8[a]	33
Past	92.9[a]	92.9[a]	14
Soil	85.9[a]	89.1[a]	64
Pihd	35.5[a]	29.0[a]	31
Hdwd	77.6[a]	83.3[a]	156
Ccut	76.1[a]	95.8[b]	71
Sghd	72.4[a]	66.7[a]	123
Pine	27.3[a]	27.3[a]	11
Watr	42.9[a]	42.9[a]	14

†Dissimilar superscripts within each particular cover class denotes a significant difference at the $\alpha = 0.10$ level of confidence based on the Newman-Keuls' range test conducted on the arcsin transformed proportions. The proportions are the relative rates of <u>omission</u> in classification.

4.3 to those in Table 4.4 indicates a tremendous shift in relative classification performance for second growth hardwood. This large apparent shift in classification accuracy determined for the second growth hardwood raises questions concerning the value of comparisons based solely on the omission component of error. There is an apparent need for a more stable index for conducting comparisons on a cover class basis.

On the basis of overall classification performance, the results obtained with test pixels confirm the results obtained with training field pixels. The use of the *SECHO per-field approach is expected to provide higher overall classification accuracies using 30 meter spatial resolution data than are achieved with the per-point GML approach. Similar improvements in PCC are expected for some individual cover classes but the results are not entirely consistent between estimates provided by training and test pixels. The larger difference between training field pixel PCC and test pixel PCC (water tupelo, marsh vegetation, pine-hardwood mix, and pine) as compared to the differences in PCC achieved with the different classifiers, indicate that the degree to which the training statistics represent the respective cover classes can be a more important factor than the classifier employed.

Flight Line CAM2N

Per-Point GML Classification Using Data of Different Spatial Resolutions

Evaluation Using Training Field Pixels. Overall classification accuracies, based on training field pixels, increased with decreasing spatial resolution only over the range of 15 to 45 meter spatial resolutions (as illustrated in Figure 4.9). Further decreases in spatial resolution beyond 45 meters resulted in an apparent decrease in overall classification accuracy. The differences in PCC level achieved with the 45 and 80 meter spatial resolution data are not statistically significant at the a = 0.10 level of confidence. All other differences among overall classification performances are significant (a = 0.10). The differences in the relationship between classification accuracy and spatial resolution observed in CAM2N as opposed to CAM1S are perhaps due primarily to differences in characteristics of the scene. Recall, from the section describing the study site, that CAM2N is located on the deeply disected Piedmont escarpment. The physiography of CAM2N results in relatively small contiguous areas occupied by the individual cover classes. This was well illustrated in the aerial photography contained in Figure 3.2. A quantitative index for comparing this scene related characteristic of CAM2N to CAM1S was presented in Tables 3.7

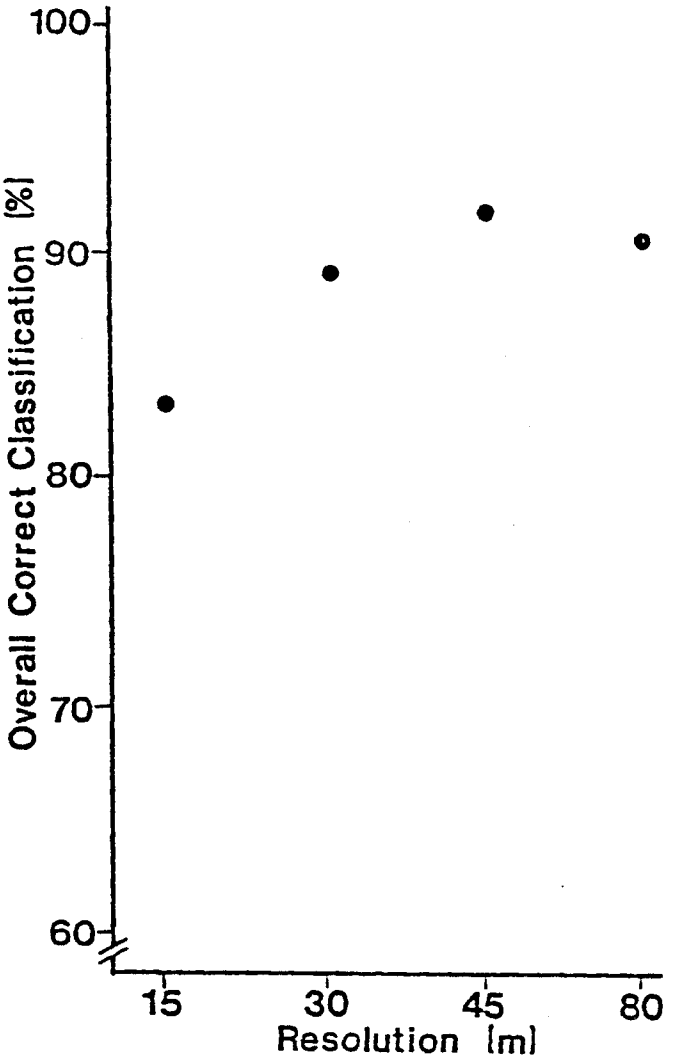

Figure 4.9 Overall Percent Correct Classification of Training Field Pixels by Spatial Resolution (Per-Point GML Classifier, CAM2N).

and 3.8. The average "field" (i.e., a contiguous area occupied by an individual cover class) size, based on the values in Tables 3.7 and 3.8, in CAM2N is about 38 percent of the average field size in CAM1S. The average number of pixels per spectral class for the cover classes of CAM2N is about 50 percent of that for CAM1S. Since the overall PCC values presented in Figure 4.9 are based on training field pixels, the relative differences in overall PCC levels observed for CAM2N may differ from those observed for CAM1S due to a critical reduction in the number of pixels used in computing the training statistics. A reduction in the number of pixels available for training the classifier was previously recognized as a natural consequence of low spatial resolution data in the context of the supervised clustering technique employed in the training phase of the analysis. While the number of training pixels obtained for CAM1S relative to the number obtained for CAM2N would provide a lower estimated variance associated with the PCC and, consequently, a more sensitive test for significant differences between PCC levels, the outcome of the tests is not thought to be determined by this factor. The arithmetic difference between the overall PCC observed for the 45 meter and 80 meter spatial resolution data in CAM2N (91.2 and 90.5 percent, respectively) is much lower than that observed in the analysis of CAM1S (91.9 and 94.5 percent, respectively). The 80 meter spatial resolution data failed to provide an improvement in the overall percent correct classification either due to :

1) cover class conditions which were invariant with respect to spatial resolution after the 45 meter resolution level,

2) due to a critical reduction in the number of pixels in some of the spectral classes such that convergence on the parameters failed to occur (see Duda and Hart, 1973 on the "unexpected problem of dimensionality"), or

3) some other factor.

The PCC by cover class achieved with the per-point GML classifier with data of each spatial resolution is illustrated by the response surface in Figure 4.10. A summary of the statistical evaluation of the differences between PCC levels achieved with data of each spatial resolution is provided for each cover class in Table 4.5. The results appear to vary considerably between cover classes. In every case, except pine, where the differences are <u>significant</u> (a = 0.10) the highest accuracies are achieved with the 45 meter spatial resolution data. In cover classes associated with high levels of spectral variability across adjacent pixels, such as clearcut and urban, the relationship between PCC and spatial resolution is not consistent with that observed in CAM1S. Classification accuracy increases in the urban class from 15 meter to 30 meter spatial resolution but differences between PCC achieved with the 30 meter, 45 meter, and 80 meter spatial resolution data were not significant (a = 0.10). In the clearcut areas, the PCC levels achieved with data of each spatial resolution were statistically different, but the highest PCC was obtained with the 45 meter spatial resolution data. The pine cover class in CAM2N has a wide range of canopy closures resulting in a considerable level of spectral variability across adjacent pixels. The PCC levels achieved in the pine cover class were statistically different at the a = 0.10 level of confidence, but the highest PCC was achieved with the 30 meter

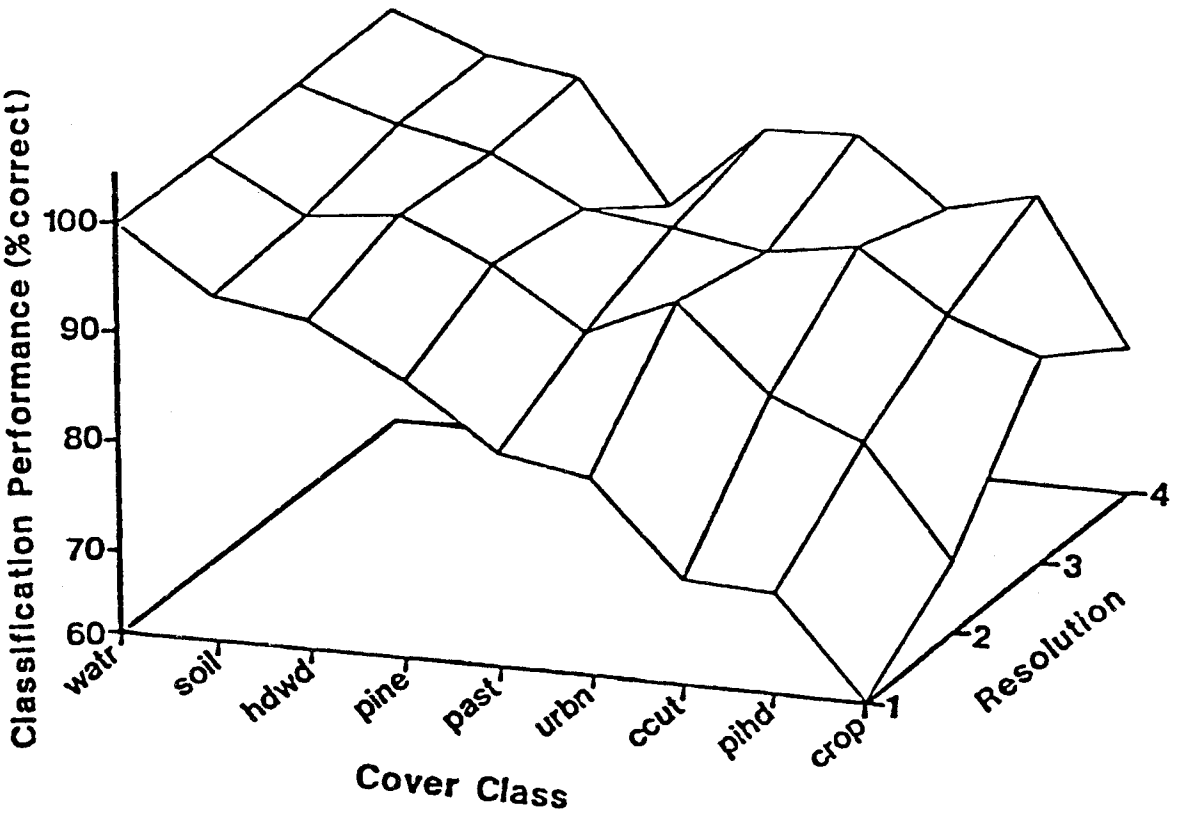

Figure 4.10 Response Surface in Percent Correct Classification by Cover Class, for each Spatial Resolution (Training Field Pixels, Per-Point GML Classifier, CAM2N).

Table 4.5 Statistical Evaluation of Classification Performances by Cover Class for each Spatial Resolution (Training Field Pixels, Per-Point GML Classifier, CAM2N).†

Cover Class	Spatial Resolution 15 Meter	30 Meter	45 Meter	80 Meter	Harmonic Mean
Watr	99.7[a]	99.5[a]	99.6[a]	100.0[a]	294.81
Soil	93.4[a]	94.5[a]	96.7[a]	96.7[a]	288.03
Hdwd	91.9[a]	95.5[b]	94.7[b]	95.3[b]	887.87
Pine	87.0[b]	91.5[d]	90.2[c]	83.7[a]	564.14
Past	80.8[a]	85.6[b]	89.4[c]	91.8[c]	401.97
Urbn	79.2[a]	89.5[b]	87.7[b]	92.5[b]	181.21
Ccut	70.4[a]	81.5[b]	89.2[d]	86.3[c]	755.53
Pihd	69.9[a]	77.8[b]	83.4[c]	88.5[d]	293.81
Crop	60.3[a]	67.2[b]	80.4[c]	74.5[c]	119.91

†Dissimilar superscripts within each particular cover class denotes a significant difference at the $\alpha = 0.10$ level of confidence based on the Newman-Keuls' range test conducted on the arcsin transformed proportions. The proportions are the relative rates of <u>omission</u> in classification.

resolution data and the lowest was achieved with the 80 meter resolution data. These evaluations are based solely on the omission error and perhaps a more meaningful index for comparing classification performance would be provided by some measure which combines the commission and omission error.

Evaluation Using Test Pixels. The overall PCC achieved for test pixels using data of each spatial resolution is provided in Figure 4.11. The overall PCC observed for the 80 meter spatial resolution data (63.3 percent) was statistically ($a = 0.10$) lower than the PCC observed for all other spatial resolutions. The differences observed among the PCC levels achieved with data of 15, 30, and 45 meters (75.3, 72.3, and 70.5 percent, respectively) were not significant at the $a = 0.10$ level of confidence. These results indicate that no real differences between PCC levels are expected when using data of any of the higher spatial resolutions. The lower PCC achieved with the 80 meter spatial resolution is believed to result, in part, from the factors discussed in the section on "training field pixel evaluation" and, in part, because of "field" size.

There is always some frequency of error associated with the location and identification of areas in a scene. As the field size decreases the requirement for higher precision of location increases in order to avoid field boundaries. The frequency of error associated with avoiding boundaries is therefore expected to increase as the field size decreases. While this is an error on behalf of the analyst to provide "pure" pixels for testing, it is also an indication of the

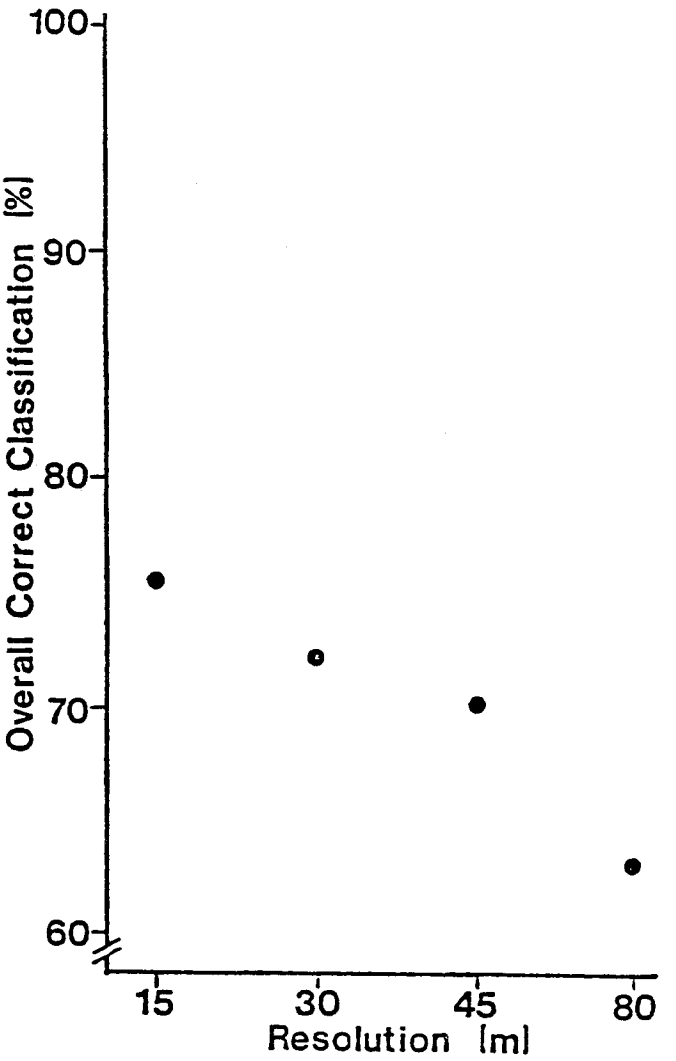

Figure 4.11 Overall Percent Correct Classification of Test Pixels by Spatial Resolution (Per-Point GML Classifier, CAM2N).

information provided by the classification. Only 376 "pure" pixels were identified by the analyst out of the 1428 provided by the sampling grid. This reduction resulted from a rigorous adherence to the test pixel inclusion criteria (i.e., that the "pixel" of the lowest spatial resolution occur in only one cover class and that the cover class be identifiable at a high level of confidence on the part of the analyst). In spite of this degree of selectiveness, the 80 meter data PCC results were significantly lower than the PCC achieved with the data of the other resolutions.

Figure 4.12 illustrates the relative PCC by cover class achieved with data of each spatial resolution. Table 4.6 provides a summary of the statistical evaluation of the differences between the PCC levels, by cover class. In general, the results are extremely variable and fail to identify the superiority of any particular resolution. The PCC of urban appears to increase with decreasing resolution, but the differences are significant ($a = 0.10$) only between the 15 meter and 80 meter resolutions. This is probably due to the high level of spectral variability across adjacent pixels associated with urban areas. However, other cover classes associated with high levels of spectral variability across adjacent pixels, such as clearcut and pine, do not demonstrate higher PCC with lower resolution. Hardwood forests in this area do not display the level of "texture" that was characteristic of CAM1S. In other cover classes (eg., soil, pine and hardwood) the higher spatial resolution data provided higher classification accuracies, but differences were generally not significant among PCC achieved with data of the higher resolutions.

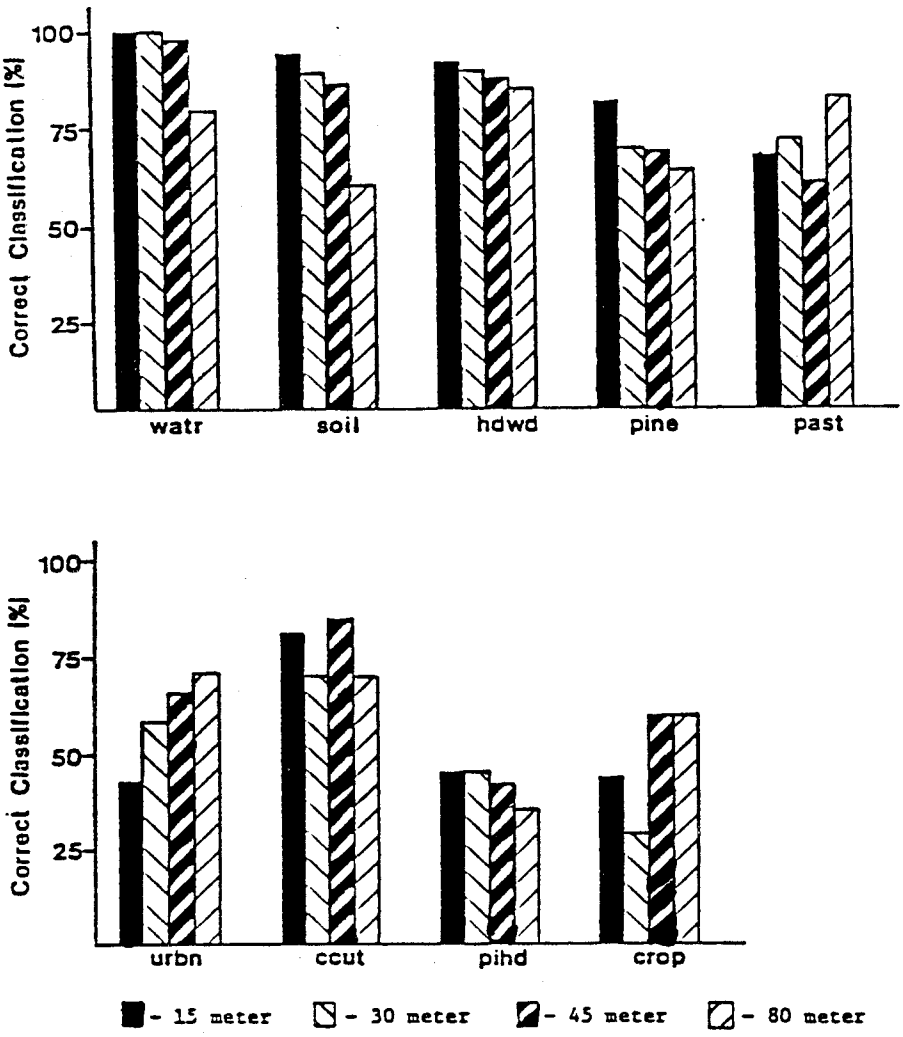

Figure 4.12 The Percent Correct Classification of Test Pixels by Spatial Resolution for each Cover Class (Per-Point GML Classifier, CAM2N).

Table 4.6 Statistical Evaluation of Classification Performances by Cover Class, for each Spatial Resolution (Test Pixels, Per-Point GML Classifier, CAM2N).†

Cover Class	Spatial Resolution 15 Meter	30 Meter	45 Meter	80 Meter	Harmonic Mean
Watr	100.0^{b}	100.0^{b}	96.7^{b}	76.7^{a}	30
Soil	96.2^{b}	88.5^{b}	84.6^{b}	57.7^{a}	26
Hdwd	92.5^{b}	90.3^{b}	87.1^{b}	80.6^{a}	93
Pine	78.9^{b}	67.6^{a}	66.2^{a}	59.2^{a}	71
Past	64.0^{ab}	72.0^{ab}	60.0^{a}	80.0^{b}	25
Urbn	42.9^{a}	57.1^{ab}	64.3^{ab}	71.4^{b}	14
Ccut	77.1^{a}	71.4^{a}	80.0^{a}	71.4^{a}	35
Pihd	45.3^{b}	45.3^{b}	40.0^{b}	32.0^{a}	75
Crop	42.9^{a}	28.6^{a}	57.1^{a}	57.1^{a}	7

†Dissimilar superscripts within each particular cover class denotes a significant difference at the $\alpha = 0.10$ level of confidence based on the Newman-Keuls' range test conducted on the arcsin transformed proportions. The proportions are the relative rates of <u>omission</u> in classification.

The differences between the training field pixel PCC levels and the test pixel PCC levels observed for CAM2N confirm the finding in CAM1S that the degree to which the training areas represent the remainder of the area to be classified is a more important factor than the spatial resolution employed in the classification. While the water, bare soil, hardwood and clearcut areas were fairly well represented by the training statistics, the urban, pine-hardwood mix, and crop were not generally well represented.

The small field size of CAM2N also appeared to be a determining factor. While the strict adherence to a "pure" pixel was intended throughout the test pixel selection procedure, the likelihood of boundary pixels being included in the test pixel set for CAM2N is believed to be much higher due to the small field size. In an area where the "pure" pixel restriction on test pixel selection resulted in three-fourths of the test pixels being rejected, the effect of the relative number of boundary pixels on classification results is expected to be large.

The lower classification accuracies achieved with the 80 meter spatial resolution data is believed to be due, in part, to: 1) the relatively low number of pixels per spectral class for the 80 meter resolution data, resulting in lack of convergence on the "population" parameters, 2) the small field sizes characteristic of the area, and 3) the relative lack of cover classes with large levels of spectral variability across adjacent pixels.

Classification Results Using *SECHO Compared to Results Using the Per-Point GML Classifier

Evaluation Using Training Field Pixels. The 30 meter spatial resolution data of CAM2N were also classified using the *SECHO classifier. While the overall PCC achieved with *SECHO (90.2 percent) was statistically greater than that achieved with the per-point GML approach (88.8 percent), the arithmetic difference was very low (1.4 percent). The percentages of training field pixels correctly classified for each cover class using *SECHO are compared with the PCC achieved with the per-point GML classifier in Figure 4.13. The statistical evaluation of the differences illustrated in Figure 4.13 are summarized in Table 4.7. The results achieved with *SECHO are statistically greater (a = 0.10) than those achieved with the per-point for urban, clearcut, pine-hardwood mix, and crop areas. The results observed in the urban and clearcut cover classes are in accordance with the design intentions of the *SECHO classifer in that it tends to accomodate higher levels of spectral variability across adjacent pixels than does the per-point approach.

The PCC achieved with the per-point classifier were statistically greater than those achieved with *SECHO for hardwood and pine forest areas. While the arithmetic differences were not very large for the hardwood class (2.0 percentage points), the difference associated with the pine forest cover class was quite large (16.1 percentage points). A possible explanation for this result is that areas of low crown closures which have illuminated ground cover visible from the reference

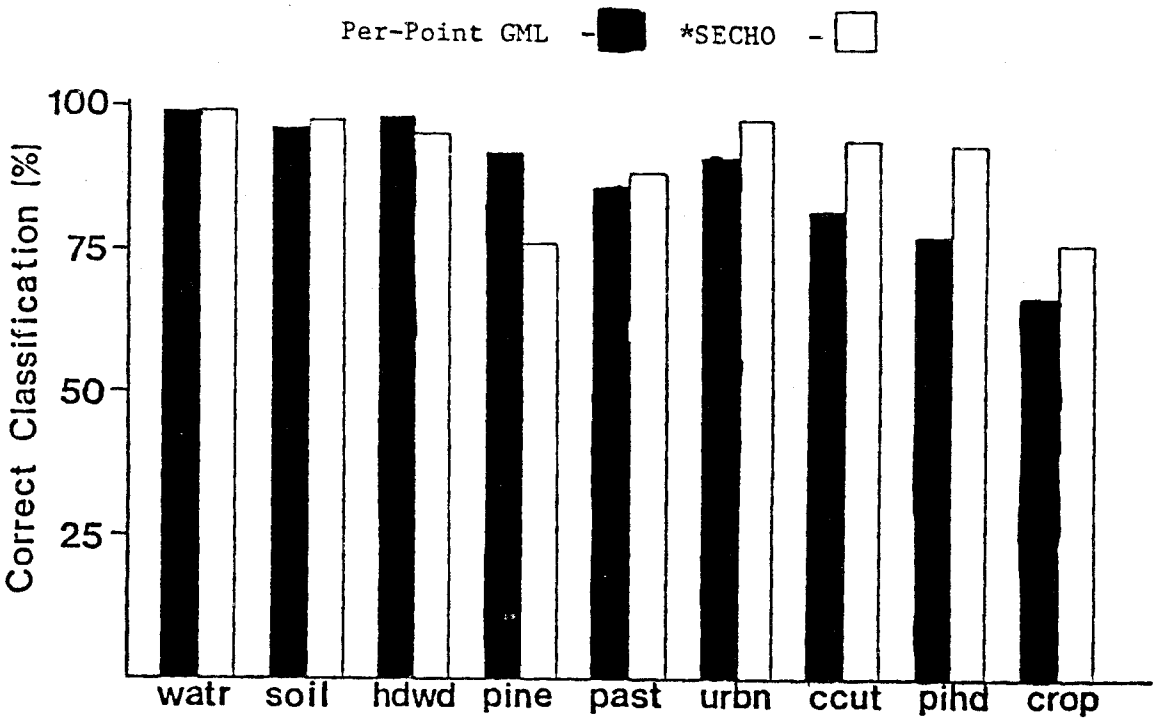

Figure 4.13 Percent Correct Classification by Cover Class Achieved with the *SECHO Classifier as Compared to the Per-Point GML Classifier using 30 Meter Spatial Resolution Data (Training Field Pixels, CAM2N).

Table 4.7 Statistical Evaluation of Classification Performances by Cover Class Achieved with the *SECHO Classifier and the Per-Point GML Classifier using 30 Meter Spatial Resolution Data (Training Field Pixels, CAM2N).†

Cover Class	Classifier: Per-Point GML	Classifier: *SECHO	Harmonic Mean
Watr	99.5[a]	99.5[a]	591
Soil	94.5[a]	94.8[a]	561
Hdwd	95.5[b]	93.5[a]	1793
Pine	91.5[b]	75.4[a]	1106
Past	85.6[a]	87.2[a]	846
Urbn	89.5[a]	96.1[b]	363
Ccut	81.5[a]	93.3[b]	1607
Pihd	77.8[a]	92.8[b]	511
Crop	67.2[a]	75.4[b]	228

†Dissimilar superscripts within each particular cover class denotes a significant difference at the $\alpha = 0.10$ level of confidence based on the Newman-Keuls' range test conducted on the arcsin transformed proportions. The proportions are the relative rates of <u>omission</u> in classification.

point of the scanner may be more similar spectrally to the pine-hardwood mix class when the measured irradiance of a 2-by-2 cell of 30 meter pixels is examined. Computations involving the commission error indicated that 97 percent of the commission error in pine-hardwood mix were actually pixels of the pine forested cover class. This same component of the commission in pine-hardwood constituted 78 percent of the omission error in the PCC of pine. Apparently, sampling the irradiances associated with pine areas with a cell of pixels results in an average spectral response very similar to pine-hardwood mix for many of the areas in pine.

Evaluation Using Test Pixels. The overall PCC of test pixels achieved with *SECHO (72.5 percent) was not statistically different from that achieved with the per-point approach (72.5 percent). Figure 4.14 illustrates the PCC levels achieved for each cover class through the use of *SECHO as compared to the per-point classifier. Table 4.8 provides a summary of the statistical evaluation of the differences in PCC level. Relatively high classification accuracies were achieved for water, bare soil and hardwood indicating that the training statistics were representative of of their respective cover classes. High classification accuracy was maintained by *SECHO for the urban, with statistically ($a = 0.10$) lower PCC levels provided by the per-point. This result indicates that the *SECHO classifier tends to perform better than the per-point classifier in the context of some degree of spectral variability. The *SECHO achieved an arithmetically higher PCC for clearcut than did the per-point (i.e., 80.0 percent versus 71.4

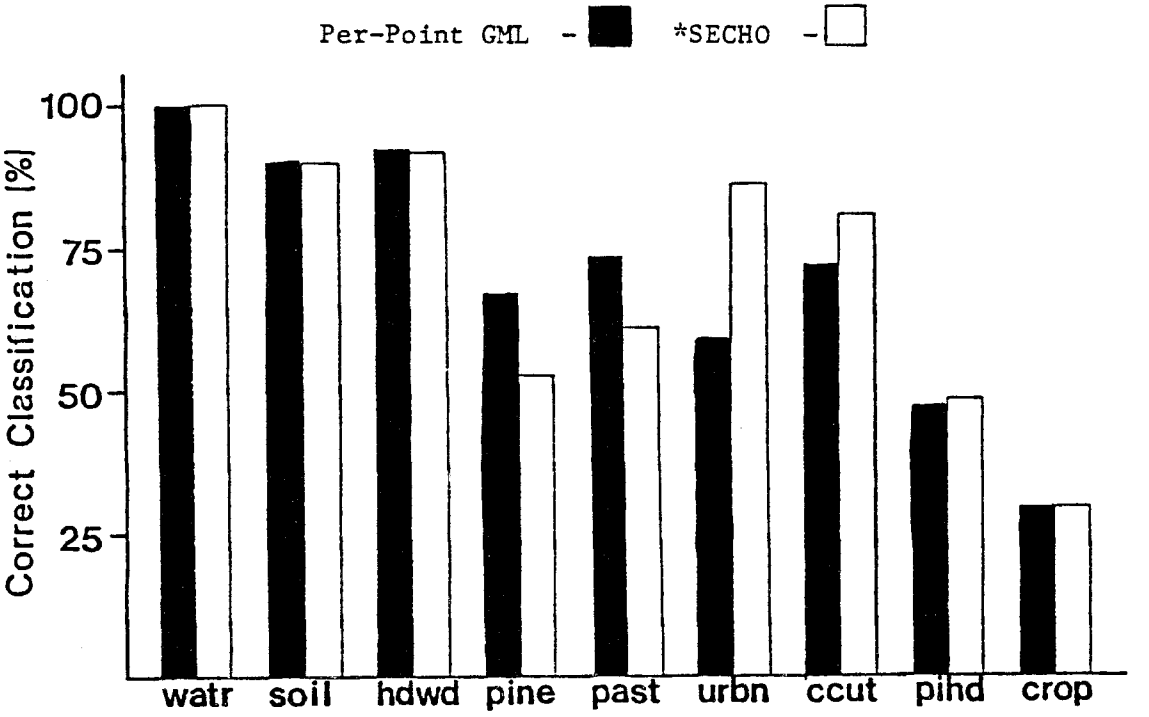

Figure 4.14 Percent Correct Classification by Cover Class Achieved with the *SECHO Classifier as Compared to the Per-Point GML Classifier using 30 Meter Spatial Resolution Data (Test Pixels, CAM2N).

Table 4.8 Statistical Evaluation of Classification Performances by Cover Class Achieved with the *SECHO Classifier and the Per-Point GML Classifier using 30 Meter Spatial Resolution Data (Test Pixels, CAM2N).†

Cover Class	Classifier: Per-Point GML	Classifier: *SECHO	Harmonic Mean
Watr	100.0[a]	100.0[a]	30
Soil	88.5[a]	88.5[a]	26
Hdwd	90.3[a]	89.2[a]	93
Pine	67.6[b]	52.1[a]	71
Past	72.0[a]	60.0[a]	25
Urbn	57.1[a]	85.7[b]	14
Ccut	71.4[a]	80.0[a]	35
Pihd	45.3[a]	46.7[a]	75
Crop	28.6[a]	28.6[a]	7

†Dissimilar superscripts within each particular cover class denotes a significant difference at the $\alpha = 0.10$ level of confidence based on the Newman-Keuls' range test conducted on the arcsin transformed proportions. The proportions are the relative rates of <u>omission</u> in classification.

percent, respectively), but this difference was not found to be significant at the a = 0.10 confidence level. The PCC for test pixels achieved for pine with the per-point classifier was statistically (a = 0.10) greater than that achieved with *SECHO. Only 53 percent of the total omission error of pine is involved in the commission error of pine-hardwood mix for the test pixels.

The differences in PCC achieved between training and text pixels for the pine, pine-hardwood mix, and crop cover classes indicates that training methods and training field selection are more important than the classifier employed.

SUMMARY AND CONCLUSIONS

This investigation provided some very important insights regarding classification accuracies achieved with multispectral scanner data of different spatial resolution used with the conventionally employed per-point GML classifier. Classification accuracies achieved with the per-point GML classifier using 30 meter spatial resolution data were also compared to classification accuracies, using the same data, obtained with the *SECHO (a per-field) classifier. These findings are summarized as:

1) The degree to which the probability density functions, employed by the classifier actually represent the spectral variability of each of the cover classes of interest is a more important determinant of classification performance than either the spatial resolution of the data or the classifier employed (over the range of resolutions and classifiers examined).

2) Provided the probability density functions represent the spectral variability associated with each cover class, higher overall classification accuracies were obtained with the use of lower spatial resolution data.

3) Higher classification accuracies using lower spatial resolution data were obtained for cover classes characterized by a relatively large degree of spectral variability across adjacent pixels (eg., old age hardwood, second growth hardwood, clearcut, and urban) as opposed to those cover classes associated with

relatively low levels of spectral variability across adjacent pixels (eg., soil, crops, pasture, and water).

4) Cover classes with very distinct spectral characteristics, in spite of relatively high levels of spectral variability across adjacent pixels (eg., water tupelo), were classified with a high degree of accuracy regardless of the spatial resolution of the data employed (over the range of resolutions examined here).

5) Higher spatial resolution data provided higher classification accuracies in areas where the cover classes occupy relatively small contiguous areas (i.e., where "field" sizes are small).

6) Provided the probability density functions represent the spectral varibility associated with each respective cover class, higher accuracies were obtained with the use of the *SECHO than with the per-point GML classifier.

7) Greater improvements in overall classification accuracies were achieved with the *SECHO versus the per-point GML classifier for areas where the "field" sizes are large as opposed to areas where the "field" sizes are relatively small.

8) Higher classification accuracies were obtained for cover classes associated with relatively high degrees of spectral variability (eg., old age hardwood, second growth hardwood, clearcut, and urban) with the *SECHO classifier as compared to the per-point GML classifier when using 30 meter spatial resolution data.

9) Training procedures which are appropriate for data of high spatial resolution are not necessarily well suited for developing training statistics for low spatial resolution data. While a supervised clustering approach, such as the one employed in this study, is well suited for high spatial resolution data, some other technique, such as the "multi-cluster blocks" approach (Flemming, 1977), may be better suited for use with data of low spatial resolution.

RECOMMENDATIONS

Investigating any particular problem always seems to be a process which rarely provides as many answers as it does questions. The avenues for further examination of the problem of spatial resolution, as well as many of the activities associated with computer-based classification of spectral data, are many. The primary recommended research activities identified while conducting this investigation are summarized below.

1) Experiments should be designed which examine various resolutions in combination with various signal-to-noise ratios. A data set with perhaps four levels of each, with a design which would allow a test for each factor effect and their interaction, would provide insight into the impact of the spatial frequency of the spectral variability associated with different cover classes as compared to the effect of the signal-to-noise ratio in the data itself. Both of these data characteristics vary with spatial resolution.

2) Each step of the analysis process was held constant for the classifications conducted with data of each spatial resolution to avoid introducing additional variables which may confound the variable of interest (i.e., spatial resolution of the data) and, therefore, obfuscate the interppretation of the results. However, to determine relative classification accuracies which would be expected in a more operational setting (i.e., where each analysis

procedure is conducted independently), a comparison is needed of classification accuracies achieved with each spatial resolution where every phase of the analysis is conducted in a way most suited for each particular resolution. High resolution MSS data lends itself well to a supervised clustering approach to training the classifier. Lower resolution MSS data is better suited for an unsupervised or "multi-clustered blocks" approach. Comparisons should be made between resolutions based on analysis steps most suited for each particular resolution.

In conjunction with this independent analysis approach, classification should be conducted with data of different spatial resolution over areas for which a "wall-to-wall" ground reference data base exists. This would provide results which indicate the degree to which the higher relative frequency of boundary pixels over-rides the effect of the lower spectral variability, both of which are associated with lower spatial resolution data.

3) The task of providing a method for determining "classification accuracy" has plagued the remote sensing community in practical applications as well as more developmental investigations. Error estimations based on observations which must satisfy some set of criteria, restrictive to one degree or another, tend to test as many factors associated with the analyst and the study area, as they do the classification performance. In the context of applications, boundary pixels classified as either of the cover classes located at the boundary is an acceptable decision, whereas the classification of that pixel into another

unassociated class is not an acceptable decision. Methods for evaluating classification results need to be examined which remove analyst bias from the selection of test pixels (eg., random stratified sampling) and which can accomodate more than one analyst defined label. This would provide a results evaluation technique which would accomodate boundary pixels and remove analyst bias involved in test pixel selection. Also, the sample size would not be restricted by some pre-defined grid size.

The "cost" associated with various instances of omission and commission are not equal across the error matrix. The classification of pine-hardwood mix as pine, or hardwood, could hardly be thought to have the same "cost" as classifying the same area as crops or pasture. A technique needs to be examined which allows the analyst to assign weights to the addresses of the error matrix. The relative value of the weight is chosen to reflect the relative "cost" associated with each particular instance of omission and/or commission. Overall classification accuracies would therefore be more meaningful for purposes of comparing classification performances.

Investigations are needed which evaluate classification results by cover class employing some combination of the error associated with omission and commission. The use of the arithmetic mean of the two components of error would apply where the interest is strictly in the probability of an erroneous labeling. Some combination such as the root mean square of the error (1-PCC) would provide a measure affected by the magnitude of

the difference between omission and commission which would provide a way to counter high accuracy estimates based on omission which are achieved at the expense of high levels of commission. The entire process of classification evaluation is in need of much attention, from sampling design to calculating a meaningful index.

4) A measure of spectral variability across neighboring pixels should be investigated to provide a numerical representation of a factor which is considered to be very important with regards to classification accuracy achieved with data of different spatial resolutions. Possible measures of the spectral variability across neighboring pixels might include : 1) the amplitude and frequency components of the Fourier series representing the variation in spectral response by line and/or column, 2) measures provided by spatial filters, 3) any one of the "texture" related measures found in the literature such as the angular second moment, contrast, and entropy of Haralick et al., (1973, 1974, 1979), or the texture I, texture II, or spatial sequency distribution presented by Herzog and Rathja (1973). The representation of spectral variability across adjacent pixels with some numerical measure would provide much additional insight into the variation in classification accuracies, with respect to cover class, observed in this study.

5) The refinement of existing algorithms and the development of new algorithms for preprocessing, training, classifying, evaluating, and post-classification processing are needed for the advancement of machine processing of remotely sensed data.

Software used for modeling and reducing the variation in response level due to variation in viewing angle should be generalized and thoroughly documented to facilitate further work with simulated TM data. Modifications on the clustering algorithm should be explored, such as the post convergence computation of cluster class variance of each channel with which to compute weights for successive iterations. This would reduce the frequency of erroneous class assignments due to the "over-importance" of channels with higher variances characteristic of unweighted, multivariate Euclidean distance measures. The *SECHO classifier should be modified to annex cells for which the likelihood ratio is highest rather than the first cell for which the likelihood ratio is greater than some threshold and/or multiple cell annexations. The processor used in evaluating the classification results (*PRINTRESULTS in the LARSYS software system) should either output a disk file of the omission and commission proportions or contain calls to statistical analysis software to facilitate results evaluation. Post classification smoothing, or reassignment, based on spatial variables, class probabilities, and overlaid ancillary data should be explored more fully. Continual refinement of the techniques and software will provide an effective means of improving current capabilities. Only through a tireless re-examination of the problems at hand, and the perspectives with which they are addressed, can we hope to push the technology forward.

LIST OF REFERENCES

REFERENCES

Anderson, J. R., E. E. Hardy, and J. T. Roach. 1972. "A Land-Use Classification System for Use with Remote-Sensor Data." Geological Survey Circular 671. p. 16.

Anderson, J. R., E. E. Hardy, J. T. Roach, and R. E. Witmer. 1976. "A Land-Use and Land-Cover Classification System for Use with Remote Sensor Data." U.S. Geological Survey Professional Paper 964, Washington D.C. p. 28.

Anderson, M. C. 1966. "Stand Structure and Light Penetration, II. A Theoretical Analysis." Journal of Applied Ecology, Vol. 3. pp. 41-54.

Anderson, T. W., 1958. An Introduction to Multivariate Statistical Analysis, John Wiley and Sons, Inc., New York, N.Y. 374 p.

Anuta, P. E. 1973. "Geometric Correction of ERTS-1 Digital Multispectral Scanner Data." LARS Information Note 103073, Laboratory for Application of Remote Sensing, West Lafayette, IN. 13 p.

Anuta, P. E. and D. F. Strahorn. 1973. "Sun Angle Effect Preprocessing with Predicted Ramp Functions." LARS Technical Memorandum T-12, 050673, Laboratory for Application of Remote Sensing, West Lafayette, IN. 7 p.

Anuta, P. E. and Nim-Yau Chu. 1979. "Multidimensional Scaling for Clustering of Dissimilar Data Types." LARS Information Note 050279, prepared for NSF, grant no. ENG-7614400. 27 p.

Atkinson, J. H. and R. E. Jones. 1963. "Atmospheric Limitations on Ground Resolution from Space Photography." SPIE, Vol. 1, 1963. pp. 39-42.

Baker, L. R. and R. M. Scott. 1975. "Electro-Optical Remote Sensors with Related Optical Sensors", in Manual of Remote Sensing, edited by R. G. Reeves, American Society of Photogrammetry. pp. 325-366.

Bartolucci, L. A. and R. B. de Castro. 1979. "Clustering of Landsat MSS Data: Certain Limitations." LARS Technical Report 060679, Laboratory for Application of Remote Sensing, West Lafayette, IN. 13 p.

Billings, W. D. and R. J. Morris. 1951. "Reflection of Visible and Infrared Radiation from Leaves of Different Ecological Groups." American Journal of Botany, Vol. 38, May 1951. pp. 327-331.

Blanchard, L. E. and Oscar Weinstein 1980, "Design Challenges of the Thematic Mapper.", IEEE Trans. on Geoscience and Remote Sensing, Vol. GE-18, No. 2, April 1980. pp. 146-160.

Clark, J. and N. A. Bryant. 1977. "Landsat-D Thematic Mapper Simulation Using Aircraft Multispectral Scanner Data." Proceedings of the Eleventh International Symposium on Remote Sensing of Environment, University of Michigan, Ann Arbor, Michigan. pp. 483-491.

Clark, Jerry, 1980. "The Effect of Resolution in Simulated Satellite Imagery on Spectral Characteristics and Computer-Assisted Land Use Classification." Master of Arts Thesis, 715-22 NASA, Jet Propulsion Laboratory. 86 p.

Cochran, William G., 1977, Sampling Techniques, 3rd edition, John Wiley and Sons, New York. 428 p.

Colvocoresses, A. P. 1980. "A Re-Examination of the Landsat MSS." Photogrammetric Engineering and Remote Sensing, Vol. 46, No. 6. pp. 765-766.

Colvocoresses, A. P. 1970. "ERTS-A Satellite Imagery." Photogrammetric Engineering and Remote Sensing, Vol. 36. pp. 555-560. pp. 555-560.

Colwell, J. E. 1974. "Vegetation Canopy Reflectance." Remote Sensing of Environment, Vol. 3, 1974. pp. 175-183.

Colwell, J. E. 1974. "Grass Canopy Bidirectional Spectral Reflectance." Proceedings of the Ninth International Symposium on Remote Sensing of Environment. April 1974. pp. 1061-1085.

Crowley, James L., 1976, "Experiments in the Analysis of Image Texture." Masters Project Report, Dept. of Electrical Eng., Carnegie-Mellon University. 141 p.

Duda, R. O. and P. E. Hart. 1973. Pattern Classification and Scene Analysis. John Wiley and Sons, New York, N. Y. p. 482.

Duggins, M. J. 1980. "The Field Measurement of Reflectance Factors." Photogrammetric Engineering and Remote Sensing, Vol. 46, No. 5, May 1980. pp. 643-647.

Flemming, Michael D. 1977. "Computer-Aided Analysis Techniques for an Operational System to Map Forest Lands Utilizing Lansat MSS Data", Master of Science Thesis, Purdue University, West Lafayette, IN. 235 p.

Gates, D. M., H. J. Keegan, J. C. Schleter, and V. R. Weidner. 1965. "Spectral Properties of Plants." Applied Optics, Vol. 4, No. 1, January 1965. pp. 11-20.

Gates, D. M. and W. Tantrapern. 1952. "The Reflectivity of Deciduous Trees and Herbaceous Plants in the Infrared to 25 Microns." Science, Vol. 115. pp. 613-616.

Gausman, H. W., W. A. Allen, and R. Cadenas. 1969. "Reflectance of Cotton Leaves and their Structure." Remote Sensing of Environment, Vol. 1, 1969. pp. 19-22.

Gausman, H. W., W. A. Allen, V. I. Myers, R. Cardenas, and R. W. Leamer. 1970. "Reflectance of Single Leaves and Field Plots of Cycocel-Treated Cotton (Gossypium hirsutum) in Relation to Leaf Structure." Remote Sensing of Environment, Vol. 1, 1970. pp. 103-107.

Gausman, H. W. 1974. "Leaf Reflectance of Near-Infrared." Photogrammetric Engineering, Vol. 40, No. 2, February 1974. pp. 183-191.

Gausman, H. W. 1977. "Reflectance of Leaf Components." Remote Sensing of Environment, Vol. 6, 1977. pp. 1-9.

Gupta, J. N., R. L. Kettig, D. A. Landgrebe, and P. A. Wintz. 1973. "Machine Boundary Finding and Sample Classification of Remotely Sensed Agricultural Data." Machine Processing of Remote Sensing Data, 1974. pp. 4B25-4B35.

Gupta, J. N. and P. A. Wintz. 1973. "Closed Boundary Finding Feature Selection and Classification Approach to Multi-Image Modeling." LARS Information Note 062773, Laboratory for Application of Remote Sensing, West Lafayette, IN. 31 p.

Gurney, Charlotte M., 1980. "Threshold Selection for Line Detection Algorithms." IEEE Trans. on Geoscience and Remote Sensing, Vol. GE-18, No. 2, April 1980. pp. 204-211.

Hammil, H. B. and T. H. Holladay. 1970. "The Effects of Certain Approximations in Image Quality Evaluation from Edge Traces." SPIE, Vol. 8, 1970. pp. 223-228.

Haralick, R. M. and K. S. Shanmugam. 1974. "Combined Spectral and Spatial Processing of ERTS Imagery Data." Remote Sensing, Vol. 3, 1974. pp. 3-13.

Haralick, Robert M., 1979. "Statistical and Structural Approaches to Texture." Proceedings of the IEEE, Vol. 67, No. 5, May 1979. pp.786-804.

Harnage, J. 1975. "Landsat-D Thematic Mapper Technical Working Group - Final Report." JSC-09797, June 1975.

Herzog, J. H. and R. C. Rathja. 1973. "Comparative Evaluation of Spatial Features in Automatic Land Use Classification from Photographic Imagery." Machine Processing of Remote Sensing Data, 1973. pp. 2A69-2A77.

Higham, A. D., B. Wilkinson, and D. Kahn. 1973. "Multispectral Scanning Systems and Their Potential Application to Earth Resources Surveys; Basic Physics and Technology." European Space Research Organization, CR-231, ESTEC Contract No. 1673/72. p. 182.

Hoffer, R. M. 1978. "Biological and Physical Considerations in Applying Computer-Aided Analysis Techniques to Remote Sensor Data", in Remote Sensing : The Quantitative Approach, edited by P. H. Swain and S. M. Davis, McGraw-Hill Publishing Co., New York, N. Y. pp. 227-289.

Idso, S. B. and C. T. de Wit. 1970. "Light Relations in Plant Canopies." Applied Optics, Vol. 9, No. 1, January 1970. pp. 177-184.

Iisaka, J. 1979. "Texture Analysis by Space Filter and Application to Forest Type Classification." Machine Processing of Remotely Sensed Data Symposium, 1979. pp. 392-393.

Jurica, G. M. and W. L. Murray. 1973. "The Atmospheric Effect in Remote Sensing of Earth Surface Reflectivities." LARS Information Note 110273, Laboratory for Application of Remote Sensing, West Lafayette, IN. 61 p.

Jurica, G. M. 1973. "Atmospheric Effects on Radiation Measurements." LARS Information Note 011573, Laboratory for Application of Remote Sensing, West Lafayette, IN. 25 p.

Jurica, G. M. and C. L. Parsons. 1974. "Atmospheric Correction of Remotely Sensed Spacecraft Data." LARS Information Note 032974, Laboratory for Application of Remote Sensing, West Lafayette, IN. 25 p.

Kailath, Thomas. 1967. "The Divergence and Bhattacharyya Distance Measures in Signal Selection", IEEE Trans. on Communication Technology, Vol. Com-15, No. 1, Feb. 1967. pp 52-60.

Kan, E. P. F. and D. A. Ball. 1974. "Data Resolution Versus Forestry Classification." JSC-09478. p. 22.

Kan, E. P. F. and D. A. Ball. 1974. "Data Resolution Versus Forestry Classification." Lockheed Electronics Company Contract NAS 9-12200, Forestry Application Exploratory Study Project. p. 32.

Kanal, L. and B. Chandrasekaran. 1971. "On Dimensionality and Sample Size in Statistical Pattern Classification." Pattern Recognition, Vol. 3, 1971. pp. 225-234.

Kast, J. L. and B. J. Davis, 1977. "Test of Spectral/Spatial Classifier." LARS Contract Report 112877. 159 p.

Kauth, R. J. and G. S. Thomas. 1976. "The Tassled Cap - A Graphic Description of the Spectral-Temporal Development of Agricultural Crops as Seen by Landsat." 1976 Machine Processing of Remotely Sensed Data Symposium. pp. 4B41-4B51.

Kauth, R. J., A. P. Pentland, and S. G. Thomas. 1977. "BLOB: An Unsupervised Clustering Approach to Spatial Preprocessing of MSS Imagery." Eleventh International Symposium for Remote Sensing of Environment, 1977. pp. 1309-1317.

Kettig, R. L. and D. A. Landgrebe. 1973. "Automatic Boundary and Sample Classification of Remotely Sensed Multispectral Data." LARS Information Note 041773, Laboratory for Application of Remote Sensing, West Lafayette, IN. 23 p.

Kettig, R. L. and D. A. Landgrebe. 1975. "Computer Classification of Remotely Sensed Multispectral Image Data by Extraction and Classification of Homogeneous Objects". LARS Information Note 050975, Laboratory for Application of Remote Sensing, West Lafayette, IN. 184 p.

Kettig, R. L. and D. A. Landgrebe. 1975B. "Classification of Multispectral Image Data by Extraction and Classification of Homogeneous Objects", LARS Information Note 062375, Laboratory for Application of Remote Sensing, West Lafayette, IN. 18 p.

Knipling, E. B. 1970. "Physical and Physiological Basis for the Reflectance of Visible and Near-IR Radiation from Vegetation." Remote Sensing of Environment, Vol. 1, 1970. pp. 155-159.

Kondratyev, K. Ya. 1969. Radiation in the Atmosphere. Academic Press, N.Y. 912 p.

Kuchler, A. W. 1967. Vegetation Mapping. New York: Ronald Press. p. 472.

Kumar, R. and L. Silva. 1974. "Statistical Separability of Spectral Classes of Blighted Corn." Remote Sensing of Environment, Vol. 3, 1974. pp. 109-115.

Kumar, R., M. Niero, A. P. Manso, L. A. M. Lucht, and M. S. S. Barros. 1979. "Classification of Areas Using Pixel-by-Pixel and Sample Classifiers." Machine Processing of Remotely Sensed Data Symposium, 1979. pp. 420-427.

Landgrebe, D. A. and R. L. Kettig. 1975. "Classification of Multispectral Image Data by Extraction and Classification of Homogeneous Objects." LARS Information Note 062375, Laboratory for Application of Remote Sensing, West Lafayette, IN. 13 p.

Landgrebe, D. A. L. Biehl, and W. Simmons. 1977. "An Empirical Study of Scanner System Parameters." IEE Transactions on Geoscience Electronics, Vol. GE-15, No. 3, July, 1977. LARS No. 110976. pp. 120-130.

Landgrebe, D. A. 1978. "The Quantitative Approach : Concept and Rationale", in Remote Sensing : The Quantitative Approach, edited by P. H. Swain and S. M. Davis, McGraw-Hill Publishing Co., New York, N.Y. pp. 1-20.

Landgrebe, D. A. 1978. "Useful Information from Multispectral Image Data : Another Look", in Remote Sensing : The Quantitative Approach, edited by P. H. Swain and S. M. Davis, McGraw-Hill Publishing Co., New York N.Y. pp. 336-374.

Lansing, Jack C. and Richard W. Cline, 1975. "The Four- and Five-Band Multispectral Scanners for Landsat." Optical Engineering, Vol. 14, No. 4, July-Aug. 1975. pp. 312-322.

Lathi, B. P., 1968. Communication Systems, John Wiley and Sons, New York. 431 p.

Latty, R. S. and R. M. Hoffer. 1980. "Waveband Evaluation of Proposed Thematic Mapper in Forest Cover Classification", Proceedings of the American Society of Photogrammetry, 1980 Fall Technical Meeting. pp. RS-2-D-1 - 12.

Mobasseri, B. G., C. D. McGillem, and P. E. Anuta. 1978. "A Parametric Multiclass Bayes Error Estimator for the Multispectral Scanner Spatial Model Performance Evaluation." LARS Technical Report 061578, Laboratory for Application of Remote Sensing, West Lafayette, IN. 272 p.

Morgenstern, J. P., R. F. Nalepka, and J. D. Erickson. 1977. "Investigation of Thematic Mapper Spatial, Radiometric, and Spectral Resolution." Proceedings of the Eleventh International Symposium on Remote Sensing of the Environment, pp. 693-701.

Morrison, Donald F., 1976. Multivariate Statistical Methods, 2nd edition, McGraw-Hill Book Company, New York. 415 p.

NASA, 1973. "Advanced Scanners and Imaging Systems for Earth Observations", NASA-SP-335, Report of a working group meeting at Cocoa Beach, Dec. 11-15. 604 p.

Nilson, T. 1970. "A Theoretical Analysis of the Frequency of Gaps in Plant Stands." Agricultural Meteorology, Vol. 8, 1971. pp. 25-38.

Noffsinger, E. B. 1970A. "Image Evaluation: Criteria and Applications." SPIE, Vol. 9, 1970. pp. 32-37.

Noffsinger, E. B. 1970B. "Image Evaluation: Criteria and Applications, Paper 2: The MTF Criterion." SPIE, Vol. 9, 1970. pp. 95-103.

Otnes, R. K. and L. Enochson,. 1978. Applied Time Series Analysis : Volume 1, Basic Techniques, John Wiley and Sons, New York, N. Y. 449 p.

Parrent, G. B. Jr. and B. J. Thompson. 1965. Physical Optics Notebook. "Article 5 - Image Formation in Terms of the Impulse Response." SPIE, Vol 3, 1965. pp. 236-242.

Phillips, T. L. 1969. "Calibration of Scanner Data for Operation Processing Programs at LARS." LARS Information Note 071069, Laboratory for Application of Remote Sensing, West Lafayette, IN.

Phillips, T. L. 1973. LARSYS Version 3 User's Manual, Laboratory for Application of Remote Sensing, West Lafayette, IN. Purdue University. Laboratory for Applications of Remote Sensing.

Rabideau, G. S., C. S. French, and A. S. Holt. 1946. "The Absorption and and Reflection Spectra of Leaves, Chloroplast Suspensions, and Chloroplast Fragments as Measured in an Ulbricht Sphere." American Journal of Botany, Vol. 33, December 1946. pp. 769-777.

Richard, R. R. 1978. "NS001-MS-Landsat-D Thematic Mapper Band Aircraft Scanner." Proceedings of the Twelth International Symposium on Remote Sensing of the Environment. pp. 719-727.

Richardson, Wyman. 1974. "A Study of Some Nine-Element Decision Rules." NASA CR-ERIM 190100-32-T. 42 p.

Richardson, Wyman and J. M. Gleason, 1975. "Multispectral Processing Based on Groups of Resolution Elements." NASA CR-ERIM 109600-18-F. 121 p.

Richardson, W., Pentland, R. Crane, and H. Horowitz. 1976. "Number of Signatures Necessary for Accurate Classification." Machine Processing of Remotely Sensed Data, 1976. pp. 3A28-3A34.

Robertson, T. V. 1973. "Extraction and Classification of Objects in Multispectral Images." Machine Processing of Remotely Sensed Data, 1973. pp. 3B27-3B33.

Robertson, T.V., K. S. Fu, and P. H. Swain. 1973. Multispectral Image Partitioning". LARS Information Note 071373; Ph.D. Dissertation, Dept. of Electrical Eng., Purdue University. 90 p.

Rohde, W. G. 1978. "Improving Land Cover Classification by Image Stratification of Landsat Data." Proceedings of the Twelfth International Symposium on Remote Sensing of the Environment. pp. 729-741.

Rohde, W. G. and C. E. Olson Jr. 1972. "Multispectral Sensing of Forest Tree Species." Photogrammetric Engineering, Vol. 38, December 1972. pp. 1209-1215.

Rosenberg, P. 1971. "Resolution, Detectability and Recognizability." Photogrammetric Engineering, Vol. 37, 1971. pp. 1255-1258.

Sadowski, F. G. and W. A. Malila. 1977. "Investigation of Techiniques for Inventorying Forested Regions: Vol. I, Reflectance Modeling and Empirical Multispectral Analysis of Forest Canopy Components." NASA Contract # NAS9-14988 ERIM 122700-35-F1. p. 142.

Sadowski, F. G. and J. Sarno. 1976. "Forest Classification Accuracy as Influenced by Multispectral Scanner Spatial Resolution." NASA Contract #NAS9-14123, May 1976. p. 130.

Sadowski, F. G. and W. A. Malila, J. E. Sarno and R. F. Nalepka. 1977. "The Influence of Multispectral Scanner Spatial Resolution on Forest Feature Classification." Proceedings of the Eleventh International Symposium on Remote Sensing of the Environment. pp. 1279-1288.

Salomonson, V. V. 1978. "Landsat-D Systems Overview." Proceedings of the Twelfth International Symposium on Remote Sensing of the Environment. pp. 371-385.

Scholz, Donna, et al., 1977. "A Case Study Using ECHO for Analysis of Multispectral Scanner Data", LARS Publication 090177, Laboratory for Application of Remote Sensing, West Lafayette, IN. 86 p.

Scott, R. M. 1964. "The Practical Applications of Modulation Transfer Functions." SPIE, Vol. 2, 1964. pp. 132-136.

Shelton, C. F. 1967. "Spatial Frequency Response of Flying-Spot-Scanner Systems." SPIE, Vol. 5, 1967. pp. 155-160.

Shull, C. A. 1929. "A Spectrophotometric Study of Reflection of Light from Leaf Surfaces." Botanical Gazette, Vol. 87, 1929. pp. 583-607.

Silva, L. F. 1978. "Radiation and Instrumentation in Remote Sensing", in Remote Sensing : The Quantitative Approach, edited by P. H. Swain and S. M. Davis, McGraw-Hill Publishing Co., New York, N. Y. pp. 21-135.

Skaley, J. E. and R. J. Hoffman. 1973. "Deriving Spectral and Spatial Features to Establish a Hierarchical Classification System." Machine Processing Symposium of Remote Sensing Data. pp. 4B1-4B5.

Slater, P. N. 1975. "Photographic Sensors for Remote Sensing", in Manual of Remote Sensing, edited by R. G. Reeves, American Society of Photogrammetry. pp. 235-324.

Slater, P. N., 1975. "Use of MTF in the Specification and First-Order Design of Electro-optical and Photographic Imaging and Radiometric Systems." Optica Acta, Vol. 22, No. 4. pp. 277-290.

Slater, P. N. 1979. "A Re-examination of the Landsat MSS." Photogrammetric Engineering and Remote Sensing, Vol. 45, No. 11, November 1979. pp. 1479-1486.

Slater, P. N. and R. A. Schowengerdt. 1972. "Sensor Performance for Earth Resource Studies." Photogrammetric Engineering, Vol. 39, February 1972. pp. 197-201.

Slater, P. N. 1980 "Author's Response", Photogrammetric Engineering and Remote Sensing, Vol. 46, No. 6. pp. 767-769.

Smedes, H. W. 1976. "The Truth About Ground Truth Maps." Proceedings of the Eleventh International Symposium on Remote Sensing of the Environment. pp. 821-823.

Smith, J. A. and R. E. Oliver. 1972. "Plant Canopy Models for Simulating Composite Scene Spectroradiance in the 0.4 to 1.05 Micrometer Region." Proceedings of the Eighth International Symposium on Remote Sensing of the Environment. pp. 1333-1353.

Steele, R. G. D. and J. H. Torrie, 1960. Principles and Procedures of Statistics, McGraw-Hill Publishing Co., New York, N. Y. 418 p.

Stoner, E. R. 1979. "Physicochemical, Site, and Bidirectional Reflectance Factor CHaracteristics of Uniformly Moist Soils", Ph.D. Dissertation, Department of Agronomy, Purdue University, West Lafayette, IN. 192 p.

Suits, G. H. 1972. "The Calculation of the Directional Reflectance of a Vegetative Canopy." Remote Sensing of Environment, 1972. pp. 117-125.

Suits, G. H. 1972. "The Cause of Azimuthal Variations in Directional Reflectance of Vegetative Canopies." Remote Sensing of the Environment, February 1972. pp. 175-182.

Swain, P. H., T. V. Robertson, and A. G. Wacker. 1971. "Comparison of the Divergence and B-Distance in Feature Selection." LARS Information Note 200871, Laboratory for Application of Remote Sensing, West Lafayette, IN. 12 p.

Swain, P. H. 1972. "Pattern Recognition: A Basis for Remote Sensing Data Analysis." LARS Information Note 111572, Laboratory for Application of Remote Sensing, West Lafayette, IN.

Swain, P. H. and R. C. King. 1973. "Two Effective Feature Selection Criteria for Multispectral Remote Sensing." LARS Information Note 042673, Laboratory for Application of Remote Sensing, West Lafayette, IN. 5 p.

Swain, P. H. 1978. "Fundamentals of Pattern Recognition in Remote Sensing", in Remote Sensing: The Quantitative Approach edited by P. H. Swain and S. M. Davis, McGraw-Hill Publishing Co., New York, N. Y. pp. 136-187.

Swain, P. H., S. B. Vardeman, and J. C. Tilton. 1980. "Contextual Classification of Multispectral Image Data." LARS Technical Report 011080, Laboratory for Application of Remote Sensing, West Lafayette, IN. p. 34.

Thompson, L. L. 1980. "More on a Re-Examination of the Landsat MSS", Photogrammetric Engineering and Remote Sensing, Vol. 46, No. 6. pp. 766-767.

Thomson, F. J. and J. D. Erickson. 1976. "A Thematic Mapper Performance Optimization Study." Proceedings of the Tenth International Symposium on Remote Sensing of the Environment. pp. 85-98.

Todd, H. N. and R. D. Zakia. 1969. Photographic Sensitometry : the Study of Tone Reproduction. Morgan & Morgan Publishers, 145 Palisade Street, Dobbs Ferry, N.Y. 312 p.

Townshend, John R. G., 1980. The Spatial Resolving Power of Earth Resources Satellites : A Review". NASA Technical Memorandum 82020, Sept., 1980. 36 p.

Triendl, E. E. 1972. "Automatic Terrain Mapping by Texture Recognition." Proceedings of the Eighth International Symposium on Remote Sensing of the Environment, Vol. I, 1972. pp. 771-776.

Tubbs, J. D. and W. A. Coberly. 1978. "Spatial Correlation and it's Effect Upon Classification Results in Landsat." Proceedings of the Twelfth International Symposium for Remote Sensing of the Environment. pp. 775-781.

Tucker, C. J., L. D. Miller, and R. L. Pearson. 1975. "Shortgrass Praire Spectral Measurements." Photogrammetric Engineering, Vol. 41, No. 9, September 1975. pp. 1157-1162.

Tucker, C. J. 1977. "Spectral Estimation of Grass Canopy Variables." Remote Sensing of Environment, Vol. 6, 1977. pp. 11-26.

Tucker, C. J. 1978. "A Comparison of Satellite Sensor Bands for Vegetation Monitoring." Photogrammetric Engineering and Remote Sensing, Vol. 44, No. 11, 1978. pp. 1369-1380.

Tucker, C. J. 1979. "Red and Photographic Infrared Linear Combination for Monitoring Vegetation." Remote Sensing of Environment, Vol. 8, 1979. pp. 127-150.

Tucker, C. J. and M. W. Grant. 1977. "Leaf Optical System Modeled as a Stochastic Process." Applied Optics, Vol. 16, No. 3, March 1977. pp. 635-642.

Wacker, A. G. 1969. "A Cluster Approach to Finding Spatial Boundaries in Multispectral Imagery", LARS Information Note 122969, Laboratory for Application of Remote Sensing, West Lafayette, IN. 24 p.

Wacker, A. G. 1972. "Minimum Distance Approach to Classification", Ph.D. Dissertation, Department of Electrical Engineering, Purdue University, West Lafayette, IN. 238 p.

Wacker, A. G. 1972. "The Effects of Subclass Numbers on Maximum Likelihood Gausian Classification." Proceedings of the Eighth International Symposium on Remote Sensing of the Environment. pp. 851-859.

Wacker, A. G. and D. A. Landgrebe. 1972. "Minimum Distance Classification in Remote Sensing." LARS Print 030772, Laboratory for Application of Remote Sensing, West Lafayette, IN. 25 p.

Welch, R. 1971. "Modulation Transfer Functions." Photogrammetric Engineering, Vol. 37. pp. 247-259.

Wiersma, D. J. and D. A. Landgrebe. 1976. "The Use of Spatial Charateristics for the Improvement of Multispectral Classification of Remotely Sensed Data." Machine Processing of Remotely Sensed Data. pp. 2A18-2A25.

Wiersma, D. J. and D. A. Landgrebe. 1979. "An Analytical Approach to the Design of Spectral Measurements in the Design of Multispectral Sensors." 1979 Machine Processing of Remotely Sensed Data Symposium. pp. 331-341.

Wooley, J. T. 1971. "Reflectance and Transmittance of Light by Leaves." Plant Physiology, Vol. 47. pp. 656-662.

Wu, C. L., D. A. Landgrebe, and P. H. Swain, 1974. "The Decision Tree Approach to Classification", LARS Information Note 090174, Laboratory for Application of Remote Sensing, West Lafayette, IN. 174 p.

Ziemer, R. E. and W. H. Tranter. 1976. Principles of Communications: Systems, Modulation and Noise. Boston: Houghton Mifflin Company. p. 513.

Zimmerman, J. 1966. "A Practical Approach Toward the Determination of Resolution Requirements." SPIE, Vol. 4. pp. 277-280.

Zwick, D. M. 1966. "The Meaning of Numbers of Photographic Parameters." SPIE, Vol. 4. pp. 205-211.

APPENDICES

APPENDIX A

APPENDIX A

$p(\omega'j|X)$ is computed from the probability function of X assuming $\omega'j$ has occurred, $p(W|\omega'j)$, which is computed from the normal distribution density function:

$$p(X|\omega'j) = \frac{1}{2\pi^{d/2}|Cj|^{d/2}} \exp\left[-\tfrac{1}{2}(X-\hat{\mu}_j)\, C_j^{-1} (X-\hat{\mu}_j)^T\right]$$

where:

X = the d-component response level vector

$\hat{\mu}_j$ = the estimated mean of the j(th) spectral class computed from the clustered training data.

C_j = the d-by-d covariance matrix of the j(th) spectral class computed from the clustered training data.

$|C_j|$ = the determinant of the covariance matrix.

The probability, $p(\omega'j|X)$, of the occurrence of the j(th) cover class, given the occurrence of some measurement X, is then computed by:

$$p(\omega'j|X) = \frac{p(X|\omega'j)\; p(\omega'j)}{p(X)}$$

where:

$$p(X) = \sum_{j=1}^{p} p(\omega'j)\; p(X|\omega'j)$$

Since $p(x)$ is a constant in the decision rule, it cancels out and the remaining rule is:

$$p(X|\omega'j)\ p(\omega'j) \geq p(X|\omega'i)\ p(\omega'i)$$

where the a priori probabilities are assumed equal for all spectral classes, the rule simplifies to:

$$p(X|\omega'j) \geq p(X|\omega'i)$$

which are computed directly from the normal distribution density functions. These functions contain other constants and available simplifications to facilitate their computation for purposes of discriminant analysis (see Duda and Hart, 1973).

APPENDIX B

Table B-1 Means and Variances by Spectral Class for 15 Meter Resolution Data (CAMIS)

Cover Class	Channels 1	2	3	4	5	6	7
SOIL1	156.23 258.68	178.70 661.78	191.37 766.05	183.28 358.64	190.06 347.39	189.30 829.57	142.43 855.30
SOIL2	128.01 98.25	125.20 213.61	128.81 256.17	134.93 237.60	144.02 173.84	145.07 178.94	141.61 1358.81
SOIL3	111.39 108.32	96.21 245.81	92.15 316.34	98.85 361.40	108.46 341.60	104.43 417.78	131.34 638.28
PAST1	107.49 13.81	93.28 29.34	81.50 80.23	149.21 189.18	162.80 92.29	131.89 88.99	196.72 282.38
PAST2	104.34 4.80	85.51 8.43	61.68 16.51	189.53 123.24	176.66 37.07	101.98 42.95	144.06 123.54
PAST3	104.27 17.62	84.95 16.75	69.57 38.83	140.94 182.55	148.79 99.52	109.21 74.31	155.78 175.28
PAST4	99.41 10.23	80.88 16.98	58.76 29.07	170.88 243.05	154.16 67.30	84.49 45.74	115.33 83.17
PAST5	97.35 6.93	73.69 13.19	51.35 15.39	164.00 144.07	134.80 86.61	62.82 30.12	87.35 72.78
CROP1	117.86 50.90	111.41 159.70	100.99 382.09	174.33 228.21	162.96 155.89	120.06 282.59	102.44 229.55
CROP2	100.46 5.98	75.77 14.58	51.86 18.42	210.04 184.30	160.56 41.38	68.50 37.53	82.17 47.51
CROP3	99.83 36.22	82.23 37.18	71.25 76.47	117.62 125.11	117.05 120.90	91.65 203.47	137.62 280.48
CROP4	96.16 9.88	76.92 37.48	58.38 54.45	150.96 193.98	127.64 140.53	65.11 87.52	96.50 198.31
PINE1	92.22 3.89	69.86 6.74	54.44 14.87	112.93 107.06	115.32 90.12	72.73 66.52	119.71 387.78
PINE2	94.20 15.65	67.83 8.30	48.84 7.33	118.38 134.83	112.48 101.65	60.48 47.80	85.10 93.28
PIHD1	91.66 12.24	68.96 5.79	55.01 13.80	108.28 60.66	109.59 46.30	69.78 36.82	127.13 428.46
PIHD2	93.95 7.15	65.55 7.86	46.74 7.64	112.56 150.88	105.79 102.26	53.70 33.52	83.84 71.28
HDWD1	92.04 4.13	66.41 6.59	44.14 3.88	165.02 67.47	141.83 40.17	66.94 25.41	79.97 44.03
HDWD2	91.08 7.03	65.64 13.16	43.58 7.22	146.41 44.64	126.98 23.44	61.63 23.86	76.75 52.37
HDWD3	85.23 14.46	58.73 11.75	39.04 8.29	123.53 111.51	107.34 74.11	52.46 15.61	72.05 25.19
SGHD1	91.27 7.98	67.30 10.77	44.24 6.01	179.50 82.61	153.89 56.49	72.90 34.98	85.41 66.53
SGHD2	87.19 32.11	62.03 22.93	40.86 7.68	155.82 67.08	134.05 42.86	63.66 22.55	80.05 90.17
SGHD3	90.86 18.08	63.71 13.46	41.26 8.00	127.13 197.06	108.62 146.48	54.02 29.24	68.49 52.50
TUPE1	95.48 8.52	80.72 15.19	51.34 4.84	184.56 75.70	156.71 40.21	77.71 14.45	80.49 108.16
TUPE2	95.50 9.25	80.69 16.03	51.87 6.35	165.03 55.27	142.01 38.15	74.06 13.97	81.76 54.24

Table B-1 Continued

Cover Class	Channels 1	2	3	4	5	6	7
TUPE3	82.86 11.99	72.80 4.70	46.38 1.35	124.37 17.12	108.93 8.71	60.59 2.42	79.16 34.53
CCUT1	101.75 46.60	83.37 67.32	74.09 195.45	120.57 178.04	134.64 85.55	113.62 158.34	192.12 597.92
CCUT2	91.41 8.69	70.71 13.44	49.87 23.57	143.67 300.66	132.11 131.40	77.78 73.27	99.51 244.16
CCUT3	96.05 18.77	75.39 37.02	63.40 117.19	106.24 226.10	112.51 165.39	88.89 100.68	135.33 232.49
CCUT4	91.00 20.55	66.18 25.39	51.28 60.98	80.25 399.46	79.03 396.86	58.46 186.16	93.72 294.05
MVEG1	102.98 26.02	79.62 81.96	66.12 194.12	109.18 75.94	122.98 70.15	90.49 120.09	124.76 209.75
MVEG2	100.75 12.24	76.90 24.25	52.43 22.06	124.31 229.76	112.03 170.94	63.53 72.48	78.89 125.75
WATR1	101.86 5.39	67.75 13.53	50.24 19.07	40.28 84.12	33.28 67.74	24.97 32.94	67.45 37.87
WATR2	104.27 5.15	79.66 8.31	61.96 12.25	38.38 4.30	29.15 6.22	20.21 2.94	39.01 5.05

Table B-2 Average Standard Deviation over all Spectral Classes in each Cover Class (CAM1S)

Cover Class	Channels 1	2	3	4	5	6	7
SOIL	12.13	18.67	20.49	17.79	16.77	20.87	30.46
PAST	3.19	4.03	5.71	13.19	8.64	7.37	11.76
CROP	4.69	7.17	9.99	13.45	10.44	11.64	13.22
PINE	2.96	2.74	3.28	10.98	9.79	7.53	14.68
PIHD	3.09	2.61	3.24	10.04	8.46	5.93	14.57
HDWD	2.83	3.21	2.51	8.48	6.60	4.63	6.30
SGHD	4.25	3.91	2.68	10.44	8.72	5.36	8.30
TUPE	3.14	3.36	1.96	6.76	5.16	3.03	7.88
CCUT	4.66	5.75	9.37	16.43	13.37	11.21	18.12
MVEG	4.30	6.99	9.31	11.94	10.73	9.74	12.85
WATR	2.29	3.28	3.93	5.62	5.36	3.73	4.20

Table B-3 Means and Variances by Spectral Class for 30 Meter Resolution Data (CAMIS)

Cover Class	Channels 1	2	3	4	5	6	7
SOIL1	154.87 243.34	177.14 635.95	189.70 705.00	181.14 320.86	188.11 308.40	189.22 513.50	143.31 767.91
SOIL2	128.42 88.26	125.67 194.42	128.85 240.09	135.62 223.42	144.49 158.03	144.83 158.41	139.44 1162.87
SOIL3	111.10 105.86	95.83 235.72	92.80 308.18	99.29 361.95	109.41 331.33	106.21 396.72	135.06 734.38
PAST1	107.48 9.79	93.05 29.30	81.10 74.74	148.14 161.33	162.16 87.59	131.79 83.29	197.08 283.63
PAST2	104.65 4.76	85.95 9.49	62.46 17.70	188.67 116.83	176.23 34.90	102.77 51.15	145.38 138.17
PAST3	104.30 19.73	85.04 22.34	69.62 52.99	141.63 162.09	148.91 97.33	108.70 88.28	154.41 196.43
PAST4	99.52 8.07	80.96 13.68	58.73 17.95	171.73 222.32	154.58 59.78	84.27 35.41	115.33 58.16
PAST5	97.60 5.56	73.76 7.60	51.20 7.15	165.09 46.32	135.90 30.41	63.37 25.85	87.51 55.28
CROP1	117.65 42.54	111.12 130.55	100.67 309.76	172.25 203.03	161.50 140.88	119.68 229.87	103.02 221.09
CROP2	100.77 5.80	76.21 16.76	52.34 22.41	210.17 176.97	160.62 39.00	68.76 40.72	82.34 40.46
CROP3	99.82 37.79	82.30 37.85	71.21 70.78	118.67 115.25	117.97 118.15	91.60 203.40	137.56 268.31
CROP4	96.08 6.16	76.84 30.63	58.46 45.40	150.22 199.89	127.02 141.36	64.76 70.29	97.05 194.62
PINE1	92.26 3.11	69.76 6.35	54.05 13.48	113.46 81.46	115.17 65.40	71.88 50.93	116.23 288.47
PINE2	94.75 15.59	67.90 8.73	48.67 5.99	118.79 104.89	112.27 83.46	59.60 40.22	83.64 73.18
PIHD1	91.69 14.58	69.46 8.39	55.44 11.86	109.79 64.06	110.61 46.92	70.28 28.63	127.44 379.38
PIHD2	94.31 6.04	65.79 7.81	46.98 7.09	112.63 119.94	105.95 85.44	53.95 29.96	84.25 54.55
HDWD1	92.12 2.48	66.21 4.29	43.92 2.64	161.01 38.26	138.32 20.72	65.29 15.45	78.90 30.02
HDWD2	91.45 4.73	66.07 11.26	43.94 5.93	146.15 30.91	127.10 16.15	61.97 19.43	77.05 43.73
HDWD3	84.52 8.75	58.21 7.59	38.78 5.89	124.69 86.81	108.22 55.82	52.82 10.90	72.92 19.29
SGHD1	91.42 7.13	67.31 9.40	44.23 5.47	175.67 55.54	150.73 38.43	71.57 29.82	84.74 55.83
SGHD2	86.10 32.01	61.11 20.54	40.46 6.09	155.12 54.63	133.78 29.75	63.66 17.06	81.08 80.84
SGHD3	91.52 13.22	64.64 9.93	41.91 6.45	131.63 126.96	112.29 92.78	56.05 16.65	68.85 34.31
TUPE1	95.44 7.53	80.55 12.71	51.29 3.64	183.49 66.36	155.89 30.81	77.28 10.74	80.27 97.30
TUPE2	95.67 7.47	80.57 12.79	51.88 4.47	164.41 45.11	141.59 36.50	74.01 12.20	81.98 37.88

Table B-3 Continued

Cover Class	Channels 1	2	3	4	5	6	7
TUPE3	82.83	72.87	46.51	124.39	109.04	60.90	79.67
	8.41	3.40	0.89	11.67	6.59	1.58	22.23
CCUT1	101.66	83.29	73.24	121.39	135.02	112.71	189.76
	39.09	50.16	145.27	163.30	73.32	123.54	463.75
CCUT2	96.86	76.45	64.94	107.61	114.36	91.23	137.69
	17.11	35.73	117.13	191.87	140.05	98.66	198.27
CCUT3	91.66	70.97	50.25	142.64	131.36	77.78	100.85
	7.20	11.70	19.19	276.54	110.55	44.09	132.54
CCUT4	91.17	66.86	52.46	83.56	83.20	62.04	98.73
	19.28	26.99	75.15	330.60	325.53	164.53	300.15
MVEG1	102.64	79.12	65.10	110.00	123.25	89.91	123.56
	22.73	73.10	174.96	58.84	51.46	102.11	204.00
MVEG2	100.76	76.83	52.67	123.72	112.42	64.49	80.16
	8.90	20.02	14.56	173.99	118.27	66.70	113.35
WATR1	102.17	68.24	50.73	40.80	33.82	25.60	67.92
	3.98	13.95	18.87	80.49	65.24	29.69	37.83
WATR2	104.41	80.03	62.62	38.64	29.21	20.44	39.31
	3.51	4.76	2.98	3.76	3.17	2.31	1.59

Table B-4 Average Standard Deviation over all Spectral Classes in each Cover Class (CAM1S)

Cover Class	Channels 1	2	3	4	5	6	7
SOIL	11.76	18.17	19.87	17.29	16.11	18.39	29.64
PAST	2.99	3.94	5.41	11.59	7.68	7.34	11.53
CROP	4.39	6.80	9.37	13.11	10.22	11.05	12.89
PINE	2.86	2.74	3.06	9.63	8.61	6.74	12.77
PIHD	3.14	2.85	3.05	9.48	8.05	5.41	13.43
HDWD	2.24	2.73	2.16	7.02	5.35	3.88	5.49
SGHD	3.99	3.58	2.45	8.70	7.10	4.56	7.44
TUPE	2.79	3.00	1.66	6.09	4.72	2.68	6.91
CCUT	4.37	5.42	8.98	15.36	12.24	10.13	16.11
MVEG	3.88	6.51	8.52	10.43	9.02	9.14	12.46
WATR	1.93	2.96	3.04	5.46	4.93	3.48	3.71

Table B-5 Means and Variances by Spectral Class for 45 Meter Resolution Data (CAMIS)

Cover Class	Channels 1	2	3	4	5	6	7
SOIL1	152.62 246.63	173.79 659.64	185.89 748.21	178.30 344.25	184.49 333.91	183.36 539.05	139.48 592.98
SOIL2	127.12 86.61	123.48 189.59	125.86 212.30	133.43 222.67	142.04 155.68	141.69 157.13	138.21 1069.18
SOIL3	109.76 106.38	93.59 210.52	90.51 268.71	96.90 379.48	107.10 318.82	103.94 321.18	132.97 579.64
PAST1	107.73 10.20	95.08 26.69	83.78 78.90	150.86 102.29	164.70 54.83	134.54 79.76	200.97 330.22
PAST2	104.39 4.44	85.71 8.82	62.26 13.67	188.24 103.33	175.84 28.35	102.46 47.88	144.46 119.86
PAST3	104.58 15.26	85.12 13.45	69.67 31.68	141.54 154.56	149.36 85.67	109.53 69.92	156.14 168.21
PAST4	99.26 8.24	80.60 14.83	58.70 18.56	170.00 216.26	153.85 60.96	84.80 35.03	116.09 56.69
PAST5	97.28 5.58	73.42 6.48	50.97 6.89	165.56 27.63	135.83 26.60	62.97 19.69	87.22 48.35
CROP1	117.17 33.34	110.97 102.32	100.26 240.79	172.19 172.26	161.31 138.40	119.76 184.19	102.93 166.94
CROP2	100.70 6.11	76.13 17.63	52.33 22.97	210.07 153.04	160.69 34.45	68.96 44.04	82.21 39.17
CROP3	99.93 36.25	82.30 37.05	70.70 65.23	120.81 138.49	119.34 121.47	91.12 182.86	135.94 238.18
CROP4	95.79 4.74	76.60 28.13	58.16 41.74	151.39 175.69	127.29 138.11	64.13 62.11	95.02 146.95
PINE1	92.25 7.66	70.09 15.31	54.52 29.43	113.06 74.83	115.12 66.99	72.54 83.15	117.07 245.34
PINE2	94.14 14.21	67.79 8.28	48.75 5.54	118.60 89.57	112.64 72.79	60.45 41.28	85.31 81.16
PIHD1	92.60 29.27	70.25 22.49	55.82 12.75	111.00 99.04	111.75 63.75	70.71 15.69	124.93 275.03
PIHD2	94.03 5.43	65.45 7.04	46.71 6.38	111.63 102.31	104.89 71.26	53.10 25.45	83.74 44.20
HDWD1	92.00 2.27	65.95 3.60	43.63 2.21	158.78 30.01	136.27 15.82	64.15 12.69	77.99 25.84
HDWD2	91.32 4.44	66.09 11.73	43.97 5.95	145.23 25.97	126.61 14.38	62.08 19.45	77.05 44.31
HDWD3	84.01 5.88	57.78 5.22	38.47 4.61	124.01 91.97	107.64 55.94	52.57 8.99	72.95 18.92
SGHD1	91.29 5.86	66.92 8.37	43.86 5.34	174.15 40.62	149.17 32.07	70.52 30.24	83.74 56.07
SGHD2	85.36 30.34	60.44 18.09	40.03 4.92	154.63 48.82	133.46 26.99	63.49 14.98	81.39 77.05
SGHD3	91.76 9.45	64.93 7.82	42.07 6.27	133.57 113.26	113.91 79.29	56.67 14.90	68.78 24.72
TUPE1	94.56 7.80	80.03 10.82	51.08 2.78	180.63 58.46	153.94 23.10	76.96 6.69	82.24 90.18
TUPE2	96.14 5.27	80.39 13.50	51.81 4.16	161.50 48.60	138.78 36.24	72.58 11.85	79.64 26.87

Table B-5 Continued

Cover Class	Channels 1	2	3	4	5	6	7
TUPE3	82.36 6.24	72.47 3.57	46.29 1.03	124.31 7.31	109.09 4.27	60.69 1.67	79.49 13.67
CCUT1	101.49 34.64	82.87 40.21	72.42 118.28	120.49 160.95	133.97 72.32	111.44 114.90	186.61 420.78
CCUT2	96.38 13.35	75.88 29.06	64.51 105.34	106.23 179.44	112.73 134.17	89.95 85.29	135.51 174.91
CCUT3	91.63 7.23	70.96 11.37	50.25 18.45	142.90 240.57	131.49 94.79	77.75 35.31	100.88 119.67
CCUT4	90.70 18.72	66.43 24.43	51.66 64.95	84.90 299.52	84.36 287.78	62.21 135.11	98.99 271.77
MVEG1	103.22 22.15	80.04 71.86	66.79 172.08	109.01 42.85	122.84 48.14	90.68 103.12	125.35 179.31
MVEG2	100.32 6.39	76.35 16.14	52.63 10.53	122.34 151.38	113.21 98.86	65.79 75.19	82.02 153.00
WATR1	103.00 14.00	76.57 8.95	57.57 8.62	82.57 231.95	67.86 156.81	42.86 33.14	70.29 377.24
WATR2	102.35 4.23	69.34 25.41	51.92 30.30	39.20 13.03	31.91 13.05	24.05 11.15	63.92 108.69

Table B-6 Average Standard Deviation over all Spectral Classes in each Cover Class (CAMIS)

Cover Class	Channels 1	2	3	4	5	6	7
SOIL	11.78	17.99	19.44	17.65	16.20	17.89	27.04
PAST	2.89	3.64	5.03	10.53	6.99	6.91	11.31
CROP	4.11	6.43	8.71	12.63	10.10	10.40	11.68
PINE	3.27	3.39	3.89	9.06	8.36	7.77	12.34
PIHD	3.87	3.70	3.05	10.03	8.21	4.50	11.62
HDWD	2.01	2.54	2.02	6.72	5.08	3.66	5.36
SGHD	3.67	3.31	2.34	8.00	6.59	4.41	7.08
TUPE	2.53	2.95	1.57	5.77	4.30	2.44	6.13
CCUT	4.14	5.01	8.37	14.72	11.70	9.38	15.29
MVEG	3.62	6.25	8.18	9.42	8.44	9.41	12.88
WATR	2.90	4.02	4.22	9.42	8.07	4.55	14.92

Table B-7 Means and Variances by Spectral Class for 80 Meter Resolution Data (CAM1S)

Cover Class	Channels 1	2	3	4	5	6	7
SOIL1	153.45 205.50	174.19 617.71	185.00 762.61	177.84 335.39	183.42 303.55	181.28 496.55	136.52 573.72
SOIL2	126.21 79.19	122.22 189.92	123.97 220.73	133.54 235.97	141.96 158.30	140.65 160.87	139.86 990.32
SOIL3	109.69 93.18	93.37 181.56	90.38 239.49	99.48 366.36	108.87 279.49	103.81 287.15	129.20 471.44
PAST1	107.89 6.22	95.61 16.84	84.39 55.43	151.94 73.35	165.89 39.87	135.39 70.49	201.39 264.49
PAST2	104.28 15.21	84.89 12.84	69.43 25.15	142.79 131.38	149.84 60.28	109.23 72.98	156.03 171.85
PAST3	104.76 4.69	86.05 9.45	62.62 17.15	189.95 73.15	176.24 22.59	102.14 50.23	146.48 118.57
PAST4	99.35 9.01	80.10 13.26	58.32 16.64	170.76 219.06	153.91 61.40	84.19 34.40	114.94 69.19
PAST5	97.17 5.70	73.48 7.72	51.22 6.72	165.17 76.52	137.30 50.04	64.65 32.51	88.00 55.45
CROP1	116.04 29.15	108.07 91.85	95.79 152.69	172.04 136.41	160.54 104.48	116.54 142.04	102.46 116.04
CROP2	100.85 5.02	76.36 15.25	52.72 18.92	208.68 154.34	160.24 34.31	69.28 37.86	82.59 40.50
CROP3	99.85 33.63	82.83 40.96	71.69 75.06	124.45 155.25	122.35 131.17	92.31 162.22	135.69 156.22
CROP4	95.67 2.72	76.54 20.75	58.28 27.64	149.50 205.28	125.74 118.95	63.74 33.40	95.24 127.13
PINE1	92.00 3.14	69.81 6.35	53.52 13.04	116.25 69.62	117.01 50.01	72.02 39.67	113.49 153.64
PINE2	94.26 14.11	67.49 9.44	48.43 6.33	117.50 79.69	110.85 63.54	58.89 34.83	83.61 67.88
PIHD1	90.44 1.20	68.81 4.30	55.13 8.12	109.69 38.90	110.38 27.58	70.63 26.25	129.81 320.43
PIHD2	94.78 8.36	66.18 12.97	47.27 9.84	112.76 94.64	106.00 75.45	53.93 34.52	84.44 33.80
HDWD1	91.90 1.84	65.75 2.75	43.55 1.81	157.79 23.40	135.35 11.07	63.69 9.01	77.57 20.44
HDWD2	91.40 3.79	66.43 11.39	44.20 5.76	145.44 22.73	127.05 13.62	62.65 19.93	77.82 47.97
HDWD3	84.27 8.43	58.16 8.35	38.88 8.07	122.82 112.85	106.86 67.01	52.77 8.58	73.39 17.68
SGHD1	91.30 5.49	67.02 7.63	43.90 5.15	172.98 36.95	148.19 28.08	70.15 29.03	83.69 46.57
SGHD2	84.15 28.30	59.41 15.61	39.69 4.13	153.62 40.27	132.93 19.61	63.43 11.63	82.42 68.84
SGHD3	91.61 11.13	65.05 7.79	42.17 6.64	135.80 82.65	115.89 55.53	57.58 11.59	69.91 34.41
TUPE1	95.07 8.00	79.70 8.60	50.74 2.28	182.26 67.59	154.93 27.15	76.22 4.72	80.44 95.33
TUPE2	95.40 6.78	79.35 13.40	51.35 3.29	163.95 21.32	141.20 13.86	73.45 7.84	80.90 37.67

Table B-7 Continued

Cover Class	Channels 1	2	3	4	5	6	7
TUPE3	81.95 0.45	72.10 2.59	45.90 0.69	123.95 3.35	108.86 1.83	60.52 0.66	79.76 9.39
CCUT1	100.92 25.28	82.22 27.35	71.13 81.36	121.15 151.31	133.90 69.68	109.80 89.85	183.08 380.03
CCUT2	91.71 6.98	71.19 11.21	51.07 32.77	143.21 231.01	131.72 88.04	78.08 29.68	101.47 118.87
CCUT3	96.39 13.59	75.87 27.43	64.56 93.31	105.56 165.97	112.00 124.40	89.46 72.07	135.41 162.87
CCUT4	90.62 17.56	66.26 24.13	51.95 79.28	84.63 285.96	83.92 278.41	61.85 142.79	99.23 261.86
MVEG1	101.66 15.95	77.62 49.96	62.62 129.32	111.24 41.90	123.66 29.95	88.93 68.00	121.45 182.76
MVEG2	100.78 7.10	76.81 17.93	52.52 8.42	123.93 107.07	112.15 75.98	64.00 56.08	79.44 97.87
WATR1	102.73 2.63	73.82 9.36	55.00 16.80	69.09 89.49	59.00 63.60	38.00 10.40	71.73 132.42
WATR2	102.32 3.65	68.89 22.72	51.49 25.49	38.87 8.43	31.77 10.18	23.77 8.79	64.64 103.08

Table B-8 Average Standard Deviation over all Spectral Classes in each Cover Class (CAM1S)

Cover Class	Channels 1	2	3	4	5	6	7
SOIL	10.96	17.37	19.32	17.61	15.57	17.30	25.71
PAST	2.79	3.44	4.65	10.43	6.75	7.12	11.21
CROP	3.77	6.11	7.66	12.72	9.61	9.15	10.23
PINE	2.76	2.80	3.06	8.64	7.56	6.10	10.32
PIHD	1.99	2.84	2.99	7.98	6.97	5.50	11.86
HDWD	2.07	2.64	2.19	6.74	5.07	3.47	5.22
SGHD	3.67	3.17	2.29	7.17	5.73	4.07	7.00
TUPE	2.03	2.73	1.39	4.89	3.43	1.93	6.32
CCUT	3.89	4.68	8.33	14.32	11.39	8.84	14.84
MVEG	3.33	5.65	7.14	8.41	7.09	7.87	11.71
WATR	1.77	3.91	4.57	6.18	5.58	3.10	10.83

Table B-9 Means and Variances by Spectral Class for 15 Meter Resolution Data (CAM2N)

Cover Class	Channels 1	2	3	4	5	6	7
CCUT1	135.21 114.79	134.39 263.64	142.12 591.41	164.82 299.12	180.38 299.20	183.88 605.43	172.57 443.92
CCUT2	106.02 37.17	84.72 65.80	74.77 140.78	122.89 145.43	136.08 134.52	118.33 285.84	189.63 587.13
CCUT3	103.94 37.44	85.09 64.82	66.01 131.21	154.97 200.55	154.06 81.73	108.67 150.25	139.22 245.98
CCUT4	100.14 25.59	77.10 54.59	56.25 111.78	139.00 377.64	133.48 181.06	82.94 160.65	112.19 500.67
CROP1	111.87 32.40	94.24 65.92	82.99 138.58	144.25 764.34	150.28 441.44	132.37 666.00	177.21 838.47
CROP2	103.59 33.72	82.99 74.57	63.28 236.12	172.24 1037.94	153.12 221.34	95.34 590.19	111.60 1746.49
HDWD1	90.42 12.56	72.64 10.47	49.07 15.26	174.50 108.99	156.58 53.60	86.54 159.16	114.72 155.08
HDWD2	93.72 10.51	71.84 13.19	46.59 8.53	191.09 112.24	162.71 68.43	77.05 81.70	89.51 76.72
HDWD3	92.23 12.00	70.32 9.50	46.61 6.51	165.83 51.05	144.84 27.96	74.34 46.12	91.45 78.89
HDWD4	93.62 10.12	70.46 10.48	47.53 11.52	144.03 106.31	127.61 61.90	68.66 39.44	86.08 101.34
PAST1	111.34 26.00	95.43 37.83	86.82 119.57	145.37 207.70	160.39 145.95	145.43 194.43	199.94 265.59
PAST2	102.90 10.27	83.71 16.29	60.02 26.71	195.18 242.06	179.49 124.02	109.84 275.35	136.74 335.06
PAST3	102.77 19.28	79.96 35.27	74.03 61.76	104.65 35.81	117.44 62.25	104.15 357.95	196.86 808.06
PAST4	101.83 30.10	85.47 31.21	70.26 56.81	149.43 226.68	151.58 123.36	113.48 127.06	164.76 509.53
PIHD1	94.25 15.64	73.82 12.94	58.17 16.08	131.54 71.04	129.49 50.41	85.16 275.50	137.24 156.14
PIHD2	91.75 14.33	69.72 7.44	48.52 11.24	143.80 81.34	130.97 43.23	68.66 97.24	99.27 121.33
PIHD3	92.62 11.39	68.85 3.18	49.56 8.28	124.09 42.23	116.24 31.05	61.96 60.24	101.13 110.41
PINE1	97.08 10.48	73.26 4.13	65.69 14.38	107.43 24.80	113.62 30.53	86.48 515.79	176.62 269.83
PINE2	95.51 8.81	71.00 5.75	56.46 13.74	113.70 30.66	113.93 26.16	78.04 346.59	130.48 126.39
PINE3	93.95 12.33	68.96 7.01	51.48 9.71	116.74 43.02	112.65 29.35	66.12 59.09	109.60 39.36
PINE4	93.81 5.67	67.31 5.98	46.91 7.24	120.78 64.69	113.04 40.21	58.21 73.17	93.34 35.39
SOIL1	143.84 190.36	147.14 410.50	160.47 571.00	160.33 431.04	170.09 294.26	184.64 375.08	202.15 570.75
SOIL2	137.99 62.78	139.86 176.06	140.96 404.35	173.40 569.88	171.16 283.52	159.39 290.97	127.50 778.93
SOIL3	119.81 60.81	107.13 178.91	108.84 313.73	117.60 250.85	127.21 246.93	129.17 444.06	147.17 1050.05

Table B-9 Continued

Cover Class	Channels 1	2	3	4	5	6	7
URBN1	161.89	163.51	168.11	169.56	174.44	180.49	189.80
	469.14	859.01	1114.95	252.37	285.94	866.65	682.75
URBN2	118.01	98.95	89.23	137.55	139.31	113.66	206.55
	114.77	164.95	255.13	385.52	428.08	402.03	767.62
URBN3	105.03	81.55	64.37	124.96	119.93	79.16	130.56
	38.62	63.70	81.15	265.72	240.83	161.81	595.85
WATR1	114.26	94.78	76.82	41.41	32.16	48.13	47.01
	70.79	182.59	237.48	105.18	58.36	1251.07	215.30
WATR2	101.87	73.53	52.38	27.27	22.46	11.39	62.56
	3.17	0.59	5.02	10.32	5.46	44.83	17.47

Table B-10 Average Standard Deviation over all Spectral Classes in each Cover Class (CAM2N)

Cover Class	Channels 1	2	3	4	5	6	7
CCUT	53.75	112.21	243.80	255.68	174.13	300.54	444.42
CROP	33.06	70.25	187.35	901.14	331.39	628.09	1292.48
HDWD	11.30	10.91	10.45	94.65	52.97	81.61	103.01
PAST	21.41	30.15	66.21	178.06	113.89	238.70	479.56
PIHD	13.79	7.85	11.87	64.87	41.56	144.33	129.29
PINE	9.32	5.72	11.27	40.79	31.56	248.66	117.74
SOIL	104.65	255.16	429.70	417.26	274.90	370.04	799.91
URBN	207.51	362.55	483.74	301.20	318.28	476.83	682.07
WATR	36.98	91.59	121.25	57.75	31.91	647.95	116.38

Table B-11 Means and Variances by Spectral Class for 30 Meter Resolution Data (CAM2N)

Cover Class	Channels 1	2	3	4	5	6	7
CCUT1	135.94 104.49	135.56 231.52	143.51 524.40	163.83 302.19	178.96 367.74	182.14 483.44	170.95 437.56
CCUT2	105.71 32.75	84.04 53.45	73.97 110.98	121.79 108.98	134.60 104.87	116.50 240.00	187.77 398.90
CCUT3	104.62 31.86	85.53 61.28	67.96 115.75	148.71 168.70	150.63 90.17	110.78 114.42	144.66 148.74
CCUT4	100.76 22.94	78.84 38.54	56.98 47.96	150.66 344.05	142.95 178.17	87.90 122.45	114.97 221.63
CROP1	112.16 31.19	94.63 57.60	84.15 147.05	143.47 777.19	150.14 436.68	133.67 395.74	173.63 841.94
CROP2	103.27 19.18	82.29 47.65	62.06 152.27	172.47 935.05	152.42 200.60	94.83 513.93	115.73 1146.64
HDWD1	90.40 11.18	72.63 9.50	49.04 11.02	173.32 88.44	155.24 43.46	85.69 118.98	113.18 131.14
HDWD2	94.09 9.08	71.66 12.48	46.46 8.04	188.12 93.32	160.37 49.84	75.35 57.26	88.21 59.70
HDWD3	92.38 10.14	70.40 7.90	46.79 5.60	166.34 36.50	145.35 19.54	74.92 31.58	91.58 71.66
HDWD4	93.87 8.49	71.08 8.72	48.07 7.37	146.88 73.98	130.01 41.75	70.44 29.72	86.51 69.91
PAST1	111.76 21.93	95.97 31.78	87.36 94.36	145.20 206.28	160.06 142.23	145.47 118.15	198.80 244.25
PAST2	103.12 8.33	83.77 13.94	59.90 21.88	196.51 175.98	180.33 91.99	110.07 269.36	136.67 255.98
PAST3	102.00 27.15	85.77 26.27	70.02 46.69	152.52 200.54	154.02 114.94	114.20 118.46	165.86 198.24
PAST4	102.86 17.59	80.21 36.22	74.24 54.22	105.33 33.78	118.07 56.89	103.90 292.00	195.37 574.44
PIHD1	95.14 12.57	74.56 12.33	58.89 12.12	132.44 58.97	130.24 39.05	88.11 208.18	137.09 104.98
PIHD2	90.60 12.07	69.79 3.61	51.69 6.83	126.28 67.15	120.57 48.45	66.56 61.04	115.85 95.42
PIHD3	93.01 9.68	68.96 2.14	48.33 5.80	132.55 90.99	121.76 52.81	63.89 47.80	95.53 44.93
PINE1	96.94 11.39	73.38 3.18	65.71 10.05	107.00 13.73	112.88 17.09	83.65 112.04	175.71 178.29
PINE2	95.72 8.45	71.37 7.63	56.79 12.39	113.68 15.47	113.91 14.85	76.59 217.90	130.08 99.72
PINE3	94.07 11.69	69.13 6.61	51.84 8.94	116.60 25.25	112.71 18.57	65.85 40.29	110.70 30.73
PINE4	94.00 4.90	67.57 6.11	47.21 7.23	121.28 42.16	113.66 27.90	59.85 64.22	94.39 29.88
SOIL1	143.39 173.61	146.39 377.51	159.03 481.18	160.61 392.32	170.30 265.73	183.34 333.13	200.66 448.32
SOIL2	137.50 52.84	139.10 154.63	140.43 353.20	172.55 565.65	170.67 274.72	159.01 240.94	131.10 406.09
SOIL3	119.78 57.48	106.83 169.49	108.83 292.98	117.82 212.29	127.66 221.19	129.81 424.32	147.36 960.23

Table B-11 Continued

Cover Class	Channels 1	2	3	4	5	6	7
URBN1	169.43 265.96	174.29 427.76	179.00 506.92	169.07 125.92	174.64 150.25	187.93 681.15	186.71 375.14
URBN2	118.30 42.10	100.23 83.23	90.20 119.16	139.40 201.03	141.86 184.09	117.00 230.66	198.37 380.42
URBN3	107.66 34.32	84.45 49.75	69.04 70.28	126.35 179.20	121.98 153.98	83.75 97.31	148.92 545.92
WATR1	115.91 55.91	97.32 146.52	79.65 195.05	42.62 72.63	32.89 38.00	45.95 1206.29	44.44 145.98
WATR2	102.06 2.19	73.67 0.52	52.47 4.26	27.34 9.58	22.55 5.12	12.47 59.25	62.82 12.06

Table B-12 Average Standard Deviation over all Spectral Classes in each Cover Class (CAM2N)

Cover Class	Channels 1	2	3	4	5	6	7
CCUT	48.01	96.20	199.77	230.98	185.24	240.08	301.71
CROP	25.19	52.62	149.66	856.12	318.64	454.83	944.29
HDWD	9.72	9.65	8.01	73.06	38.65	59.39	83.10
PAST	18.75	27.05	54.29	154.14	101.52	199.49	318.23
PIHD	11.44	6.03	8.25	72.37	46.77	105.67	81.77
PINE	9.11	5.88	9.65	24.15	19.60	108.61	84.66
SOIL	94.64	233.88	375.79	390.08	253.88	332.79	604.88
URBN	114.13	186.91	232.12	168.72	162.77	336.37	433.83
WATR	29.05	73.52	99.65	41.11	21.56	632.77	79.02

Table B-13 Means and Variances by Spectral Class for 45 Meter Resolution Data (CAM2N)

Cover Class	Channels 1	2	3	4	5	6	7
CCUT1	135.84 83.59	135.17 188.74	142.33 400.14	164.30 272.72	179.98 305.69	182.74 328.25	171.80 321.52
CCUT2	105.39 33.28	83.40 53.10	73.22 107.72	121.01 81.02	133.46 82.69	114.28 196.31	186.08 367.14
CCUT3	105.73 36.50	87.24 73.97	70.62 145.43	148.96 137.87	151.39 71.17	113.52 127.70	146.15 146.33
CCUT4	100.57 20.25	78.75 30.81	57.52 36.10	149.03 288.53	143.09 152.13	90.08 97.92	120.69 194.08
CROP1	112.54 23.48	95.02 50.02	85.02 84.18	143.54 783.15	150.52 426.71	125.96 216.12	177.62 608.98
CROP2	103.98 41.08	83.37 89.57	64.77 308.81	168.21 1033.63	150.79 206.53	97.52 735.12	113.69 1023.63
HDWD1	90.03 11.38	72.48 10.36	49.03 13.80	171.80 81.40	154.17 40.89	84.73 71.72	114.17 122.94
HDWD2	94.22 10.84	71.46 11.79	46.21 8.13	185.85 85.48	158.40 41.56	75.18 133.63	86.94 56.39
HDWD3	92.51 11.79	70.46 10.44	46.87 6.52	165.51 30.05	144.82 17.55	74.85 56.98	91.22 71.71
HDWD4	94.01 6.71	71.21 7.99	48.42 6.12	145.68 75.42	129.45 45.26	70.84 33.46	87.62 58.79
PAST1	111.10 23.82	95.07 34.53	86.57 86.05	142.91 144.03	157.97 124.48	144.04 136.10	197.51 226.06
PAST2	102.94 8.28	83.58 16.73	60.15 24.13	194.35 190.87	179.07 102.36	110.72 223.06	138.11 292.63
PAST3	101.27 25.12	84.99 25.55	69.58 46.30	152.16 193.34	153.55 112.61	113.30 117.14	167.05 141.36
PAST4	102.83 14.75	80.12 32.03	74.42 50.07	104.47 19.43	117.32 40.53	104.30 289.57	193.11 498.11
PIHD1	95.86 11.70	75.27 17.06	59.42 20.53	133.69 47.49	131.10 31.96	89.93 195.84	136.03 97.43
PIHD2	89.12 5.63	69.85 2.20	52.07 5.89	129.07 89.82	123.75 50.54	64.98 119.78	121.64 74.61
PIHD3	93.05 9.94	69.17 2.36	48.72 5.17	131.20 79.76	120.95 45.27	65.39 25.09	97.24 43.57
PINE1	98.32 27.73	74.92 34.91	66.04 27.54	108.12 22.53	113.04 14.79	82.16 37.23	171.04 233.04
PINE2	95.79 7.16	71.58 7.94	56.58 12.64	115.08 26.56	114.87 21.02	77.09 209.65	128.14 114.30
PINE3	93.91 12.65	69.42 6.68	52.02 7.87	117.73 36.11	113.58 22.90	66.11 45.43	110.75 31.30
PINE4	93.51 4.02	67.02 4.89	46.61 5.71	121.26 39.49	113.49 23.07	59.39 53.65	94.10 32.14
SOIL1	149.53 66.94	156.16 159.81	168.20 223.81	169.96 438.25	177.37 243.79	189.78 186.23	188.84 872.77
SOIL2	134.50 44.02	133.61 124.65	136.54 242.96	163.31 572.37	164.39 241.42	156.41 160.24	140.42 606.35
SOIL3	118.71 46.67	105.18 132.39	106.80 230.48	117.82 175.94	127.24 171.30	127.83 363.16	146.37 897.71

Table B-13 Continued

Cover Class	Channels 1	2	3	4	5	6	7
URBN1	172.50 121.10	177.83 148.17	183.67 148.27	170.67 53.88	176.00 92.40	190.50 302.30	181.33 193.47
URBN2	118.00 30.83	99.51 68.12	88.77 95.09	137.60 159.00	138.85 160.43	112.77 220.75	190.13 266.74
URBN3	107.08 19.46	83.80 28.14	68.92 39.12	127.80 133.94	124.18 106.51	85.41 70.78	152.09 358.22
WATR1	114.36 61.02	94.90 172.68	76.83 235.41	41.62 116.93	32.17 55.80	48.36 1043.60	45.79 138.17
WATR2	101.84 2.06	73.49 0.37	52.28 4.48	27.21 9.90	22.41 5.05	11.19 44.55	62.66 10.43

Table B-14 Average Standard Deviation over all Spectral Classes in each Cover Class (CAM2N)

Cover Class	Channels 1	2	3	4	5	6	7
CCUT	43.41	86.66	172.35	195.03	152.92	187.54	257.27
CROP	32.28	69.80	196.50	908.39	316.62	475.62	816.30
HDWD	10.18	10.14	8.64	68.09	36.32	73.95	77.46
PAST	17.99	27.21	51.64	136.92	95.00	191.47	289.54
PIHD	9.09	7.21	10.53	72.36	42.59	113.57	71.87
PINE	12.89	13.60	13.44	31.17	20.44	86.49	102.70
SOIL	52.54	138.95	232.42	395.52	218.84	236.54	792.28
URBN	57.13	81.48	94.16	115.60	119.78	197.94	272.81
WATR	31.54	86.52	119.95	63.41	30.43	544.08	74.30

Table B-15 Means and Variances by Spectral Class for 80 Meter Resolution Data (CAM2N)

Cover Class	Channels 1	2	3	4	5	6	7
CCUT1	137.12 80.11	136.91 177.48	144.47 390.80	164.94 214.61	180.29 262.61	183.50 272.09	169.79 268.78
CCUT2	105.55 29.56	83.92 51.61	73.47 116.07	123.27 88.88	134.79 82.19	114.54 170.58	181.63 272.20
CCUT3	105.37 39.70	87.17 72.68	69.62 158.12	154.66 107.37	154.13 34.88	111.31 94.55	138.67 160.39
CCUT4	100.34 15.42	77.85 28.44	57.59 37.39	142.58 178.14	138.78 90.74	88.96 74.10	125.45 257.32
CROP1	111.52 23.76	94.52 58.43	84.84 133.89	141.32 617.31	147.36 281.83	129.12 152.36	168.56 602.17
CROP2	102.96 11.88	81.69 32.54	62.04 82.84	161.96 540.68	147.92 165.36	89.54 351.22	123.27 923.49
HDWD1	93.64 52.93	77.18 64.15	55.73 132.83	169.67 149.29	156.45 63.63	92.61 65.31	129.58 102.19
HDWD2	89.84 8.46	70.70 5.03	47.38 3.74	167.23 50.46	148.21 29.28	78.97 13.09	102.52 37.18
HDWD3	94.24 5.88	70.39 10.30	46.15 7.43	173.21 90.46	149.13 40.27	73.11 52.65	85.24 31.40
HDWD4	94.02 7.19	71.30 7.65	48.80 8.28	146.43 86.57	130.96 42.38	71.81 57.14	90.44 125.54
PAST1	111.34 18.13	95.34 26.94	86.05 91.35	146.82 207.02	161.42 147.12	144.21 104.88	197.63 179.97
PAST2	102.74 7.90	83.17 13.68	60.20 18.75	192.03 218.59	177.17 113.24	108.17 176.74	137.09 184.73
PAST3	102.52 22.26	85.93 25.57	72.24 38.54	147.98 206.16	152.33 119.98	117.93 92.42	170.43 97.73
PAST4	102.55 12.69	79.35 25.63	73.96 38.64	104.49 8.38	116.96 29.84	102.16 222.34	195.71 290.70
PIHD1	95.06 13.39	74.21 11.02	58.65 15.21	131.71 40.40	129.38 26.19	88.00 76.79	135.38 98.85
PIHD2	88.62 3.29	69.85 2.30	51.85 4.62	129.88 83.07	124.00 45.04	64.19 103.44	121.54 75.14
PIHD3	92.98 11.82	69.30 3.35	48.97 5.87	131.00 80.33	121.05 40.75	66.02 12.65	98.44 48.65
PINE1	98.73 39.22	75.64 46.86	67.09 51.69	109.45 38.88	114.73 38.42	85.09 91.49	169.55 209.88
PINE2	95.72 6.07	71.67 7.16	56.41 10.88	115.87 23.52	115.15 15.16	72.98 23.72	125.34 42.96
PINE3	93.33 9.54	68.26 6.00	50.22 9.37	117.79 21.41	112.71 15.86	64.91 62.41	106.72 34.70
PINE4	94.05 5.04	67.88 6.49	46.85 7.74	126.82 65.27	117.38 37.45	60.70 57.97	92.54 23.10
SOIL1	145.21 71.40	147.53 167.05	158.53 250.38	159.53 178.82	169.42 135.93	183.89 193.33	198.53 264.04
SOIL2	134.40 41.32	133.56 124.75	137.44 245.13	160.58 651.98	161.89 304.79	154.82 149.27	139.30 359.20
SOIL3	116.79 40.91	102.13 112.90	102.31 205.43	120.67 246.55	129.49 207.89	126.13 393.22	147.05 699.42

Table B-15 Continued

Cover Class	Channels 1	2	3	4	5	6	7
URBN1	163.75 74.92	162.75 230.92	166.00 296.67	157.00 418.00	161.25 548.92	167.00 1146.00	193.25 216.25
URBN2	116.00 18.51	96.55 50.56	85.30 72.58	134.90 125.99	136.32 124.28	109.57 205.84	186.70 256.18
URBN3	108.00 14.23	85.08 21.28	70.53 30.03	128.89 123.82	124.94 78.63	85.89 45.99	152.36 141.72
WATR1	110.11 94.34	88.93 208.92	71.56 242.88	44.85 293.05	35.19 179.85	41.11 267.33	53.70 308.06
WATR2	101.93 1.18	73.45 0.33	52.13 2.63	26.92 2.87	22.24 1.01	11.13 39.89	62.72 6.34

Table B-16 Average Standard Deviation over all Spectral Classes in each Cover Class (CAM2N)

Cover Class	Channels 1	2	3	4	5	6	7
CCUT	41.20	82.55	175.59	147.25	117.60	152.83	239.67
CROP	17.82	45.49	108.37	579.00	223.59	251.79	762.83
HDWD	18.62	21.78	38.07	94.19	43.89	47.05	74.08
PAST	15.25	22.96	46.82	160.04	102.54	149.09	188.28
PIHD	9.50	5.55	8.56	67.93	37.32	64.29	74.21
PINE	14.97	16.63	19.92	37.27	26.72	58.90	77.66
SOIL	51.21	134.90	233.64	359.12	216.20	245.27	440.89
URBN	35.89	100.92	133.09	222.60	250.61	465.94	204.72
WATR	47.76	104.62	122.75	147.96	90.43	153.61	157.20

APPENDIX C

APPENDIX C

NEWMAN-KEULS' RANGE TEST ON THE ARCSIN TRANSFORMED PROPORTIONS

The arcsin transformation is conducted to transform the binomially distributed proportions (percent correct classification) into a normal distribution. This is conducted in order to employ statistical tests which are designed in relation to populations having normal distributions. The test employed throughout this analysis is the Newman-Keuls' range test. This test was chosen since it provides inference concerning statistically significant differences over a range, or set of values. The sequence of steps involved in the test is provided here for benefit of: 1) repeating the procedure in follow-on experimentation, 2) elucidating the implications of certain variables, such as sample size, 3) providing a basis with which the inferences can be more fully appreciated.

The proportion of correct classification (PCC) by cover class are computed by:

$$PCC_{ir} = \left(\sum_{j=1}^{k} P_{ij} \Big/ \sum_{j=1}^{n} P'_{ij} \right) \qquad \text{(C-1)}$$

where:

P_{ij} = a pixel labeled as the i(th) cover class by the classifier and labeled as the i(th) cover class in the r(th) spatial resolution data by the analyst (k such pixels occur).

P'_{ij} = a pixel labeled by the analyst as the i(th) cover class, in the r(th) spatial resolution. (n such pixels occur) $\{P_{ij} \in P'_{ij} \; ; \; k \leq n\}$

The arcsin transformation is conducted for all PCC_{ir} for all of the cover classes and achieved with data of the four spatial resolutions.

$$*PCC_{ir} = \sin^{-1}(PCC_{ir})^{\frac{1}{2}} \qquad \text{(C-2)}$$

The variance (σ^2) of the transformed PCC_{ir} is now provided by:

$$\sigma_i^2 = (821/N) \qquad \text{(C-3)}$$

where:

821 = a derived constant relating sample size to the arcsin transformed distribution (see Steel and Torrie, 1960).

N = the number of samples with which the PCC were calculated. Since a variance common to all spatial resolutions (or any variable for which tests across factor levels will be conducted) is desired, the harmonic mean of the number of samples taken for each resolution is empolyed (i.e., N = harmonic mean).

The harmonic mean is a weighted average, where the weight is proportional to the inverse of the relative magnitude of each element included in the average. The harmonic mean is, therefore, a mean value of lower magnitude than the arithmetic mean in every case where the elements are not equal (the harmonic mean equals the arithmetic mean where the elements are equal). The harmonic mean is regarded as more appropriate than the arithmetic mean for estimating a common variance among factor levels (eg., each resolution) sampled at different

intensities, since the lowest sampling intensity has the greatest weight in determining the mean. The harmonic mean is computed by:

$$HM = m / \sum_{r=1}^{m} \frac{1}{n_r} \qquad \text{(C-4)}$$

where:

HM = harmonic mean

m = the number of elements included in the mean.

n_r = the number of pixels sampled in computing the proportion correctly classified using the r(th) spatial resolution.

The normalized standard deviation σ_i computed for each cover class is then multiplied by the appropriate tabulated percentile (q) of the Studentized Range Distribution (see Neter and Wasserman, 1974; Appendix Table A-9, or Steel and Torrie, 1960; Appendix Table A-9.A). The arcsin transormation provides a test conducted with infinite degrees of freedom associated with the mean square error and therefore provides a sensitive test provided the number of samples are sufficient. The transformed proportions are arranged in descending or ascending order. Differences between the ordered transformed proportions which are greater than the $\sigma(q)$, computed for the corresponding range, are considered "real" or significant at the α-level for which the q value was obtained. The range test is generally conducted sequentially starting with a comparison of the highest and lowest values and proceeding down to neighboring pairs of values. If the highest and lowest are not found to differ significantly, then all values are considered equal.

The following example is provided by the pine-hardwood class of the training data from CAMIS:

		(i=pihd)	
	PCC_{ir}	$*PCC_{ir}$	n_r
r = 15	83.7	66.19	1273
r = 30	89.8	71.37	314
r = 45	91.6	73.15	143
r = 80	95.1	77.21	61

The harmonic mean is computed:

$$HM = 4/(1/1273 + 1/314 + 1/143 + 1/61)$$
$$= 146.22$$

The standard deviation is computed:

$$\sigma = (821/146.22)^{\frac{1}{2}}$$
$$= 5.615$$

The percentiles of the Studentized Range Distribution are obtained:

	2	3	4
$\alpha = 0.10$	2.33	2.90	3.24

The smallest significant differences are computed:

$\alpha = 0.10$	(2.33)	(2.90)	(3.24)
$q\sigma =$	13.083	16.283	18.192

These are compared to the differences associated with the rank ordered *PCC

66.19	71.37	73.15	77.21

Since 77.21 - 66.19 = 11.02 < 18.192 all differences are insignificant at $\alpha = 0.10$. This result is then denoted by:

66.19^a	71.37^a	73.15^a	77.21^a